Electron Transfer in Cytochrome *c* Oxidase: The Rate of Electron Equillibration Between Cytochrome *a* and Copper A

Thesis by
Joel E. Morgan

In Partial Fulfillment of the Requirements
for the Degree of
Doctor of Philosophy

California Institute of Technology
Pasadena, California

1989

(Submitted August 10, 1988)

In the pursuit of learning, every day something is acquired.
In the pursuit of Tao, every day something is dropped.

Lao Tsu

translated by Gia-Fu Feng and Jane English

ACKNOWLEDGEMENTS

First, I would like to thank the following people who have contributed directly to my graduate research: **Sunney Chan**, my graduate research advisor who gave me the space to make mistakes, and to learn from them, and forced me to be independent; **David Blair**, **D.J. Jang**, **Mark Li**, and **Craig Martin**, who collaborated with me on projects here at Caltech; **Mostafa El-Sayed**, **Harry Gray**, and **Michael Hoffman**, who generously lent me their equipment and laboratories; **Larry Henling**, who helped me run mass spec. more times than either of us would like to remember; **Eric Betterton**, who helped me set up the stopped-flow T-jump apparatus and taught me to use it; **Bruce Vogelaar**, who helped me with the data analysis; and the members of the technical staff here at Caltech, especially, **Siegfried Jenner**, glass blower to the gods, and **Tom Dunn**.

I would also like to thank the following people for contributing their insight into the questions raised by this work: **James Alben**, **Jerry Babcock**, **Jimmy Cowan**, **Walther Ellis**, **Mark Ondrias** and **Mary Selman**.

I am very thankful to **Elise Gabriel** for being my guardian angel while this thesis was in preparation.

I would also like to thank **all of the people who have been part of the Chan Group** while I have been at Caltech, especially: **Bob Copeland**, **Elise Gabriel**, **Jeff Gelles**, **Thomas Nilsson**, **Paul Smith**, **Hsin Wang**, and **Steve Witt**, who have worked on the oxidase project, and with whom I

have shared the sorrows of isolating this enzyme, and the joys of thinking about how it might work; and **Joe Falke, Kathy Kanes, Scott Ross, Paula Watnick** and **Denise Worthen**. I'm going to miss you guys!

Finally, I wish to thank my mother and father for their love and support, and for giving me the truck.

ABSTRACT

Intramolecular electron transfer in partially reduced cytochrome *c* oxidase has been studied by means of perturbed equilibrium techniques. We have prepared a three electron reduced, CO inhibited form of the enzyme in which cytochrome *a* and copper A are partially reduced an in intramolecular redox equilibrium. When these samples were photolyzed using a nitrogen laser (0.6 μs, 1.0 mJ pulses) changes in absorbance at 598 nm and 830 nm were observed which are consistent with a fast electron from cytochrome *a* to copper A. The absorbance changes at 598 nm have an apparent rate of 17,200 ± 1,700 s^{-1} (1σ), at pH 7.0 and 25.5 °C. These changes were not observed in either the CO mixed valence or CO inhibited fully reduced forms of the enzyme. The rate is fastest at about pH 8.0, and falls off in either direction, and there is a small, but clear temperature dependence. The process was also observed in the cytochrome *c* -- cytochrome *c* oxidase high affinity complex.

This rate is far faster than any rate measured or inferred previously for the cytochrome *a* -- copper A electron equilibration, but the interpretation of these results is hampered by the fact that the relaxation could only be followed during the time before CO became rebound to the oxygen binding site. The meaning of our our measured rate is discussed, along with other reported rates for this process. In addition, a temperature-jump experiment on the same system is discussed.

We have also prepared a partially reduced, cyanide inhibited form of the enzyme in which cytochrome *a*, copper A and copper B are partially

reduced and in redox equilibrium. Warming these samples produced absorbance changes at 605 nm which indicate that cytochrome *a* was becoming more oxidized, but there were no parallel changes in absorbance at 830 nm as would be expected if copper A was becoming reduced. We concluded that electrons were being redistributed from cytochrome *a* to copper B. The kinetics of the absorbance changes at 605 nm were investigated by temperature-jump methods. Although a rate could not be resolved, we concluded that the process must occur with an (apparent) rate larger than 10,000 s^{-1}.

During the course of the temperature-jump experiments, we also found that non-redox related, temperature dependent absorbance changes in fully reduced CO inhibited cytochrome *c* oxidase, and in the cyanide mixed valence enzyme, took place with an (apparent) rate faster that 30,000 s^{-1}.

TABLE OF CONTENTS

List of Figures

Abbreviations.

CHES, (2-[N-Cyclohexylamino]ethanesulfonic acid).

CN+1, see page 114.

CNMV, cyanide mixed valence compound of cytochrome *c* oxidase.

CNOx, fully oxidized cyanide inhibited cytochrome *c* oxidase.

COMV, CO mixed valence compound of cytochrome *c* oxidase.

COMV+1, see page 26.

COFR, CO inhibited, fully reduced cytochrome *c* oxidase.

Cu_A, copper A.

Cu_B, copper B.

ENDOR, electron nuclear double resonance.

EPR, electron paramagnetic resonance.

EXAFS, extended x-ray absorption fine structure.

Fe_a, cytochrome *a* .

Fe_{a_3}, cytochrome *a*3.

k_{app}, apparent rate constant.

k_f, rate constant of forward process.

k_r, rate constant of reverse process.

MES, (2-[N-Morpholino]ethanesulfonic acid).

MOPS, 3-[N Morpholino]propane sulfonic acid.

MWCO, molecular weight cut off (of dialysis tubing etc.)

NADH, Nicatinamide adenine dinucleotide, reduced form.

NHE, neutral hydrogen electrode.

PMT, photomultiplier tube.

σ, standard deviation.

T-J, temperature-jump.

Tween-20, Polyoxyethylenesorbitan monolaurate.

Tween-80, Polyoxyethylenesorbitan monooleate;

Chapter I

Introduction

The work presented in this thesis is an investigation of the kinetics of electron equilibration between cytochrome *a* and copper A of cytochrome *c* oxidase. The introduction is divided into four parts:

1) a general introduction to cytochrome *c* oxidase, its physiological role, its isolation, and its structural and kinetic properties;

2) a more detailed introduction to some of the electron transport properties of the enzyme which provide a context for the measurements presented later;

3) a brief introduction to perturbed equilibrium kinetic measurements;

4) an introduction to the properties of the enzyme which are exploited to make this measurement possible.

The first part of the introduction may be skipped by the reader who is familiar with cytochrome *c* oxidase since the remaining parts of the introduction are written to be somewhat self contained.

1. Cytochrome *c* oxidase.

The process of mitochondrial electron transport ends with the reduction of dioxygen to water by cytochrome *c* oxidase. Ferrocytochrome *c* is oxidized, dioxygen is reduced, and the free energy resulting from this reaction is converted into an electrochemical potential across the inner mitochondrial membrane, a potential which ultimately drives the production of ATP (see Wikström et al., 1981 for a review). To accomplish this energetic coupling, the enzyme employs two concurrent mechanisms. One mechanism is a direct consequence of the redox chemistry of the enzyme. The conversion of one

molecule of dioxygen to water requires four electrons and four protons. When this reaction is catalyzed by cytochrome *c* oxidase, the electrons enter the enzyme from the outer (cytosolic) side of the membrane, and the protons are consumed from the inner (matrix) side. In this manner, the membrane sidedness is exploited to produce a charge separation and a proton gradient across the membrane.

Coupled to this transmembrane electron transfer is an electrogenic proton pump. As electrons flow through the enzyme, protons are pumped out of the mitochondrial matrix and into the cytosol. The stoichiometry of this vectorial proton pumping process can be as high as one proton per electron. Thus, for every electron which passes through the enzyme, one proton is consumed, and up to one proton is pumped, resulting in a maximum proton per electron stoichiometry of two. (Wikström et al., 1981)

The cytochrome *c* oxidases of eukaryotic organsims are made up of as many as twelve different polypeptides. Of these, most are encoded on nuclear genes, but the three largest (subunits I, II and III), are encoded in the mitochondrial genome. These three ("mitochondrial") subunits appear to make up the functional core of the enzyme. Subunits I and II are thought to contain all of the redox active metal centers (Wikström et al., 1981; Holm et al., 1987). Subunit III appears to play a role in the pumping of protons. If this subunit is removed, the stoichiometry of the proton pump falls from about 0.9 H^+/e^- to approximately half of that (Sarti et al., 1985).

The molecular events catalyzed by cytochrome *c* oxidase are mediated by four redox-active metal centers, two coppers and two heme irons. One iron and one copper, cytochrome *a*3 (Fe_{a_3}) and copper B (Cu_B), form the site of

oxygen binding and reduction. The remaining two centers, cytochrome *a* (Fe_a) and copper A (Cu_A), serve to accept electrons from cytochrome *c* and pass them on to the oxygen binding site (Blair et al., 1983). A recent study by Wikström and Casey (1985) showed that these latter metal centers are the most likely sites of the redox-linked proton pumping function. (The structure and function of the metal centers will be discussed in much more detail below.)

In eukaryotic organisms, cytochrome *c* oxidase is an integral membrane protein found in the inner (coupling) membrane of the mitochondrion. Some properties of the enzyme can be studied in whole mitochondria, but for most work, a detergent solubilized preparation is used. The most popular source for the enzyme is beef heart. The original studies of proton pumping were done with whole mitochondria (Wikström, 1977), but most recent work has used the isolated enzyme reconstituted into lipid vesicles. (These topics are reviewed by Wikström et al., 1981.)

The isolated beef heart cytochrome *c* oxidase is a dimer. The dimer can be dissociated, and the monomers are active in electron transfer, but there are some indications that the dimer may be neccessary for proton pumping activity (Finel and Wikström, 1986). The enzyme isolated from some organisms; for example, sharks, is monomeric (Georgevich et al., 1983; Wilson et al., 1980). However, this may be an artifact of isolation, and it is not clear whether monomers exist under physiological conditions.

Metal Centers.

As there is no high resolution crystal structure for cytochrome *c* oxidase, the present identification of metal center ligands and structures, and the measurements of distances between metal centers, have come from spectroscopic studies. Some additional information about the metal center structures has come from the amino acid sequences for the enzyme (Wikström et al., 1985). Holm et al. (1987) and Chan et al. (1987), have used the spectroscopic and protein data together to model some of the metal centers. Current knowledge about the metal center structures has been reviewed by Blair et al. (1983), and much of the following discussion is based on this source.

Ligands to metal centers. All four metal centers are structurally and spectroscopically distinct. Both irons are contained in the unusual heme A, which differs from the heme of cytochrome *c* in that it bears a formyl group and a long isoprenoid chain on its periphery. Resonance Raman and EPR studies with model compounds (Babcock et al., 1981; Peisach, 1978) have indicated that both of the axial ligands of Fe_a are histidines. EPR and isotope incorporation studies (Stevens and Chan, 1981) have shown that one of the axial ligands to Fe_{a_3} is histidine. The other axial position is part of the catalytic site for oxygen reduction. As well as oxygen, Fe_{a_3} can also bind other external ligands including carbon monoxide, nitric oxide and cyanide.

Cu_A is a spectroscopically unique biological metal center. In the oxidized form it has at least one histidine and one cystiene ligand, and the available spectroscopic and amino acid sequence data are consistent with a structure with two histidine and two cystiene ligands (Martin, 1985; Martin et

al., 1988; Li et al., 1987; Holm et al., 1987). Chan et al. (1987) have proposed that Cu_A may exchange ligands upon reduction. Cu_B is EPR silent in most states of the enzyme. It is known from EXAFS and ENDOR studies, that in the oxidized state, Cu_B has three nitrogen (or oxygen) bearing ligands, two of which are probably histidines, and one heavier (S or Cl) ligand (Li et al., 1987; Witt, 1988). Like Fe_{a_3}, Cu_B makes up part of the catalytic site for oxygen reduction. Cu_B has also been reported to external ligands including NO, and under some circumstances CO (Fiamingo et al., 1982; Brudvig et al., 1980).

Intermetal distances. Most of what is known about the distances between the metal centers also comes from spectroscopic studies.

1) Fe_a to Cu_A. It has been found that the EPR saturation properties of Cu_A depend on the oxidation state of Fe_a, but no effects on line width have been observed. Based on these observations, and measurements of the EPR saturation properties of Cu_A in different states of the enzyme, Brudvig et al. (1984) calculated a distance of between 13 and 26 Å, while Goodman and Leigh (1985) calculated a distance between 8 and 13 Å.

2) Fe_a to Fe_{a_3}. A number of measurements of this distance have been made. Based on electronic spin relaxation rates in the azide inhibited compound of the enzyme, Goodman and Leigh (1987) calculate a distance of 19 ± 8 Å. Brudvig et al. (1984) have calculated a distance of 20 Å, based on a reinterpretation of earlier EPR studies of the nitrosyl adduct of $Fe_{a_3}{}^{2+}$.

3) The best established intermetal distance in the enzyme is that between Fe_{a_3} and Cu_B. The oxidized enzyme reacts with azide and NO to produce a species conatining $Fe_{a_3}{}^{2+}$-NO, and $Cu_B{}^{2+}$ at the oxygen binding site. Magnetic interaction between the two spins gives rise to a triplet signal, from

which a distance of 3.4 Å between "spin centers" has been calculated (Stevens et al., 1979; Blair et al., 1983). A value of 3.8 Å for the iron to copper distance has been calculated from EXAFS measurements by Powers et al. (1979).

The distances of the various metal centers from the surface of the protein or the membrane have been studied by means of EPR relaxation measurements employing soluble paramagnetic probes such as dysprosium complexes. In studies on the enzyme reconstituted into phospholipid vesicles, distances of about 2.1 to 2.2 nm were found for Fe_a and Cu_A, and 3.5 nm for Fe_{a_3} (Ohnishi et al., 1985). The authors caution that the absolute numbers are not highly reliable and should principally be used for comparison with one another. They conclude that Fe_{a_3} is more deeply buried that either Fe_a or Cu_A which are both buried to about the same extent.

Redox potentials. The redox potential of cytochrome *c* is about 260 mV (v. NHE, Taniguchi et al., 1982), and the redox potential for the reduction of oxygen to water is about 810 mV (see Wikström et al., 1981). This span defines the range of potentials over which cytochrome *c* oxidase operates, as well as the amount of energy available to be conserved. In the native enzyme the redox potentials of Cu_A and Fe_a are about 288 mV and 340 mV respectively, fairly close to that of cytochrome *c* . In the absence of oxygen the redox potential of Fe_{a_3} is around 270 to 310 mV, and has been found to vary from batch to batch of enzyme. The redox potential of Cu_B cannot be measured directly because there is no appropriate spectroscopic signature. Lindsay et al. (1975) obtained a value of about 340 mV by an indirect method. In the functioning enzyme, the effective potentials of Fe_{a_3} and Cu_B will be much

higher due to the presence of oxygen and partially reduced oxygen intermediates in the active site (Lindsay et al., 1975).

Redox interactions. The redox potentials of the metals in cytochrome *c* oxidase can vary depending on whether other metal centers in the enzyme are reduced or oxidized (Goodman 1984; Blair et al., 1986). There is an anticoöperative interaction of 40 mV between Fe_a and Cu_A, which means that when Fe_a is reduced, the redox potential of Cu_A is lowered by 40 mV; i.e., it is 40 mV more difficult to reduce. In addition, there are anticoöperative interactions between Fe_a and Fe_{a_3} (-35 mV), Fe_a and Cu_B (-35 mV) and between Fe_{a_3} and Cu_B (-35 mV). The redox potentials given above are all "upper asymptotic" potentials, meaning that these are the potentials when all of the other sites are oxidized.

Optical spectra. The visible spectra of Fe_a and Fe_{a_3} overlap to a large extent, and this together with the interactions between the metal centers has made the interpretation of the visible spectrum of the enzyme a significant problem. At one time, the interactions observed in redox titrations were attributed to spectral interactions; that is, to the influence of the redox state of one site on the visible extinction coefficient of another site (reviewed in Wikström et al., 1981). Such spectral interactions do exist; for example, the redox state of Cu_B has been found to influence the visible extinction coefficient of Fe_{a_3} (Blair et al., 1982). However, spectral interactions have been shown to be small compared to the redox interactions (Blair et al., 1982; Blair et al., 1986, Ellis et al., 1986; Goodman et al., 1984; Wang et al., 1986; Wikström, 1981). Some controversy still exists, but it is now centered on the

spectra of intermediates during the oxygen reaction (see for example Brunori and Gibson, 1983, Hill et al., 1986).

In a way, this controversy has brought the field back around a full circle. The currently accepted deconvolution of the visible spectrum into contributions from Fe_a and Fe_{a_3} comes from a 1966 paper by Vanneste. According to this source, the contributions from Fe_a and Fe_{a_3} to the reduced-minus-oxidized absorption difference at 445 nm are 45% and 65% respectively, while the contributions at 605 nm are about 80% and 20% respectively. Oxidized Cu_A gives rise to a broad, weak absorbance centered at around 830 nm which has an extinction of about 2.3 mM^{-1} (Boelens and Wever, 1980). Thus, the reduction of Fe_a is usually observed at 605 nm, and the reduction of Cu_A at around 830 nm.

Kinetics.

Steady-state kinetics: Cytochrome *c* oxidase catalyzes the reduction of dioxygen to water together with the oxidation of ferrocytochrome *c* . Under typical experimental conditions the enzyme will oxidize a maximum of 30 to 600 molecules of cytochrome *c* per second. A great deal of work has been devoted to the study of this reaction at steady state by classical enzyme kinetics methods. The oxidation of cytochrome c^{2+} can be followed spectrophotometrically (Smith, 1955), and the consumption of oxygen can be followed polarographically by means of an oxygen electrode (Ferguson-Miler et al., 1976). In the steady state reaction, when the cytochrome *c* concentration is varied, two kinetic phases are typically observed, each with a

different maximum turnover number (TN_{max}) and K_m. These values depend on pH, ionic strength, and the detergent used to solubilize the enzyme (Sinjorgo et al., 1986). Binding studies have demonstrated that cytochrome *c* oxidase binds cytochrome *c* with two different affinities, which correlate fairly well with the K_m values of the two kinetic phases. This was originally interpreted in terms of two catalytically active cytochrome *c* binding sites on the oxidase (Ferguson-Miller et al., 1976). More recently, it has been suggested that there may only be one catalytic cytochrome *c* binding site, and that the binding site which has the lower affinity acts allosterically (Speck et al., 1984; Sinjorgo et al., 1986). In the present context, the maximum turnover number which is of interest is the one corresponding to the fastest phase, and in what follows, TN_{max} will always refer to that number.

Reduction kinetics. When electrons enter the enzyme from cytochrome *c* , Fe_a and Cu_A are the first metal centers to be reduced. From these two centers, the electrons are passed through the molecule to Fe_{a_3} and Cu_B where the reduction of dioxygen to water occurs. The kinetics of reduction can be studied either during an approach to steady state, with oxygen present, or as a terminal process, in the absence of oxygen or in the presence of an inhibitor such as cyanide.

The initial reduction of Fe_a and Cu_A is fast. In stopped flow experiments, with or without oxygen present, biphasic reduction is observed at both metal centers. Either the two metal sites are reduced synchronously, or Cu_A lags slightly (Antalis and Palmer, 1982; Andréasson et al., 1972; Wilson et al., 1975). The actual order of electron transfer these two sites is still not known. (The issue is discussed in more depth below.) In these experiments,

initial rates between 10^6 and 3×10^7 $M^{-1}s^{-1}$ have been measured for the reduction of Fe_a, in a variety of different enzyme preparations. Slightly higher rates have been measured using temperature-jump and by pulsed radiolysis techniques (Greenwood et al., 1976; Van Buuren et al., 1974).

The metals of the oxygen binding site are subsequently reduced by an intramolecular transfer of electrons from Fe_a and Cu_A. Initially, this process is far slower than the reduction of Fe_a and Cu_A. $Fe_{a_3}{}^{2+}$–CO is photolabile. Under anaerobic condition, when there is CO in the sample, the extent of reduction of Fe_{a_3} can be unambiguously determined from the amplitude of absorbance changes which occur when the sample is illuminated. (This is sometimes referred to simply as "photosensitivity.") In the presence of CO, Fe_{a_3} is reduced with a half time of 1.2 s (Gibson et al., 1965). In the presence of oxygen, steady state turnover is reached at a similarly slow rate (Antonini et al., 1977). These rates are clearly too slow to account for the steady state turnover of the enzyme which presumably involves the same intramolecular electron transfer step.

This can be accounted for in part by a hysteresis in the oxidized state of the enzyme. When the enzyme has been kept in the oxidized state for several hours, for example, after the isolation proceedure, the approach to steady state turnover is slow as described above, However, if the enzyme has been recently reduced and reoxidized, the approach to steady state in the presence of air, and the onset of photosensitivity in the presence of CO, both occur about five times faster (Colosimo et al., 1981). The slower state is known as the "resting" enzyme, while the faster state resulting from turnover is known as "oxygen-pulsed" or more recently "pulsed" enzyme. Like the resting enzyme,

the pulsed enzyme is fully oxidized. However, based on its EPR spectrum, ligand binding properties and chemical reactivities the chemical configuration at the oxygen binding site is thought to be different from that of the resting enzyme. The pulsed enzyme decays to resting with a half-life of about 45 minutes at ice temperature (Armstrong et al., 1983; Brudvig et al., 1981; Colosimo et al., 1981). The difference in intramolecular electron transfer rates between the pulsed and resting enzyme is probably due to the ligation state of the oxygen binding site (Brudvig et al., 1981).

Reoxidation kinetics. Fully reduced cytochrome *c* oxidase contains four reducing equivalents, enough to reduce one molecule of dioxygen to water. The reoxidation of the reduced enzyme is much faster than the reduction of the oxidized enzyme. Upon contact with air, the enzyme is reoxidized within five milliseconds, a time consistent with steady state turnover rates (Hill and Greenwood, 1984a). Since this is within the dead time of a typical stopped flow measurement, other techniques have been used to study this reaction. The two techniques which are commonly used both rely on CO as a photolabile inhibitor of the reduced enzyme.

Most of the information about intermediates in the reduction of oxygen has come from a technique called "triple trapping," in which the reaction is carried out at very low temperatures. This technique, developed by Britton Chance and colleagues (1975). The CO inhibited, reduced enzyme is first cooled to -20 °C, a temperature at which the reaction with oxygen is very slow. Oxygen is then introduced, in the dark, and the sample is frozen as a glass to 77 K. At this temperature, $Fe_{a_3}{}^{2+}$–CO can be photolyzed with continuous illumination, and the reaction with oxygen will not proceed. Once the

photolysis is complete, the sample can be warmed in a controlled way, and the reaction will go forward. The mechanism of oxygen reduction is reviewed by Wikström et al. (1981) and Hill et al. (1986) (see also, Witt, 1988).

In these experiments, Fe_a and Cu_A are reoxidized at different rates. This has led some workers to suggest that direct electron transfer to the oxygen binding site from each of these metal centers is possible (Blair et al., 1985).

In order to study this reaction at room temperature, a technique known as "flow flash" has been developed (Gibson and Greenwood, 1963). In the flow-flash experiment, CO inhibited cytochrome *c* oxidase and oxygen containing buffer are mixed, exactly as they would be in a stopped-flow experiment. In the dark, the dissociation rate of CO is very slow (0.03 s^{-1} , Boelens et al., 1982), and the reactants can be mixed without the reaction proceeding to a significant extent. Once mixing is complete, $Fe_{a_3}{}^{2+}$–CO is photolyzed with an intense flash of light, and the reaction with oxygen begins within a microsecond.

Flow flash experiments have revealed that the reoxidation of Fe_a and Cu_A is multiphasic. $Fe_{a_3}{}^{2+}$ is reoxidized at a rate of 30,000 s^{-1}. Cu_B may be reoxidized simultaneously, but since it cannot be observed, there is no way to know. Surprisingly, it appears that 40% of Fe_a is reoxidized simultaneously with Fe_{a_3}. Following this initial phase, 60% of Cu_A is reoxidized at 7000 s^{-1}, and finally the balance of Fe_a and Cu_A are reoxidized at 700 s^{-1} (Hill and Greenwood, 1984a). These data have been interpreted in terms of a branching mechanism for the reoxidation of the enzyme in which there are two different subpopulations of the enzyme, and in each population, Fe_a and Cu_A donate electrons to the oxygen binding site with different rates. According to this

scheme, 40% of the enzyme molecules follow a pathway in which Fe_a is reoxidized first, and 60% follow a pathway in which Cu_A is reoxidized first (Hill and Greenwood, 1984a, Hill et al., 1986).

More steady state kinetics. Another class of steady state kinetics experiments has been carried out in which the levels of reduction of Fe_a and Cu_A are monitored during enzyme turnover. Under turnover conditions, Fe_a is significantly more reduced that Cu_A (Thörnström et al., 1988, Brzezinski et al.; 1986). This is in accord with the fact that the redox potential of Fe_a is higher than that of Cu_A in the native enzyme (Blair et al., 1986). As the pH of the sample is increased, the steady state reduction level of Fe_a increases (Moroney et al., 1984), even though the pH dependence of the midpoint potential of Fe_a would predict the opposite behavior (Blair et al., 1986).

In a steady state experiment, when the reductant runs out, the enzyme becomes reoxidized. If there is cytochrome *c* present, Cu_A and cytochrome *c* become reoxidized more or less together, but the reoxidation of Fe_a lags significantly (Brzezinski et al., 1986; Wilson et al., 1975).

2.The role of Fe_a and Cu_A in electron transport.

Fe_a and Cu_A accept electrons from cytochrome *c* and pass them on to the oxygen binding site. As discussed above, it is still not known whether electrons from cytochrome *c* go first to Fe_a, Cu_A, or directly to both sites (See Brunori et al., 1981). Similarly, the results of the flow flash experiment suggest that electrons may be able to go directly from both centers to the oxygen binding site, but this is also not certain. In terms of the functioning of

the enzyme, these questions are important because at least one of these two metal centers plays a role in coupling the flow of electrons to the pumping of protons (Wikström and Casey, 1985).

In order for the flow of electrons to drive a proton pump, the two processes must be kinetically linked; that is, the transfer of an electron must not be allowed to occur without the pumping of a proton, and protons must not be able to back-flow. Thus, electron transfer into and out of a coupling site would be expected to be gated. These issues have received considerable attention (Wikström et al., 1981; Blair et al., 1986), and I will not attempt to deal with them in any depth here. For the present it is enough to point out that any model proposed for redox driven proton pumping in this system must be consistent with the electron transfer pathways

Because the redox potentials of Fe_a and Cu_A are close to that of cytochrome *c* , the intramolecular electron transfer from Fe_a and/or Cu_A to the oxygen binding site is the only step in the electron transport pathway of the enzyme which has enough free energy to drive the pumping of a proton (Chan et al., 1987). The measured stoichiometry of the proton pumping activity is as high as 0.9 H^+/e^- (Sarti et al., 1985), and if as is commonly assumed, the inherent stoichiometry of the coupling mechanism is one H^+/e^-, then almost every electron must pump a proton. (This assumption is discussed by Chan et al., 1987). It is possible that both Fe_a and Cu_A could be coupling sites, and that electron transfer to the oxygen binding site from either of these two centers would pump a proton. However, this kind of redundancy seems unlikely, and if it is not the case, only electron transfers out of one of the two sites will drive the proton pump (Blair et al., 1985). This in turn would lead to

the conclusion that in order to achieve a 0.9 H^+/e^- stoichiometry, almost every electron would have to go from the coupling site to the oxygen binding site.

A number of electron pathways are possible. The classical model held that electrons flowed from cytochrome *c* to Fe_a, then to Cu_A and from there to the oxygen binding site. More recently, it has been suggested that Fe_a could receive electrons from cytochrome *c* , and also donate them to the oxygen binding site, while Cu_A would be in fast redox equilibrium with Fe_a, in an electron transfer *cul de sac* (Wikström et al., 1981), or that electrons could enter Cu_A first and then move to the oxygen binding site via Fe_a (Holm et al., 1987). The unequal and biphasic reoxidation of Fe_a and Cu_A has led to the suggestion that both Fe_a and Cu_A could donate electrons directly to the oxygen binding site (Blair et al., 1985, Hill et al., 1986).

In order to approach this issue, it will be helpful to break it up into some smaller questions and to define some terminology (see Brunori et al., 1981). Given what is known about the system, the following questions can be asked: 1) How many binding sites for cytochrome *c* does cytochrome *c* oxidase have? 2) How many of these cytochrome *c* binding sites are catalytic (or electron transfer competent)? 3) Which metal center(s) can be reduced directly from a cytochrome *c* bound at a particular binding site? A binding site could be associated with "electron entry ports" to Fe_a or Cu_A or both. 4) Are electrons exchanged between Fe_a and Cu_A quickly on the time scale of reduction or turnover; that is, is the electron transfer rate between these two centers fast enough to be consistent with a model in which electrons must pass through both Fe_a and Cu_A on their way from cytochrome *c* to the oxygen

binding site? 5) Which of these metal centers is capable of transferring electrons to the oxygen binding site?

The existence of two binding sites for cytochrome *c* is well established (Ferguson-Miller et al., 1976, and see review by Capaldi et al., 1982), but none of these other issues has been settled.

One central aspect of this problem is the rate of electron equilibration between Fe_a and Cu_A. If both Fe_a and Cu_A are to participate in a single pathway, the rate of electron transfer between these two sites must be fast enough to support the turnover rate of the enzyme. If, on the other hand, both Fe_a and Cu_A are capable of donating electrons directly to the oxygen binding site, a fast Fe_a to Cu_A electron transfer rate could short-circuit an electron gating mechanism related to the proton pump (see Blair et al., 1985). In addition, there is always the possiblility that the Fe_a -- Cu_A electron transfer rate could be one of the rates controlled by the enzyme as part of its gating mechanism. In the rest of this introduction, I will focus on a few kinetic results which pertain to the Fe_a -- Cu_A electron equilibrium rate.

The initial entry of electrons into Fe_a and Cu_A is fast. In many experiments, the reduction of these two sites track together, and this has been taken as evidence of fast electron equilibration between them. For example, Andréasson et al. (1972) studied the reduction of cytochrome *c* oxidase by ferrocytochrome *c* in a stopped flow experiment. They observed biphasic kinetics at every wavelength they followed. The kinetic data were parametrized, plotting the change in absorbance at 550 nm, which corresponds to the oxidation of ferrocytochrome *c*, against the change at other wavelengths. For the first part of the reaction, plots of absorbance

change at 550 nm against 445, 605 and 830 nm were all linear. (This was only the case for the anaerobic experiments.) At the time the authors interpreted this to mean that only Fe_a was being reduced in the first phase of the reaction. The idea that only one site was being reduced provided a convenient explanation for the fact that the same kinetic behavior was observed at several wavelengths. The large change at 830 nm was explained by assigning 40% to the reduced-minus-oxidized extinction at that wavelength to Fe_a. This is no longer a tenable explanation since it is now known that Cu_A dominates the 830 nm absorbance (Beinert et al., 1980). Thus Fe_a and Cu_A must have been accepting electrons synchronously. (This is discussed by Wikström et al., 1981).

Antalis and Palmer (1982) reported a similar stopped flow experiment. They studied the reduction of both native, and cyanide inhibited cytochrome *c* oxidase by ferrocytochrome *c* and concluded that Fe_a and Cu_A were reducing in parallel. They proposed a model in which there is only one catalytic site for cytochrome *c* , and in which Fe_a and Cu_A are in fast redox equilibrium. Electrons entering the oxidase would equilibrate rapidly between Fe_a and Cu_A, but the reduction would be biphasic because the entry of the second electron would have to wait for the dissociation of the cytochrome *c* which brought the first electron. As the authors pointed out, one difficulty with this model is that it requires the redox potentials of Fe_a and Cu_A to be approximately equal. Equilibrium electrochemical measurements, have shown that the redox potential of Fe_a is 48 mV higher than that of Cu_A in the cyanide inhibited enzyme (Goodman, 1984), and is approximately the same in the native oxidase (Blair et al., 1986). With this large a potential difference, and a fast redox

equilibration between Fe_a and Cu_A, the reduction of Fe_a should clearly lead the reduction of Cu_A (See Copeland et al., 1987).

Antalis and Palmer (1982) explain their results by postulating that the redox potential difference between Fe_a and Cu_A which controls the initial reduction of the enzyme, is much smaller than that measured electrochemically. If this were the case, the electrons in Fe_a and Cu_A should eventually redistribute in accord with the equilibrium potentials. Antalis and Palmer report no such redistribution, even though they follow their reactions for several seconds.

There is one report of such a redistribution in an experiment in which cytochrome *c* oxidase was reduced by pulse radiolysis through the mediation of cytochrome *c* (Van Buuren et al., 1974). In the first part of the reaction, cytochrome *c* oxidase accepted electrons from cytochrome *c* at a rate of about 6×10^7 $M^{-1}s^{-1}$. In this phase, two equivalents of ferrocytochrome *c* were oxidized for every equivalent of Fe_a reduced. This was followed by a phase in which there was very little additional oxidation of cytochrome *c*, but the reduction level at Fe_a doubled. The authors interpreted these results as 1) the fast reduction of both Fe_a and Cu_A to approximately the same extent, followed by 2) a slower redistribution of electrons to the thermodynamically predicted distribution. The authors also note that the redistribution occurred on a time scale of hundreds of milliseconds and would be too slow to have a role in turnover. This redistribution could occur either because of a slow change in the redox potentials of Fe_a and Cu_A or because these two metal centers were each reduced rapidly but independently, and then the electron populations equilibrated via a slow Fe_a -- Cu_A electron transfer. The latter explanation

requires the assumption that Fe_a or Cu_A do not equilibrate via cytochrome *c* . It should be noted that the experiment was performed in a low ionic strength buffer (5mM phosphate), in the presence of 40 mM methanol.

In all the above experiments, Fe_a and Cu_A appeared to reduce synchronously. However, other workers have reported experiments in which this was not the case. Wilson et al. (1975) reported a stopped flow study in which cytochrome *c* oxidase was reduced by ferrocytochrome *c* , in the presence of oxygen. At lower concentrations of cytochrome*c* plots of $\Delta A(550)$ (oxidation of cytochrome *c*) v. $\Delta A(605)$ (reduction of Fe_a) were linear. As the concentration of cytochrome *c* , and hence the rate of the reaction, was increased, the curve became nonlinear. Relatively more Fe_a was reduced at the beginning of the reaction and less toward the end. This kind of nonlinearily could arise in two ways, either if the reduction of Fe_a was followed by a slower intramolecular reduction of Cu_A or, as described above, if Fe_a and Cu_A were in fast equilibrium, but the potential of Cu_A was significantly lower than that of Fe_a. The fact that the non-linearity occurred only at the faster rates suggests that it is kinetic and not thermodynamic in nature. The stoichiometry of the complete reaction was constant, shown by the fact that the linear and nonlinear traces both came to the same endpoint.

Parallel experiments were also carried out at higher enzyme concentrations where the 830 nm band could be observed. In these experiments, the absorbance changes at 830 nm sometimes lagged behind the absorbance changes at 605 nm but were never faster. In fact, the authors reported that at high concentrations of cytochrome *c*, the disppearance of the

830 nm band proceeded at a rate which was independent of the cytochrome *c* concentration and had a half time of about 8 ms (Wilson et al., 1975).

A similar delay between the reduction of Fe_a and Cu_A has been observed when the cytochrome *c* oxidase was reduced with phenazine methosulfate (PMS) under anaerobic conditions (Halaka et al., 1984). In these experiments, Fe_a was reduced with a second order rate of 3×10^5 $M^{-1}s^{-1}$, but a definite lag phase was observed in the reduction of Cu_A (followed at 830 nm), and a rate of about 20 s^{-1} for the Fe_a to Cu_A electron transfer rate was resolved by simulating the kinetics of the system. This rate was not signficantly concentration dependent (Barnes, 1986). The lack of concentration dependence argues against a thermodynamic explanation for the lag between the reduction of Fe_a and Cu_A.

Greenwood et al. (1976) reported a temperature-jump experiment in which a sample containing CO inhibited cytochrome *c* oxidase and cytochrome*c* was poised at a reduction level at which the cytochrome*c* , Fe_a and Cu_A were all partially reduced. A sudden increase in temperature was followed by an electron redistribution from Fe_a to cytochrome *c* . The relaxation was biphasic. The two phases were interpreted to be 1) a fast reëquilibration between Fe_a and cytochrome *c*, followed by 2) a slower reëquilibration involving Cu_A as well. The fast phase was analyzed to give electron transfer rates of 9×10^{-6} $M^{-1}s^{-1}$ from cytochrome *c* to Fe_a, and 8.5×10^{-6} $M^{-1}s^{-1}$ for the reverse reaction. The slower phase, which was also somewhat concentration dependent, had a relaxation time constant of 40 to 100 s^{-1}. This was inferred to be the Fe_a -- Cu_A electron equilibration rate. As discussed above, the reduction of Fe_a by cytochrome *c* has itself been shown to

be biphasic (Antalis and Palmer, 1982). Therefore, it is possible that the biphasic behavior observed in this T-jump experiment does not arise from slow Fe_a -- Cu_A redox equilibration.

The only direct measurement of the Fe_a -- Cu_A electron transfer rate comes from a study of electron redistribution after photolysis of the CO mixed valence (COMV) compound. The COMV is a form of the enzyme in which the metal centers of the oxygen binding site are reduced, with CO bound to $Fe_{a_3}{}^{2+}$, while Fe_a and Cu_A remain oxidized. When $Fe_{a_3}{}^{2+}$–CO was photolyzed in the absence of oxygen, the CO rebinds at a rate of about 66 s^{-1} (Boelens et al., 1982). A redistribution of electrons was observed between the photolysis and the time that CO recombined with $Fe_{a_3}{}^{2+}$ (Brzezinski et al., 1987, Boelens et al., 1982). First, a subpopulation of Cu_A became reduced at a rate of about 14,200 s^{-1}, and then, a subpopulation of Fe_a was reduced at a rate of about 500 s^{-1} (Brzezinski et al., 1987). The reduction of Cu_A has also been reported by Boelens et al. (1982) and it is generally agreed to be a fast electron transfer from the oxygen binding site. Fe_a could be reduced either by an electron transfer from the newly reduced Cu_A, or by a direct electron transfer from the oxygen binding site. Brzezinski et al. (1987) preferred the former interpretation. Both the rate and the extent of reduction of Fe_a were found to be strongly pH dependent, the rate decreasing, and the extent of reduction increasing with increasing pH. From the extents of reduction at both metal sites, the forward (Fe_a to Cu_A) and backward rates were calculated to be: k_f = 400 s^{-1} and k_r = 120 s^{-1} (at pH 7.4). The authors point out that the forward rate is faster that the turnover rate of the enzyme, which under these conditions is about 50 s^{-1}.

Thus, rates ranging from 20 s^{-1} (Halaka et al., 1984) to over 600 s^{-1} (Antalis and Palmer, 1982) have been measured for the Fe_a to Cu_A electron transfer rate, in a variety of states of the enzyme, and using a variety of techniques. Some of these results appear to be contradictory, and none of them are completely unambiguous. The goal of the present work was to measure this rate directly using a perturbed equilibrium approach similar to that of Greenwood et al. (1976).

3. Perturbed-equilibrium kinetic measurements.

The investigations of electron transfer between Fe_a and Cu_A presented in this thesis all involve perturbed-equilibrium measurements. Such measurements are made by poising the experimental system at an equilibrium position, rapidly changing the sample conditions so as to move the position of this equilibrium, and following the kinetics as the system relaxes into its new equilibrium. This method has the advantage that it can be used to study systems such as intramolecular equilibria fairly directly. One disadvantage is that the size of the equilibrium shift can be small.

For simple $A \leftrightarrow B$ systems such as the intramolecular transfer of an electron between two metal centers, the first-order relaxation rate observed is the sum of the forward and backward rate constants. The analysis of relaxation rates for more complicated systems involving multiple components is discussed by Hiromi (1979). In what follows, I will discuss the application of this technique to the Fe_a --Cu_A electron equilibration in terms of the physical chemistry of the enzyme.

4. Applying perturbed equilibrium methods to the Fea --CuA electron transfer.

The ideal system in which to study the Fe_a -- Cu_A electron equilibration would be one in which Fe_a and Cu_A in each molecule made up an electronically isolated pair, exchanging electrons with each other, but unable to accept or donate to any other metal center. There would not be electron exchange with the metal centers of the oxygen binding site, or between molecules. Each Fe_a, Cu_A pair would share one electron so that a shift in equilibrium constant would produce the maximum population change. These conditions can be approximated fairly closely in a real system, by starting with the carbon monoxide-mixed-valence (COMV) compound of the enzyme, in which the metal centers of the oxygen binding site are both reduced, and then adding in one more electron equivalent to be shared between the two low potential metal centers. In the following section, I will discuss the preparation and properties of this CO-mixed-valence-plus-one-electron (COMV+1) system in terms of the physical chemistry and enzymology of cytochrome *c* oxidase. (This COMV+1 system has been used in magnetic resonance studies by Brudvig et al., 1984 and in low temperature "triple trapping" studies by Blair et al., 1985.)

The carbon monoxide mixed valence compound. When the metal centers of the oxygen binding site (Fe_{a_3} and Cu_B) are both reduced, carbon monoxide will bind to $Fe_{a_3}{}^{2+}$. With carbon monoxide bound, $Fe_{a_3}{}^{2+}$ and $Cu_B{}^{+}$ behave as a cooperative, two-electron donor with very high potential (Lindsay et al., 1975). The redox potentials of Fe_a and Cu_A are much lower than those of the CO-

inhibited oxygen binding site, and this difference in redox potentials makes it possible to prepare a mixed valence form of the enzyme in which Fe_{a_3} and Cu_B are in the reduced form, and Fe_a and Cu_A are both oxidized. The nature of this CO-mixed valence (COMV) compound is clearly illustrated by the classical proceedure for its preparation (Greenwood et al., 1974): The enzyme is first reduced fully using a small excess of reductant. CO is then added, and finally, a small excess of ferricyanide is added as an oxidant. The ferricyanide reoxidizes Fe_a and Cu_A virtually completely, but the redox potential of the CO-bound oxygen binding site is sufficiently high that the ferricyanide will not reoxidize Fe_{a_3} and Cu_B. One drawback to this method of preparation is that $Fe_{a_3}{}^{2+}$-CO is photolabile, and when the sample is illuminated, $Fe_{a_3}{}^{2+}$ and $Cu_B{}^{+}$ will donate electrons to ferricyanide.

Fortunately, the COMV compound can be prepared without addition of a chemical oxidant by incubating the resting (fully oxidized) form of the enzyme under an anaerobic CO atmosphere at room temperature for about eight hours. Apparently, reduction of Fe_{a_3} and Cu_B occurs by means of a water-gas shift type reaction in which carbon monoxide is oxidized to carbon dioxide (Bickar et al., 1984). A second molecule of carbon monoxide then binds to $Fe_{a_3}{}^{2+}$. The COMV compound made in this way is also photolabile, but in the absence of a high potential electron acceptor the electrons remain in the enzyme and the CO can rebind to $Fe_{a_3}{}^{2+}$ (Boelens and Wever, 1979; Boelens and Wever, 1980; Boelens et al., 1982.)

Fe_a--Cu_A electron equilibrium in the CO mixed valence compound. The redox potentials of Fe_a and Cu_A in the CO-inhibited enzyme are very similar. At 25°C, the potentials are approximately 288 mV (v. NHE), for Fe_a (when Cu_A is oxidized), and 276 mV for Cu_A (when Fe_a is oxidized, see below; Wang et al., 1986; Ellis et al., 1986). This translates into an equilibrium constant of 0.68 for electron distribution between the two metal centers. Thus, when one electron equivalent of reductant is added to a sample of the CO-mixed valence (COMV) compound, both Fe_a and Cu_A become partially reduced. This "CO mixed valence-plus-one-electron" (COMV+1) sample will contain four subpopulations: 1) a COMV population, in which Fe_a and Cu_A are both in the oxidized form; 2) a three electron reduced population in which Fe_a is reduced, and Cu_A is oxidized; 3) a three electron reduced population in which Cu_A is reduced and Fe_a is oxidized; and 4) a fully reduced (COFR) population in which both Fe_a and Cu_A are in the reduced form (see figure I.1). All of these species will be in equilibrium through intermolecular elecron exchange, but the two three electron reduced populations, 2) and 3) will also be in equilibrium through an intramolecular electron transfer between Fe_a and Cu_A. This intramolecular electron transfer is the process of interest in this study. In principle, it should be possible to measure the rate of this process by causing a sudden shift in the redox potential difference between Fe_a and Cu_A, and observing the reëquilibration between populations 2) and 3) above. In the absence of an electron mediator, this intramolecular electron exchange would be expected to be much faster than the exchange of electrons between enzyme molecules. If there is reason to believe that the observed process is an intermolecular one, this question can be addressed experimentally since an

Figure I.1.

The redox equilibria in CO inhibited cytochrome *c* oxidase. The transitions which must occur through intermolecular processes are indicated by broken arrows. The solid arrows indicate the intramolecular Fe_a -- Cu_A redox equilibrium.

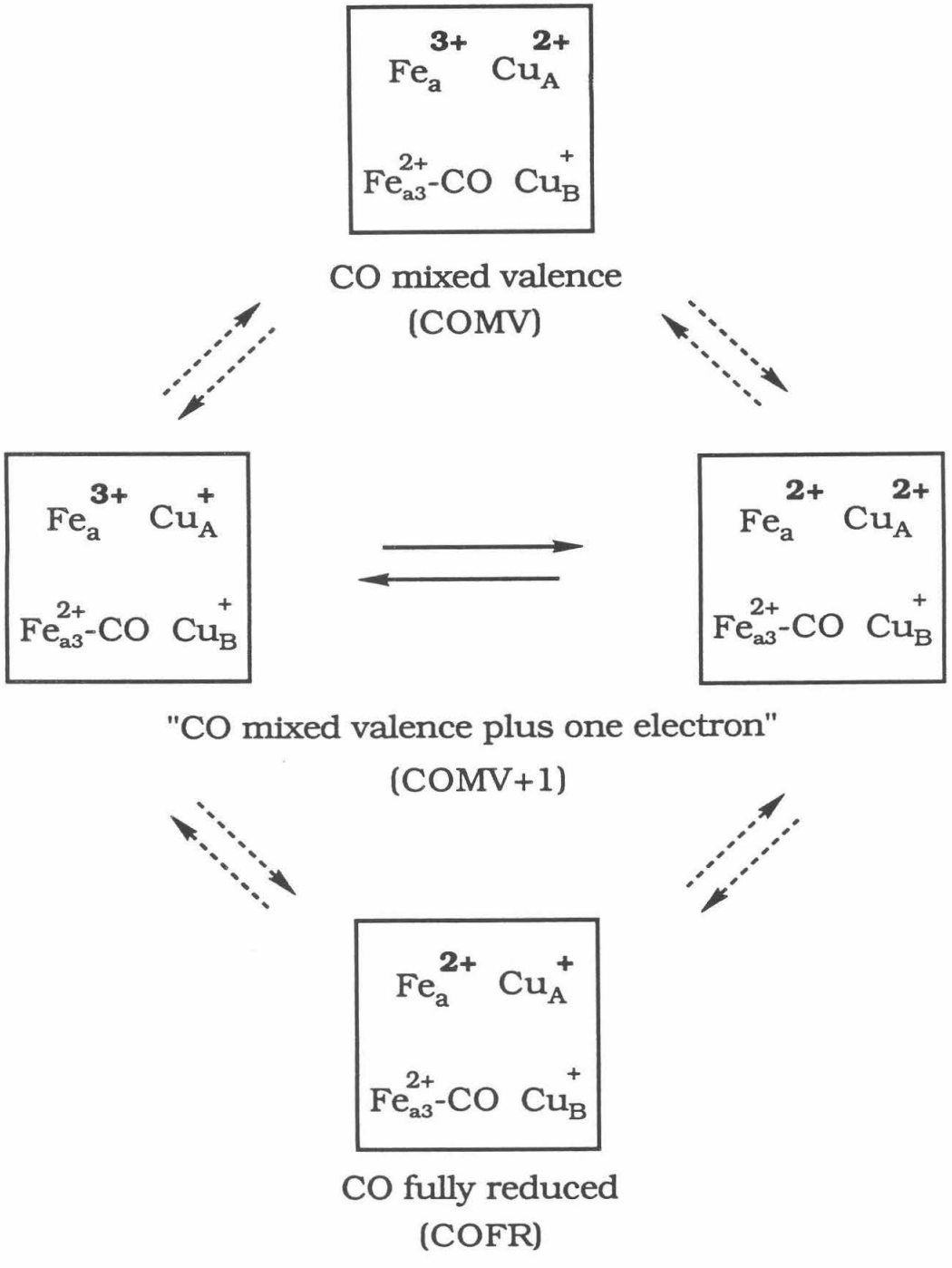
Fe_a^{3+} Cu_A^{2+}
Fe_{a3}^{2+}-CO Cu_B^{+}
CO mixed valence
(COMV)
Fe_a^{3+} Cu_A^{+}
Fe_{a3}^{2+}-CO Cu_B^{+}
Fe_a^{2+} Cu_A^{2+}
Fe_{a3}^{2+}-CO Cu_B^{+}
"CO mixed valence plus one electron"
(COMV+1)
Fe_a^{2+} Cu_A^{+}
Fe_{a3}^{2+}-CO Cu_B^{+}
CO fully reduced
(COFR)

intermolecular process should vary as a function of concentration while an intramolecular process should not. (The concentration dependence was not studied in these experiments because the exchange of electrons between cytochrome *c* oxidase molecules is known to be slow; Antonini et al., 1970.)

The amplitude of the observed reëquilibration will depend on the size of this three electron reduced subpopulation in the sample. One factor which contributes to the size of the three electron reduced subpopulation is that there is a redox anticoöperativity of about 40 mV between the Fe_a and Cu_A; when Fe_a is reduced, the redox potential of Cu_A is lowered by 40 mV and vice versa (Ellis et al., 1986, Wang et al., 1986; redox anticooperativity is discussed in detail by Blair et al., 1986.) The result of this anticoöperativity is that even though the upper asymptotic redox potentials of Fe_a and Cu_A in the CO-inhibited enzyme are almost identical, the entry of a second electron into the low-potential metal centers is energetically much less favorable that the entry of the first electron. This has the effect of increasing the subpopulation of three electron reduced enzyme at the expense of the two- and four-electron reduced subpopulations. Without this anticoöperativity, 50% of the molecules in a COMV+1 sample would be at the three electron level of reduction. Because of the anticoöperativity, this number is expected to be 69% (see Copeland et al., 1987).

Perturbing the Fe_a --Cu_A equilibrium. As described above, COMV+1 sample contains a large subpopulation of enzyme molecules in which there is an intramolecular redox equilibrium between Fe_a and Cu_A. It should be possible to measure the rate of this equilibration by making a small sudden shift in the equilibrium and following the relaxation kinetics of the system.

In the experimental part of this thesis, two approaches to perturbing this equilibrium are presented. In chapter II an experiment is described in which the $Fe_{a_3}{}^{2+}$-CO at the oxygen binding site is photolyzed by a brief laser flash. Although Fe_a and Cu_A are not involved in the binding of CO, and in fact, are some distance from the oxygen binding site (Goodman and Leigh, 1987; Brudvig et al., 1984), changes in the optical spectrum indicate that photolysis of $Fe_{a_3}{}^{2+}$-CO is followed by a fast electron reëquilibration from Fe_a to Cu_A (k_{app} = 17,200 s^{-1}). The mechanism by which an event at the oxygen binding site could cause a change in the potentials of Fe_a and Cu_A is unknown, but presumably a protein conformational change is involved. (The events surrounding the photolysis of $Fe_{a_3}{}^{2+}$-CO have been studied extensively by Fiamingo et al., 1982; Boelens and Wever, 1979; Boelens and Wever, 1980; Boelens et al., 1982).

In chapter III a temperature-jump approach to the study of this same equilibrium is presented. For such an experiment to work, the difference between the redox potentials of Fe_a and Cu_A must change with temperature. Ellis et al. (1986) and Wang et al. (1986) have measured the redox potentials of Fe_a and Cu_A in the COMV compound as a function of temperature, but their results are not sufficiently precise to decide whether this experiment would be possible. (In fact, their mean values predict a change which would be too small to measure.) In the present experiments, it has been shown that when the temperature of a COMV+1 sample is raised, the distribution of electrons shifts to favor Cu_A. This population change is large enough that it should be feasible to observe it using the T-jump apparatus. Thus far the reëquilibration has not been unambiguously observed in the T-jump apparatus, but the

experiment is still in progress. As a side benefit, these experiments have shown that the spectral band shifts which have been observed upon raising the temperature of cytochrome *c* oxidase (Orii and Miki, 1979) occur very quickly ($k_{app} > 20{,}000\ s^{-1}$). In chapter IV, a similar temperature-jump study on the cyanide inhibited compound of the enzyme is reported.

References.

Andréasson, L.E., Malmström, B.G., Strömberg, B.G. and Vänngård, T. (1972)*FEBS Lett.* **28**, 297-301.

Andreev, I.M., Myakotina, O.L., Popova, E.Yu. and Konstantinov, A.A. (1983) *Biokhimiya*, **48**, 219-223.

Antalis, T.M. and Palmer, G. (1982) *J. Biol. Chem.* **257**, 6194-6206.

Antonini, E., Brunori, M., Colosimo, A., Greenwood, C. and Wilson, M.T. (1977) *Proc. Natl. Acad. Sci. U.S.A.* **74**, 3128-3132.

Antonini, E., Brunori, M., Greenwood, C. and Malmström B.G. (1970) *Nature*, **228**, 936-937.

Armstrong, F., Shaw, R.W. and Beinert, H. (1983) *Biochim. Biophys. Acta*, **722**, 61-71.

Babcock, G.T., Callahan, P.M., Ondrias, M.R. and Salmeen, I. (1981) *Biochemistry*, **20**, 959.

Barnes, Z.K. (1986) Ph.D. Thesis, Michigan State University.

Beinert, H., Hansen, R. and Hartzell, C.R. (1976) *Biochim. Biophys. Acta*, **423**, 339-355.

Beinert, H., Hansen, R. and Hartzell, C.R. (1980) *Biochim. Biophys. Acta*, **591**, 458-470.

Bickar, D., Bonaventura, C. and Bonaventure, J. (1984) *J. Biol. Chem.* **259**, 10777-10783.

Blair, D.F., Bocian, D.F., Babcock, G.T. and Chan, S.I. (1982) *Biochemistry*, **21**, 6928-6935.

Blair, D.F., Ellis, W.R. Jr., Wang, H., Gray, H.B. and Chan, S.I. (1986) *J. Biol. Chem.* **261**, 11524-11537.

Blair, D.F., Martin, C.T., Gelles, J., Wang, H., Brudvig, G.W., Stevens, T.H. and Chan, S.I. (1983) *Chem. Scr.* **21**, 43-53.

Blair, D.F., Witt, S.F. and Chan, S.I. (1985) *J. Am. Chem. Soc.* **107**, 7389-7399.

Boelens, R. and Wever, R. (1979) *Biochim. Biophys. Acta*, **547**, 296-310.

Boelens, R. and Wever, R. (1980) *FEBS Lett.* **116**, 223-226.

Boelens, R., Wever, R. and Van Gelder, B.F. (1982) *Biochim. Biophys. Acta*, **682**, 264-272.

Brudvig, G.W., Blair, D.F. and Chan, S.I. (1984) *J. Biol. Chem.* **17**, 11001-11009.

Brudvig, G.W., Stevens, T.H. and Chan, S.I. (1980) **19**, 5275-5285.

Brudvig, G.W., Stevens, T.H., Morse, R.H. and Chan, S.I. (1981) *Biochemistry*, **20**, 3912-3921.

Brunori, M., Antonini, E. and Wilson, M.T. (1981) in *Metal Ions In Biological Systems*, (H. Sigel, ed.) vol. 13. pp. 187-228.

Brunori, M. and Gibson, Q.H. (1983) *EMBO J.* **2**, 2025-2026.

Brzezinski, P. and Malmström, B.G. (1987) *Biochim. Biophys. Acta*, **894**, 29-38.

Brzezinski, P., Thörnström, P.E. and Malmström, B.G. (1986) *FEBS Lett.* **194**, 1-5.

Capaldi, R.A., Darley-Usmar, V., Fuller, S. and Millett, F. (1982) *FEBS Lett.* **138**,

1-7.

Chan, S.I., Li, P.M., Nilsson, T., Gelles, J., Blair, D.F. and Martin, C.T. (1987) in *Proc. of the Fourth Int. Conf. on Oxidases.*

Chance, B., Saronio, C. and Leigh, J.S. (1979) *Biochem. J.* **177**, 931-941.

Colosimo, A., Brunori, M., Sarti, P., Antonini, E. and Wilson, M.T. (1981) *Israel J. Chem.* **21**, 30-33.

Copeland, R.A., Smith, P.A., Chan, S.I. (1987) *Biochemistry*, **26**, 7311-7316.

Ellis, W.R. Jr., Wang, H.W., Blair, D.F., Gray, H.B. and Chan, S.I. (1986) *Biochemistry*, **25**, 161-167.

Ferguson-Miller, S., Brautigan, D.L. and Margoliash, E. (1976) *J. Biol. Chem.* **251**, 1104-1115.

Fiamingo, F.G., Altschuld, R.A., Moh, P.P. and Alben, J.O. (1982) *J. Biol. Chem.* **257**, 1639-1650.

Finel, M. and Wikström, M. (1986) *Biochim. Biophys. Acta*, **851**, 99-108.

Georgevich, G., Darley-Usmar, V.M. and Capaldi, R.A. (1983) *Biochemistry*, **22**, 1317-1322.

Gibson, Q.H. and Greenwood, C. (1963) *Biochem. J.* **86**, 541-554.

Gibson, Q.H., Greenwood, C., Wharton, D.C. and Palmer, G. (1965) *J. Biol. Chem.* **240**, 888-894.

Goodman, G. (1984) *J. Biol. Chem.* **259**, 15094-15099.

Goodman, G. and Leigh, J.S. Jr. (1985) *Biochemistry*, **24**, 2310-2317.

Goodman, G. and Leigh, J.S. Jr. (1987) *Biochim. Biophys. Acta*, **890**, 360-367.

Greenwood, C., Brittain, T., Wilson, M. and Brunori, M. (1976) *Biochem. J.* **157**, 591-598.

Greenwood, C., Wilson, M.T. and Brunori, M. (1974) *Biochem. J.* **137**, 205-215.

Halaka, F.G., Barnes, Z.K., Babcock, G.T. and Dye, J.L. (1984) *Biochemistry*, **23**, 2005-2011.

Haltia, T., Puustinen, A. and Finel, M. (1988) *Eur. J. Biochem.* in press.

Hill, B.C. and Greenwood, C. (1984a) *Biochem. J.* **218**, 913-921.

Hill, B.C. and Greenwood, C. (1984b) *FEBS Lett.* **166**, 362-366.

Hill, B.C., Greenwood, C. and Nicholls, P. (1986) *Biochim. Biophys. Acta*, **853**, 91-113.

Hiromi, K. (1979) *Kinetics of Fast Enzyme Reactions*, N.Y., Halsted Press.

Holm, L., Saraste, M. and Wikström, M. (1987) *EMBO J.* **6**, 2819-2823.

Li, P.M., Gelles, J., Chan, S.I., Sullivan, R.J. and Scott, R.A. (1987) *Biochemistry*, **26**, 2091-2095.

Li, P.M., Morgan, J.E., Nilsson, T., Ma, M. and Chan, S.I. (1988) *Biochemistry*, in press.

Lindsay, J.G., Owen, C.S. and Wilson, D.F. (1975) *Arch. Biochem. Biophys.* **169**, 492-505.

Martin, C.T. (1985) Ph.D. Thesis, California Institute of Technology, Pasadena, CA.

Martin, C.T., Scholes, C.P. and Chan, S.I. (1988) *J. Biol. Chem.* in press.

Moroney, P.M., Scholes, T.A. and Hinkle, P.C. (1984) *Biochemistry*, **23**, 4991-4997.

Ohnishi, T., Harmon, H.J. and Waring, A.J. (1985) *Biochem. Soc. Trans.* **13**, 607-611.

Orii, Y. and Miki, T. (1979) in *Cytochrome Oxidase*, (T.E. King et al., eds.) Elsevier/North-Holland Biomedical Press, pp. 251-256.

Peisach, J. (1978) in *Frontiers of Biological Energetics*, Vol. 2, (P.L. Dutton, J.S. Leigh and A. Scarpa, Eds.) pp. 873-881.

Powers, L., Blumberg, W.E., Chance, B., Barlow, C.H., Leigh, J.S. Jr., Smith, J., Yonetani, T., Vik, S. and Peisach, J. (1979) *Biochim. Biophys. Acta*, **546**, 520-538.

Raitio, M., Jalli, T. and Saraste, M. (1987) *EMBO J.* **6**, 2825-2833.

Sarti, P., Jones, M.G., Antonini, G., Matatesta, F., Colosimo, A., Wilson, M.T. and Brunori, M. (1985) *Proc. Natl. Acad. Sci. U.S.A.* **82**, 4876-4880.

Sinjorgo, K.M.C., Steinebach, O.M., Dekker, H.L. and Muijsers, A.O. (1986) *Biochim. Biophys. Acta*, **850**, 108-115.

Smith, L. (1955) in *Methods in Biochemical Analysis*, Vol. 2, (D. Glick, Ed.)

Speck, S.H., Dye, D. and Margoliash, E. (1984) *Proc. Natl. Acad. Sci. U.S.A.* **81**, 347-351.

Stevens, T.H. and Chan, S.I. (1981) *J. Biol. Chem.* **256**, 1069-1071.

Stevens, T.H., Brudvig, G.W., Bocian, D.F. and Chan, S.I. (1979) *Proc. Natl. Acad. Sci. U.S.A.* **76**, 3320-3324.

Taniguchi, V.T., Ellis, W.R. Jr., Cammarata, V., Webb, J., Anson, F.C. and Gray, H.B. (1982) in *Electrochemical and Spectrochemical Studies of Biological Redox Components* (Kadish, K.M., ed) pp. 51-68, American Chemical Society Advances in Chemistry Series 201, Washington D.C. Wiley, N.Y., pp. 427-434.

Thörnström, P.E., Brzezinski, P., Fredriksson, P.O. and Malmström, B.G. (1988) *Biochemistry*, **27**, 5441-5447.

Van Buuren, K.J.H., Van Gelder, B.F., Wilting, J. and Braams, R. (1974) *Biochim. Biophys. Acta*, **333**, 421-429.

Vanneste, W.H. (1966) *Biochemistry*, **5**, 838-848.

Wang, H., Blair, D.F., Ellis, W.R. Jr., Gray, H.B. and Chan, S.I. (1986)*Biochemistry*, **25**, 167-171.

Wikström, M.K.F. (1977) *Nature*, **266**, 271-273.

Wikström, M. (1981) in *Interaction Between Iron and Proteins in Oxygen and Electron Transport*, (C. Ho and W.C. Eaton, eds), Elsevier, New York.

Wikström, M. and Casey, R.P. (1985) *J. Inorg. Biochem.* **23**, 327-334.

Wikström, M., Krab, K. and Saraste, M. (1981) *Cytochrome Oxidase, A Synthesis*, Academic Press, New York.

Wikström, M., Sataste, M. and Penttilä, T. (1984) in *The Enzymes of Biological Membranes*, vol. 4. (A.N. Martonosi, ed.), Plenum.

Wilson, M.T., Greenwood, C., Brunori, M. and Antonini, E. (1975) *Biochem. J.* **147**, 145-153.

Wilson, M.T., Lalla-Maharajh, W., Darley-Usmar, V., Bonaventura, J., Bonaventura, C.and Brunori, M. (1980) *J. Biol. Chem.* **255**, 2722-2728.

Witt, S.N. (1988) Ph.D. Thesis, California Institute of Technology, Pasadena, CA.

Chapter II

Flash Photolysis Studies of the Electron Equilibration Between Cytochrome *a* and Copper A

Introduction.

The last chapter described the preparation of three electron reduced, CO inhibited samples of cytochrome *c* oxidase in which the Fe_a -- Cu_A electron equilibration rate could be studied by perturbed equilibrium methods. In this chapter the first of two experiments designed to shift this redox equilibrium and measure the rate of reëquilibration is described. In this experiment the Fe_a -- Cu_A redox equilibrium was perturbed by photolyzing $Fe_{a_3}{}^{2+}$–CO in the oxygen binding site. Between the time that CO was photolyzed, and when it recombined a few milliseconds later, a fast electron redistribution from Fe_a to Cu_A was observed.

Materials and Methods.

Materials. Cholic acid from U.S. Biochemical was purified by three-fold recrystallization from 50:50 water-ethanol. NADH pre-weighed in vials was obtained from Sigma. Sephadex G-200 (particle size 40-120 μM) was obtained both from Sigma and Pharmacia. Sodium dithionite was obtained from GFS Chemicals. Tween-20 for general use (dialysis buffers used in the prep. etc.) was obtained from Sigma. Purified Tween-20 as a 10% aqueous solution, stored under nitrogen in sealed vials, was obtained from Pierce. Argon for anaerobic work was made oxygen free by passing it through a column of manganese oxide on vermiculite. Carbon monoxide from Matheson ("Matheson Purity") was used without further purification.

Cytochrome *c* oxidase was isolated by the method of Hartzell and Beinert (1974). The procedure consists of two detergent solubilizations followed by an ammonium sulfate precipitation. The first detergent (Triton X-114) removes cytochrome bc_1 and some other proteins from the mitochondrial membranes but does not solubilize the oxidase. The second detergent (sodium cholate) solubilizes the membranes and the oxidase along with them. The enzyme is then isolated by means of a series of ammonium sulfate precipitations. Finally, the enzyme is dialyzed against buffer to remove the ammonium sulfate, and then frozen and stored at -80°C in small vials until used.

Enzymatic activity was assayed by spectrophotometrically monitoring ferrocytochrome *c* oxidation (Smith, 1955).

Horse heart cytochrome *c* (Type VI) was obtained from Sigma and generally used without further purification. However, cytochrome *c* which was used in the preparation of the cytochrome *c* --cytochrome *c* oxidase high affinity complex ("caa_3 complex") was purified by ion exchange chromatography by the procedure of Brautigan et al. (1978).

Preparation of the cytochrome c*--cytochrome* c *oxidase high affinity complex.* Under conditions of low ionic strength, cytochrome *c*, and cytochrome *c* oxidase form a high affinity complex (Kuboyama et al., 1962; Veerman et al., 1980; Hill and Nicholls, 1980). The caa_3 complex used in these experiments was made by a modification of the method of Kuboyama et al. (1962). The principle of the preparation is as follows: The two enzymes are first mixed together, with cytochrome *c* in excess, in a buffer of medium ionic strength in which complex formation is minimal. After gentle sonication to break up aggregated enzyme, the mixture is dialyzed into a buffer of low ionic

strength in which the complex forms. Finally, the complex is resolved from excess cytochrome *c* by gel (size exclusion) chromatography.

Cytochrome *c* and cytochrome *c* oxidase were first mixed in a 4:1 equivalent ratio in buffer of moderate ionic strength (50-100 mM buffer.) Tween-20 (purified 10% solution, see above) was added to bring the total concentration to 1% (see Veerman et al., 1980). Kuboyama et al. (1962) report the use of buffers containing only 0.1% Emasol No. 1130, which is identical to Tween-20. However, our experience has been that the caa_3 complex is better solubilized in 1% Tween-20, and that even with a detergent concentration of 0.5%, it tends to precipitate. After the addition of detergent, the headspace over the mixture was flushed with argon in order to minimize oxidation during the sonication step, and the tube capped. The mixture was then sonicated for about ten minutes using a bath sonicator (Lab Supplies Co. model G11SP1T) containing crushed ice and water. After sonication, the mixture was dialyzed against low ionic strength buffer (5 mM Na phosphate, 1.0% Tween-20, pH 7.0 or 7.4) for 4 to 6 hours (VWR 12,000-14,000 MWCO dialysis tubing), centrifuged (30 min, 15K RPM, Sorvall SS34 rotor) to remove precipitated protein and then eluted through a column of Sephadex G-200 (40-120 μM particle size, column height: 13 cm) with a similar buffer. The flow rate was about 5 mlh^{-1}, and was controlled by passing the effluent through a length of narrow column tubing (Intramadic PE-10.) Fractions were collected and the relative amounts of cytochrome *c* and cytochrome *c* oxidase determined from their visible spectra in the reduced form. For this purpose, samples were diluted into a strong buffer (0.5 M Tris-Cl or NaMOPS) and solid sodium dithionite was added to reduce the samples. They were not made anaerobic beforehand. Visible

spectra for this purpose were measured on a Beckman DU-7 spectrophotometer. All procedures leading to experimental samples were carried out at 4°C, but the *c:aa3* assay was performed at room temperature.

Sample Preparation. Samples for kinetic studies were prepared in concentrated form at pH 7.4 and then diluted as necessary to achieve the desired concentration and pH. The CO-mixed valence (COMV) compound was made by incubating the resting enzyme under CO at room temperature for about eight hours (see Bickar et al., 1984). These samples could then be diluted into buffers of various pH values. This transfer was performed aerobically. The enzyme became reoxidized, but once the solution was made anaerobic again, with CO, the COMV compound was regenerated within minutes. The original formation of COMV compound from resting enzyme requires hours at room temperature and is very slow at lower temperatures, but once the enzyme has been reduced and reoxidized, the regeneration of the COMV compound takes only a few minutes, even at ice temperature (Nicholls and Chanady, 1981; Morgan et al. 1985).

The three electron reduced CO inhibited (COMV+1) samples were made as follows. 1) The CO-mixed valence compound was made as described above. 2) One electron equivalent of NADH solution was added aerobically. 3) The sample was made anaerobic again with CO. 4) The sample was incubated in the refrigerator until it was three-electrons reduced (usually about 12 hours). The level of reduction was estimated from the sample's visible spectrum. (In practice, the three-electron level of reduction was only a target. What was important was that the sample contain a significant population of the three-

quarter reduced species.) 5) The three-electron reduced sample was diluted anaerobically into CO containing buffer of the desired final pH.

When the NADH was added, there was enough air in the solution to reoxidize the enzyme. In spite of this, it was only neccessary to add one electron-equivalent of NADH to reach the three-electron reduction level. As described above, when the sample was made anaerobic again with CO, the COMV compound was regenerated within minutes. This regeneration occurred much more quickly than the reduction of the enzyme by NADH. Thus, Fe_{a_3} and Cu_B were reduced quickly -- presumably by CO -- leaving only the low-potential metal centers to be reduced by NADH.

The anaerobic dilution of the COMV+1 samples was accomplished by transferring the concentrated sample into a cell containing anaerobic diluting buffer. The transfer was carried out by syringe, under argon-flush, in the dark. First, the diluting buffer was made anaerobic and saturated with CO. Next, both the sample cell and the cell containing the dilution buffer were attached to the vacuum line with "argon flush" adapters. These fittings provide an opening into the anaerobic cell, while the atmosphere in the cell is guarded by a counterflow of anaerobic gas. Although both the sample and the diluting buffer were under CO atmosphere, an argon, not CO, flush was used for the transfer (we're not that crazy!) A gas tight syringe (Hamilton, Reno, NV) with a very long needle was used to transfer the sample. Once the enzyme solution had been transferred, the dilute solution was de-aerated once with argon and five times with CO before the lights were turned back on.

We found that the purity of Tween-20 used in the diluting buffer was critical. Unless specially purified Tween-20 (see above) was used, the samples

reoxidized upon dilution. In the case of the COMV compound, this was not a problem since under an atmosphere of CO, the COMV compound was regenerated after oxidation. However, in the case of the COMV+1 samples this had the effect of converting them to the COMV compound. The fully reduced CO inhibited compound was prepared in the same way as the COMV+1, except that about twice as much NADH was added. Reduction with a large excess of reductant (NADH or sodium dithionite) was not workable since these reductants absorb strongly at the wavelength of the laser.

Visible spectra of the samples were measured before and after the kinetic experiments. In most cases, some increase in the level of reduction was observed, presumably due to photoreduction. After all other measurements were finished, the samples were opened to air and their pH measured.

Continuous Illumination Measurements. Visible spectra were recorded under continuous illumination conditions using a modified Beckman Acta CIII spectrophotometer. A helium-cadmium laser (Liconix 4240NB) operated at 445 nm was used for illumination. The laser beam was made collinear with the spectrophotometer sample beam using a dichroic mirror (Chorion). In order to superimpose the laser beam onto the probe beam slit profile, the laser was diffused to a circle the size of the slit height using a concave lens, and then refocused onto the slit profile with a cylindrical lens. The laser beam was antiparallel to the probe beam. The spectrophotometer was operated in dual beam mode. The reference and sample beam exit windows from the sample chamber were covered by 500 nm cutoff filters to keep the laser light out of the PMT.

Kinetic Measurements. Transient changes in absorbance after photolysis were measured as follows: (See figure II.1 for a block diagram of the optical bench.) Photolysis was accomplished with 337 nm pulses from a N_2 laser (Photochemical Research Associates LN1000) run at a repetition rate of 5 Hz. The photolyzing laser pulses had an energy of about 1.0 mJ with a temporal pulse width of about 0.6 ns. The laser beam was made colinear with the probe light beam (in the opposite direction) by means of a dichroic mirror and was focused to a spot size of about 2 mm. Probing light was produced by a 75 W tungsten lamp powered by a regulated DC power supply (Kikusui Electronics PAD). The light from the tungsten lamp was passed through filters, the sample, filters, and then focused into a 0.25 m monochromator (Jarrell-Ash 82-410). The purpose of the first set of filters was to minimize sample heating and photolysis by the probe beam. The second set of filters was used to minimize entry of laser light into the monochromator and to reject other potential stray light. For the 830 nm measurements, RG715 and RG9 filters were placed before the monochromator to cut off all visible light (50% T at 730 nm). The wavelength selected probe light was detected by a photomultiplier tube. (PMT for measurements in the visible range, RCA 1P28A; for measurements in the near IR, Hammamatsu R406 GA7630.) The PMT output, shorted across a 3900 Ω resistor, was recorded with a transient digitizer (Biomation 805), which was interfaced to a microcomputer (Apple II+). Unless otherwise indicated, signals were averaged for 1024 transients. Temperature control was maintained with a Beckman water jacketed cell holder (model INS-TW) attached to a refrigerated water bath.

Figure II.1.

Block diagram of the apparatus used in the nanosecond transient absorption experiment.

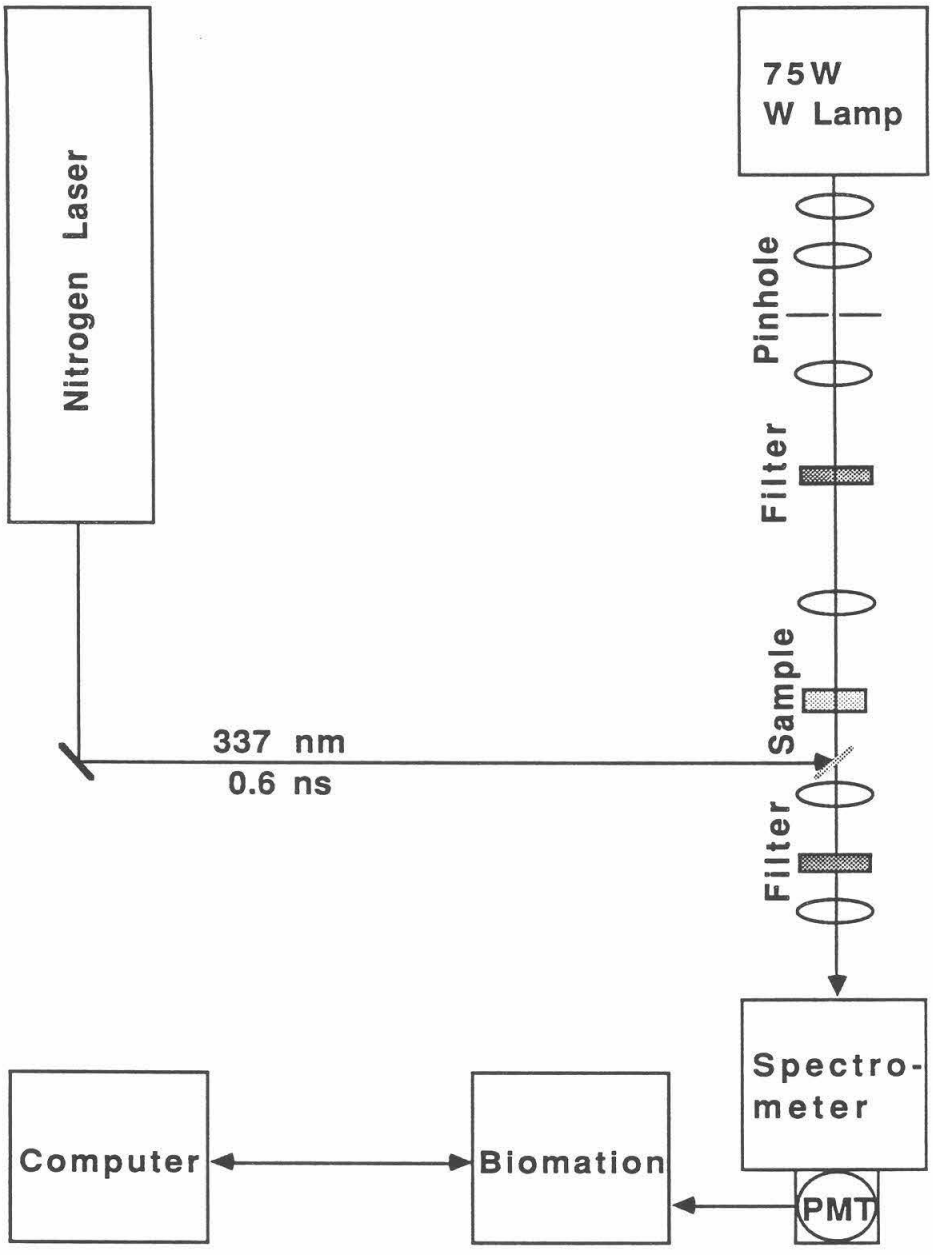
Nitrogen Laser
75W
W Lamp
Pinhole
Filter
Sample
337 nm
0.6 ns
Filter
Spectro-
meter
Computer
Biomation
PMT

Other kinetic measurements were made using a flash lamp system which has been described elsewhere (Milder et al., 1980), modified as follows: Fiber optics were used to guide the probe light from the lamp to the sample cell, and then, from the sample cell to the input slit of the monochromator. To achieve vibrational isolation, the optical apparatus was mounted on a half inch thick aluminum plate supported by two inches of polyurethane foam. The photomultiplier output was amplified by a 100X amplifier, and instead of the Biomation, an AT-compatible computer equipped with a Microway A2D-160 A/D conversion board was used. Amplified and non-amplified PMT output were recorded on two separate channels.

Calculations and Data Analysis.

Equilibrium redox calculations. The calculation of subpopulations in the partially reduced enzyme was carried out as described by Copeland et al. (1987) using a computer program written by Paul Smith.

Baseline subtraction. The timing and trigger circuitry introduced a significant background signal into the data. For this reason, background ("dark") data were acquired, with the laser and the probe lamp both shuttered. The raw kinetic data and the dark data were then used together to calculate a data set in absorbance units. This calculation was carried out by means of a computer program (see SASHIMI in Appendix) which used the dark data 1) to subtract out the background electronic signals, and 2) to give a dark reference voltage. The program then converted the raw data (proportional to transmittance) into relative absorbance data. What is meant by relative

absorbance is that within a given kinetic trace, the changes are in correct absorbance units, but that the entire data set is subject to an unknown offset.

In the case of the 830 nm data, 4096 transients were acquired, and so new "dark" baselines had to be collected as well. In the case of the 1 μs per point data (figure II.4), when the data were processed, a significant amount of trigger circuit artifact (apparently an exponential decay) was still apparent in the pre-flash part of the data. In order to correct for this, the pre-flash part of the the raw data for each of the samples and the background were fit to a single exponential. The amplitude of these fitted exponential functions was used to scale the baseline to match each data set. (The baseline offset, IMAX, was not scaled.) Even after this manipulation, the pre-flash part of the data did not subtract to give a flat baseline. Thus, these 830 nm data are not as reliable as the data taken at other wavelengths. The 10 μs per point 830 nm data (figure II.6) were handled in the normal way.

Determination of rates. The absorbance data were then analyzed using two other computer programs. Initial data analysis was accomplished with a program written in our laboratory (see MAGURO in Appendix.) This program allowed the data to be displayed graphically on the screen, and the portion of the data to be fitted could be selected using a cursor. Data were fit to a single exponential decay of the form: $C_1 + C_2 * e^{(-kt)}$, using an IMSL library routine called ZXSSQ which uses a minimum of the sum of squares -- finite difference Levenberg-Marquardt algorithm. All of the kinetic plots in this chapter were made by this program.

One limitation of the ZXSSQ routine is that it does not use analytical derivatives in the algorithm, and therefore the statistical information

available for the fit is limited, For this reason, some of the data were re-analyzed using another program (NUFIT, courtesy of Bruce Vogelaar) which was capable of more extensive statistical analysis and could also fit the data to a double as well as a single exponential function.

In the case of a double exponential function, the data were fit to an equation of the form: $C_1 + C_2 * e^{(-k1t)} + C_3 * e^{(-k2t)}$. In some instances, k_2 (the rate of CO rebinding), had been measured, and could be supplied and held constant while the other four parameters were allowed to vary. In other cases, all five paramenters were allowed to vary. The type of fit used in a given instance is indicated in the figure caption.

In order for the NUFIT program to calculate uncertainties in the fitted parameters, uncertainties for the measured data had to be supplied. These uncertainties were estimated by first fitting the function and finding the average of the residuals. The standard deviation for the residuals was then used as the uncertainty in the original data points. This resulted in a X^2 (chi-squared) value of one for the fit.

In some instances, more than one data set was acquired for a given set of conditions. When the fitted rates for these data were compared, there was more variation than could be accounted for by the uncertainties calculated for the fit. The uncertainty of the measurement was therefore estimated from a series of rates measured at 25.5 °C between pH 6.5 and 7.5 (see figure II.7). The mean rate was 17,163 s^{-1}, and the standard deviation was 1,669 s^{-1}, whereas the uncertainties calculate by NUFIT were typically less than 600 s^{-1}. This larger uncertainty was used in all cases except in the temperature dependence

(figure II.8) where the uncertainties in the fitted rates were plotted. In that case, all of the data were obtained from the same sample on the same day.

Results.

Figure II.2 shows the visible absorption spectra of CO-mixed valence (COMV) cytochrome *c* oxidase, the CO bound fully reduced (COFR) enzyme, and a sample poised at an intermediate three electron level of reduction (COMV+1). As described above, the COMV and COFR are well defined two- and four-electron reduced states of the enzyme, while the three electron reduced COMV+1 sample is an equilibrium mixture containing small populations of COMV and COFR, and a large population of three electron reduced molecules in which two electrons are effectively held at the oxygen binding site, and the third electron is shared between Fe_a and Cu_A (see figure I.2.)

The redox states of both Fe_a and Cu_A can be monitored optically. Reduced Fe_a gives rise to an absorption band at 605 nm, and oxidized Cu_A gives rise to a broad absorption centered at around 830 nm. Figure II.2 shows that as Fe_a and Cu_A become more reduced, the 605 nm band increases in intensity, while the absorbance at 830 nm decreases. The absorption peak at 590 nm which dominates the alpha band of the COMV is characteristic of CO bound $Fe_{a_3}{}^{2+}$ (Vanneste, 1966). The intensity of this band remains relatively constant as Fe_a and Cu_A go from oxidized to reduced.

$Fe_{a_3}{}^{2+}$-CO is photolabile. The photolysis of this species is accompanied by a shift in the alpha band. There is an absorbance decrease at 590 nm and an increase above 600 nm (Wikström, 1981; Greenwood et al., 1974). This

Figure II.2.

Visible absorption spectra of CO inhibited cytochrome oxidase at the two-, three-, and four-electron reduction levels. COMV (a, dots), COMV+1 (b, dots and dashes), COFR (c, solid line). The inset shows the 830 nm region of the same spectra expanded vertically. All three traces in the inset were drawn in solid lines so that the noise could be reproduced. Enzyme concentration: 48 μM, path length: 10 mm, temperature: 21.5 °C, pH: 7.4.

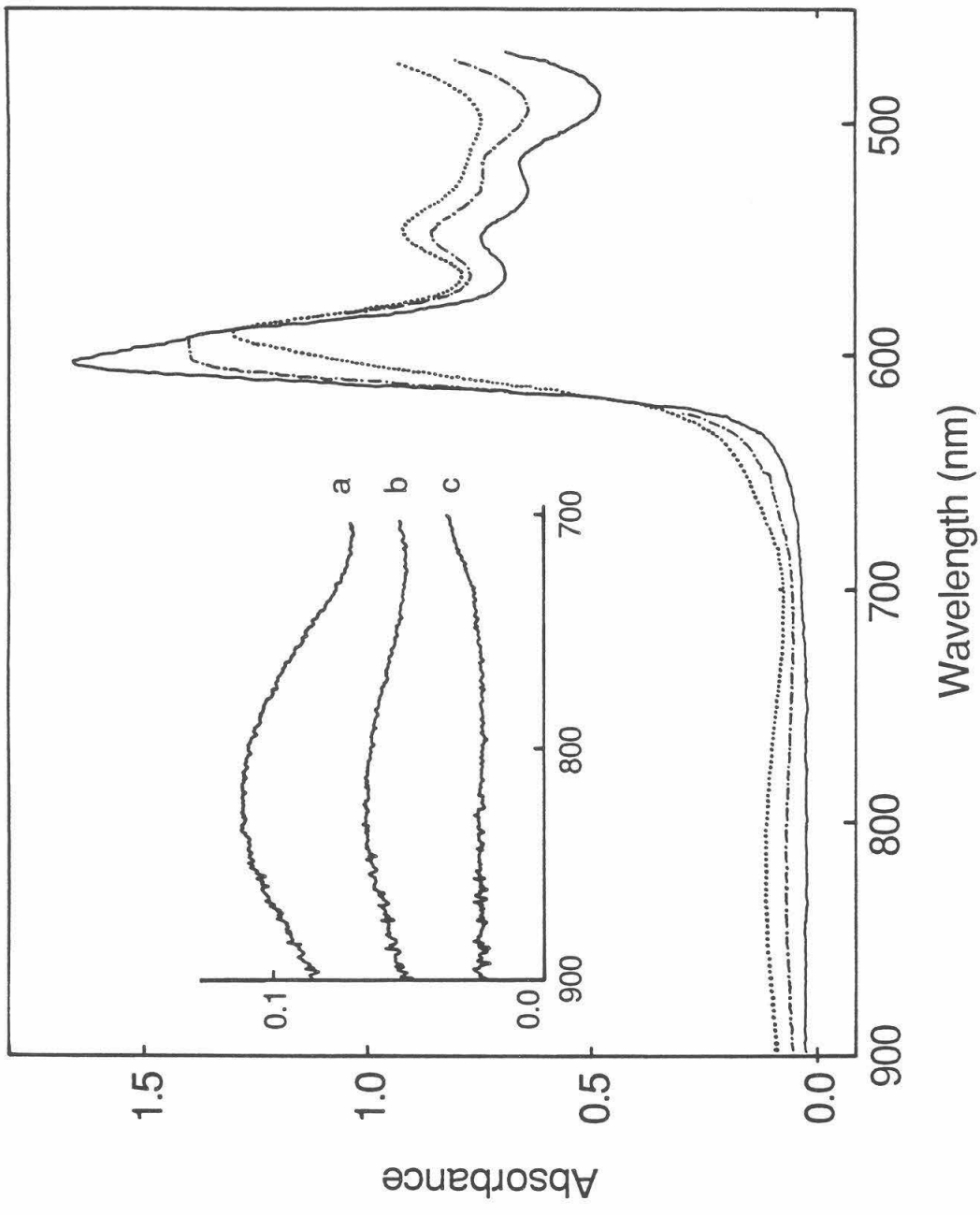
Absorbance
1.5
1.0
0.5
0.0
900
800
700
600
500
Wavelength (nm)
a
b
c
0.1
0.0
900
800
700

spectral change interferes with the observation of Fe_a at 605 nm. However, 598 nm is an isosbestic wavelength for the absorbance changes associated with this photolysis, and the Fe_a reduced-minus oxidized band, centered at 605 nm, still has about 75% of its intensity at 598 nm. Thus, by observing at 598 nm, Fe_a can be followed without interference from the absorbance changes associated with photolysis. This technique has been used to study electron transfer in the COMV compound after photolysis. (Brzezinski and Malmström, 1987).

The approach taken in the present experiment was to photolyze a COMV+1 sample and look for absorbance changes at 598 and 830 nm, which could indicate an electron reequilibration between Fe_a and Cu_A. Photolysis was accomplished using nanosecond pulses from a nitrogen laser, and the resulting changes in absorbance were followed on a microsecond time scale. Unless otherwise noted, the data presented are the average of 1024 transients.

Figure II.3 shows the absorbance changes in COMV+1 and COMV samples at 598 nm following a laser pulse. In the COMV+1, there was a decrease in absorbance with an apparent first order rate of 17,200 ± 1,700 s^{-1} (1σ, see Materials and Methods). No corresponding change was observed in the COMV. The same experiments were repeated, observing at 830 nm (figure II.4.) At this wavelength, there was an initial increase in absorbance in both samples, during the dead time of our measurement (see Boelens et al., 1982). In the COMV+1 sample, this increase was followed by a decrease which had an apparent first order rate of about 13,500 s^{-1} (see below). Again, no corresponding change was seen in the COMV sample.

These results are consistent with photolysis in the COMV+1 sample being followed by a fast electron reëquilibration between Fe_a and Cu_A, at an

Figure II.3

Absorption changes at 598 nm following photolysis by 0.6 ns laser pulse. A. COMV; B. COMV+1. Enzyme concentration (aprox.): 27 μM, path length: 10 mm, temperature: 25.5 °C, buffer: 150 mM NaMOPS, 0.5% Tween-20, pH: 7.16. 1024 transients averaged. The fit shown is a single exponential fit, apparent rate: 22,179 s^{-1}.

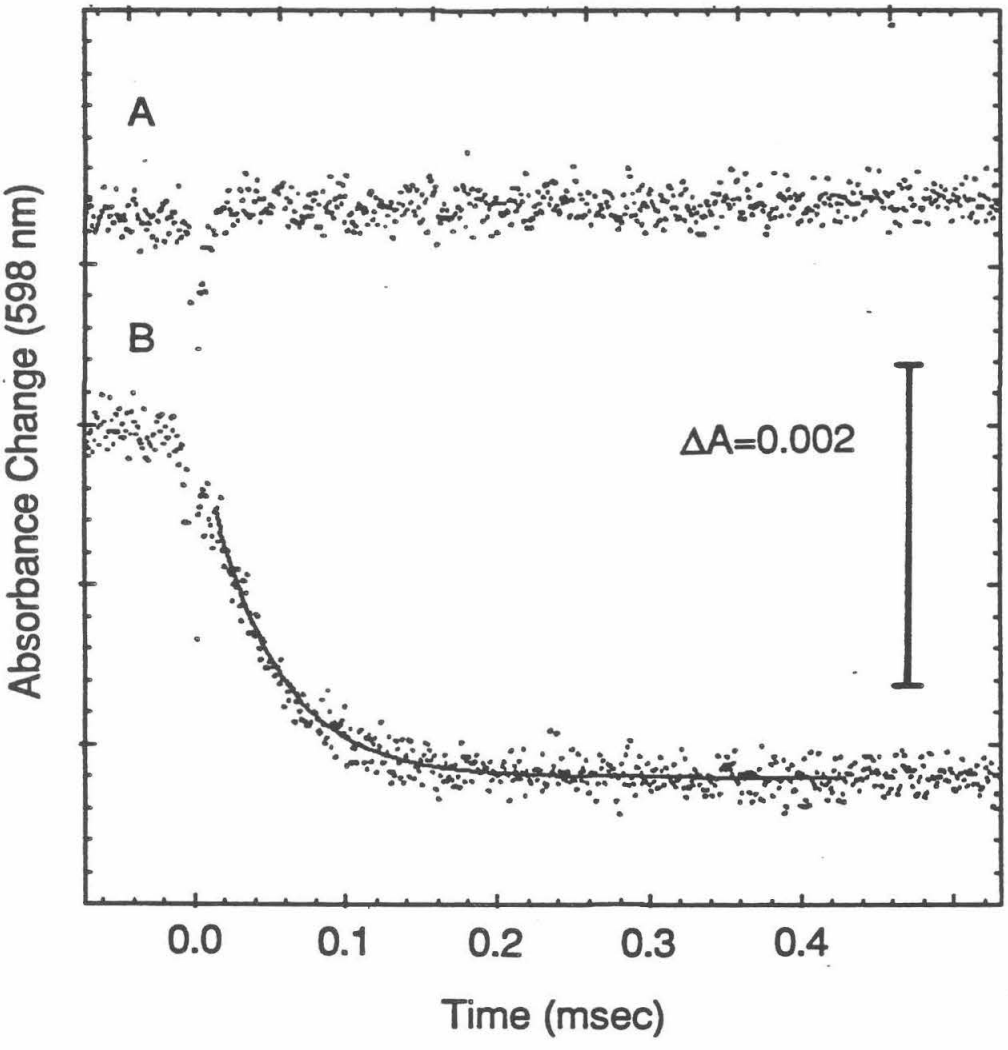
A
B
ΔA=0.002
Absorbance Change (598 nm)
0.0
0.1
0.2
0.3
0.4
Time (msec)

Figure II.4

Absorbance changes at 830 nm following photolysis by 0.6 ns laser pulse. A. COMV; B. COMV+1. 4096 transients averaged. Because the number of scans was different, a different "dark" baseline was collected. However, when the data were processed using this baseline, a significant amount of trigger circuit artifact (apparently an exponential decay) was still apparent in the pre-illumination part of the data. In order to correct for this, the pre-illumination part of the the raw data for both samples and the background were fit to a single exponential. The extents in the fitted exponential functions were used to scale the baseline to match each data set. The baseline offset (IMAX in the SASHIMI computer program, see materials and methods) was not scaled. All other conditions are the same as for figure II.3. The fit shown is a single exponential fit, apparent rate: 14442 s^{-1}.

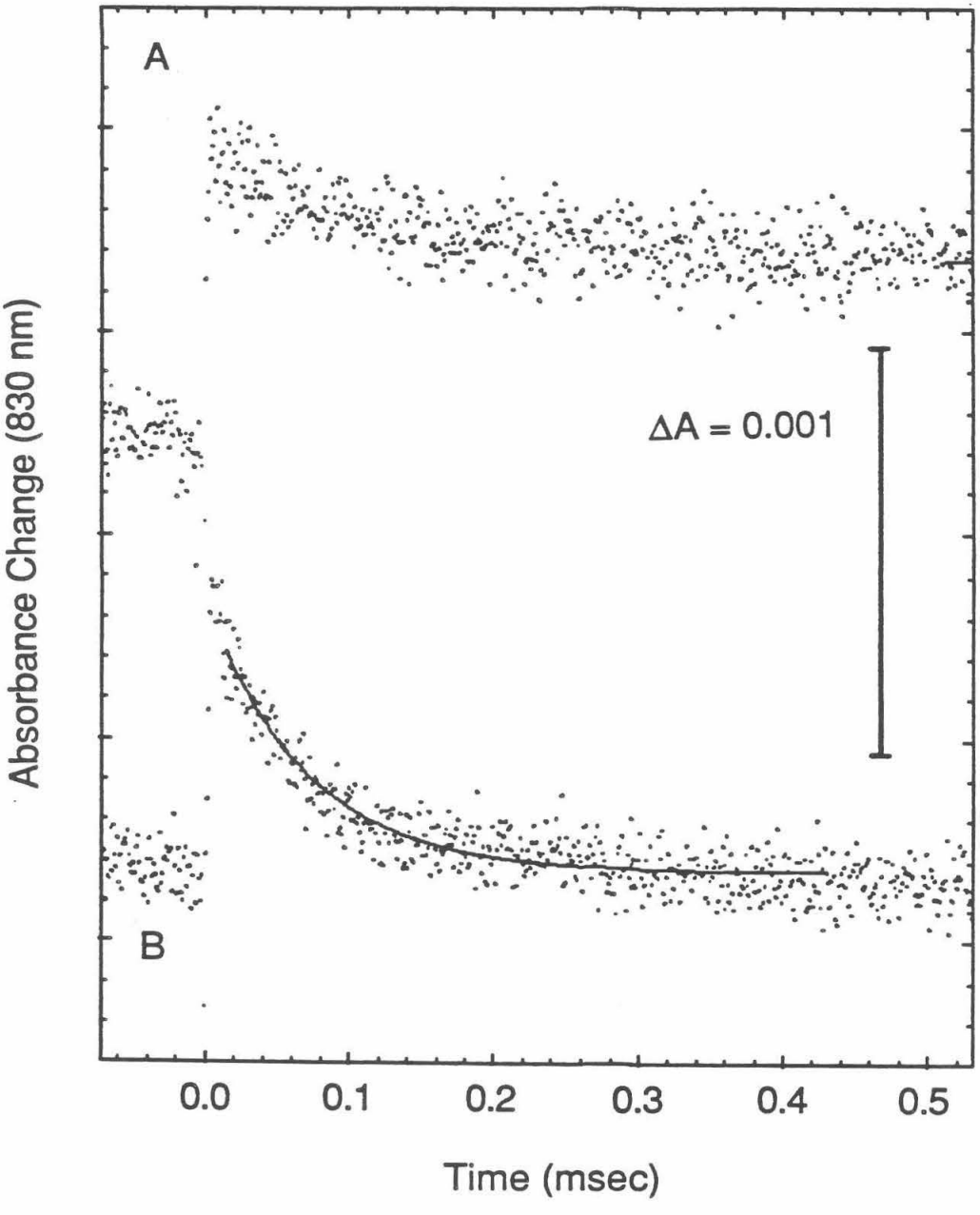
A
B
ΔA = 0.001
Absorbance Change (830 nm)
0.0
0.1
0.2
0.3
0.4
0.5
Time (msec)

apparent rate of about 17,200 s^{-1}. The absorbance changes which occur on this time scale are seen only in the COMV+1 sample where there is a subpopulation of enzyme in which electron redistribution between Fe_a and Cu_A is possible; no corresponding changes are observed in the COMV or COFR samples (data for the latter not shown). The direction of the absorbance changes (a decrease at both 598 and 830 nm) is consistent with the simultaneous oxidation of Fe_a and reduction of Cu_A. However, the data from 598 and 830 nm do not agree perfectly. The relative magnitude of the absorbance changes (based on the amplitude of the single exponential fitted curves) indicates that about 1.5 times as much Cu_A is reduced as Fe_a is oxidized, but this is almost certainly within the experimental uncertainty (see below). The apparent rate observed at 830 nm is slower; about 13,500 s^{-1}, as opposed to 17,200 s^{-1}. This difference in rates can probably be accounted for, at least in part, by the fact that there was a problem with baseline subtraction for the 830 nm data and some artificial baseline scaling had to be used (see Data Analysis in Materials and Methods). For this reason, more confidence should be placed in the data acquired at 598 nm.

In some COMV samples, we observed absorbance changes which were similar to those seen in the COMV+1 samples, but smaller. This apparently occurred because the enzyme had become photoreduced, and some of the COMV compound had been converted into COMV+1 (see below). However, no absorbance changes attributable to electron redistribution in the COMV compound were observed in these experiments.

A COMV+1 sample was also prepared using the cytochrome *c* -- cytochrome *c* oxidase (1:1) high affinity complex. The absorbance changes at

598 nm which followed photolysis in this sample were essentially the same as those described above for the COMV+1 samples containing only cytochrome *c* oxidase. (The data for the high affinity complex are not shown.)

Figure II.5 shows the absorbance changes in the COMV+1 sample at 590 nm and at 598 nm on a longer time scale. As discussed above, the major contribution to the absorption intensity at 590 nm arises from $Fe_{a_3}{}^{2+}$-CO, and the decrease and subsequent increase in absorbance at this wavelength are thought to reflect the photolysis and rebinding of CO. As would be expected, the initial decrease in absorbance corresponding to photolysis is too fast to be resolved by our apparatus (Findsen et al., 1987). The first part of the recombination which follows, can be fitted to a rate of 135 s^{-1}. This rate is generally in agreement with the rates observed at 590 nm in the COMV. This suggests that the recombination of $Fe_{a_3}{}^{2+}$–CO is not significantly affected by redox states of Fe_a and Cu_A, in agreement with the findings of Boelens et al. (1982). It should be noted, however, that in some of the COMV samples, an early slow phase was observed at 590 nm (data not shown).

At 598 nm, in the COMV+1 sample, the rapid decrease in absorbance was followed by a return to the original level at an apparent rate of 131 s^{-1} which is almost almost identical to the rate of the recovery phase observed at 590 nm. Apparently, the electron population returned to its original distribution at a rate controlled by the recombination of $Fe_{a_3}{}^{2+}$–CO. This is to be expected, since the apparent rate of the electron equilibration is much faster than the recombination of $Fe_{a_3}{}^{2+}$–CO. It should be pointed out that the kinetic trace in figure II.5a was not measured exactly at the isosbestic point. There is a significant initial deflection before the 17,200 s^{-1} phase begins. This initial

Figure II.5

Absorbance changes at 598 nm and 590 nm in COMV+1 sample following photolysis by 0.6 ns laser pulse. All conditions are the some as for figure II.3 except that no special baseline manipulation was used. Fits shown are single exponential fits, apparent rates, A: 132 s^{-1}; B: 135 s^{-1}.

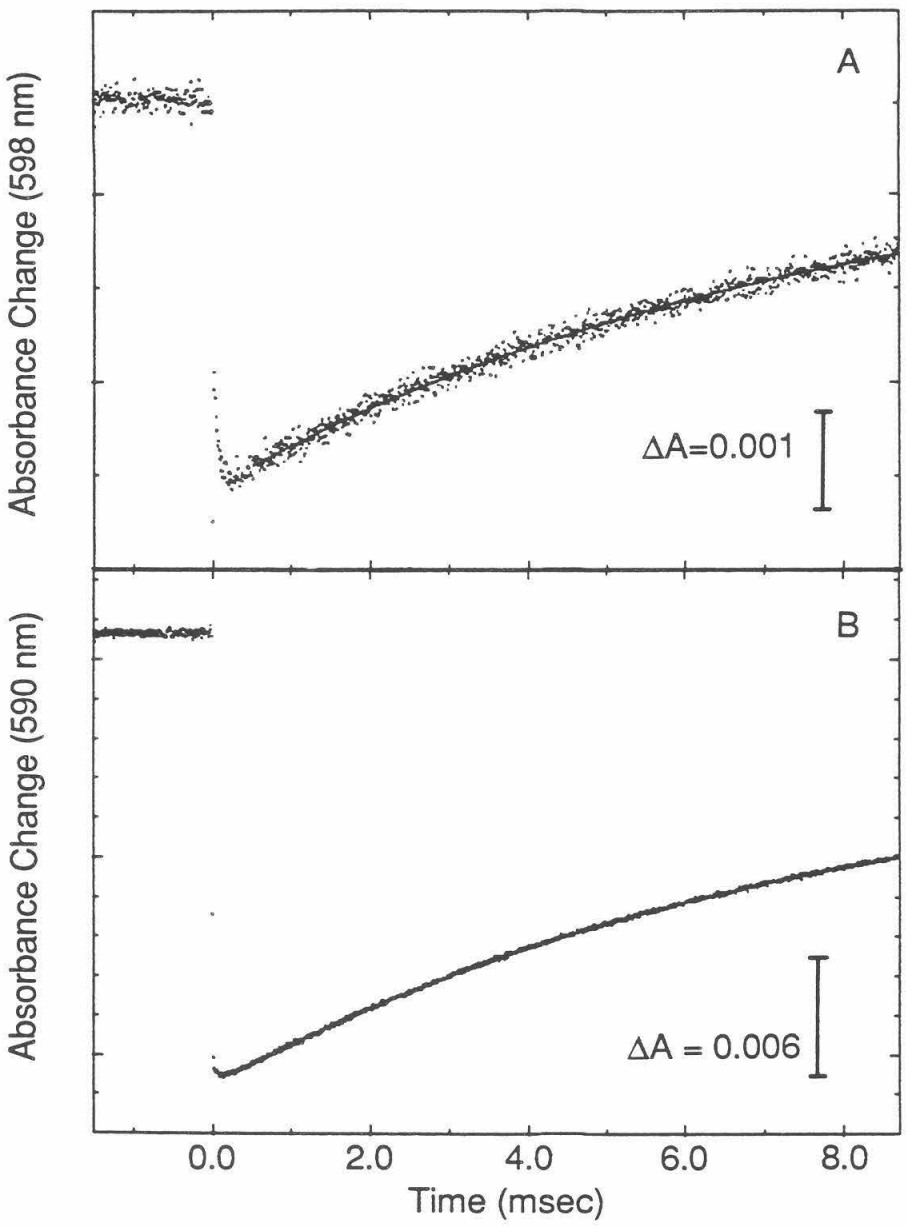
A
B
Absorbance Change (598 nm)
Absorbance Change (590 nm)
ΔA=0.001
ΔA = 0.006
0.0
2.0
4.0
6.0
8.0
Time (msec)

deflection is a contribution from the photolysis itself. There should be a corresponding contribution from the CO rebinding in the recovery part of this trace, and this could influence the measured rate. However, the corresponding data for a sample at pH 6.76 were measured almost exactly on the isosbestic point (there is no jump in absorbance in the dead time), and in this case the recovery phase has a similar rate (143 s^{-1}.) In this connection it should be noted that the isosbestic wavelength for the photolysis of $Fe_{a_3}{}^{2+}$–C O is pH dependent. At pH 7.0 the isosbestic point is at 598 nm, but at pH 9.0 it is close to 600 nm. One consequence of this is that the isosbestic does not always correspond to the same point on the Fe_a alpha band, and so the applicable Fe_a reduced-minus-oxidized extinction coefficient also changes with pH.

At 830 nm, in the case of the COMV+1 sample, the initial increase in absorbance was exactly offset by the decrease during the 13,500 s^{-1} phase, and the absorbance had already returned to baseline levels after 200 μs (see figure II.2). This appeared to rule out a recovery phase, and no data were taken at longer times. However a recovery phase was observed at 830 nm in the case of the COMV compound. As shown in figure II.6, the initial increase in absorbance at this wavelength was followed by a return to its original level with a rate of about 100 s^{-1}.

Figure II.7 shows the pH dependence of the apparent rate. What is clear from these data is that the rate is fastest at about pH 8.0 and falls off in either direction. Figure II.8 shows the temperature dependence of the apparent rate. The changes in the rate as a function of temperature are much smaller than those observed by changing the pH. Based on the uncertainties used in the pH data set (see Data Analysis in Materials and Methods), this temperature

Figure II.6

Absorbance changes at 830 nm in COMV sample following photolysis by 0.6 ns laser pulse. 4096 transients were averaged. All other conditions were the same as for figure II.3. The fit shown is a single exponential fit, apparent rate: 104 s^{-1}.

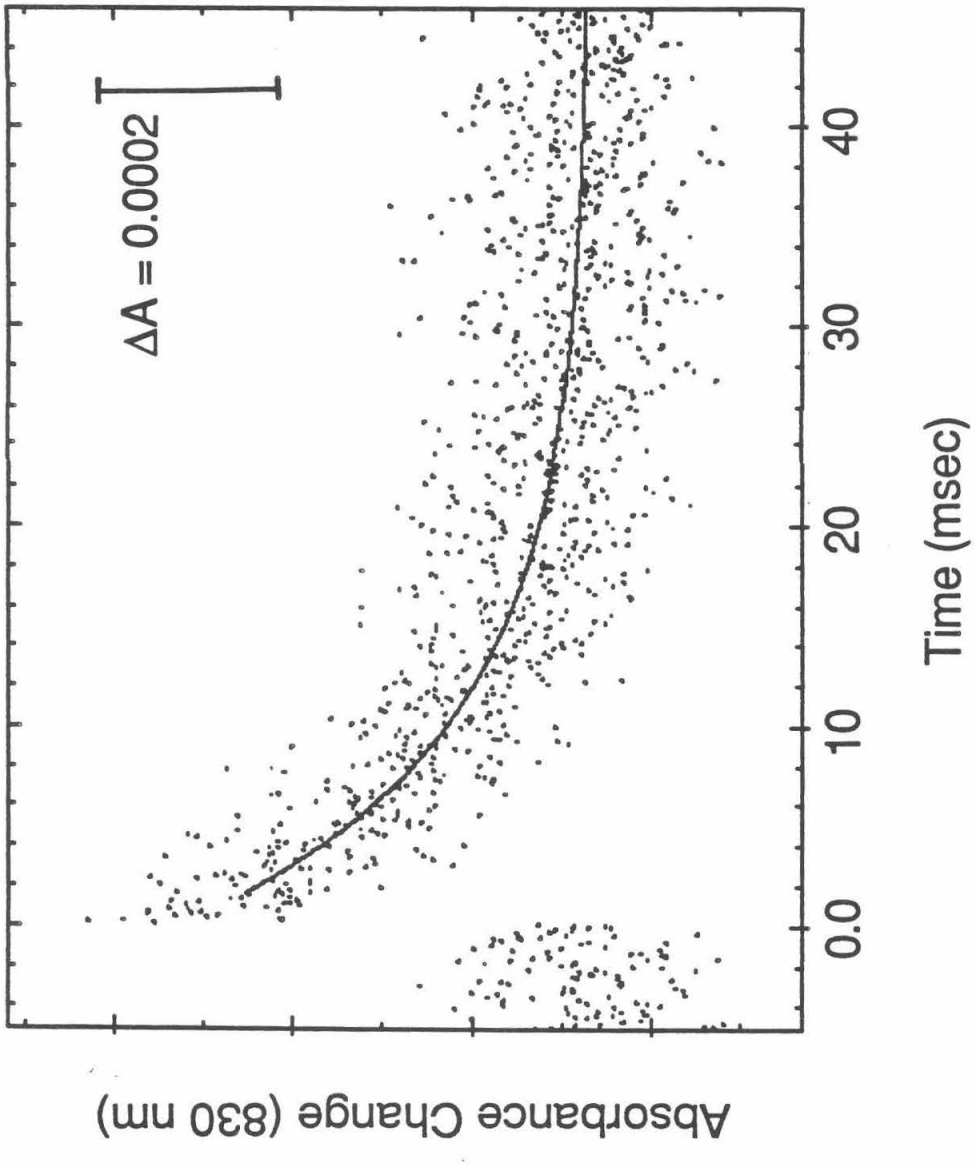
ΔA = 0.0002
0.0
10
20
30
40
Time (msec)
Absorbance Change (830 nm)

Figure II.7

pH Dependence of the Fast Absorbance Change at 598 nm (25.5 °C). Buffers: pH 8.3 and above 150 mM NaCHES, 0.5% Tween-20; below pH 8.3 150 mM NaMOPS, 0.5% Tween-20. Solid dots: 4 parameter fit; open dots: 3 parameter fit. Error bars: 1σ, (see data analysis in materials and methods).

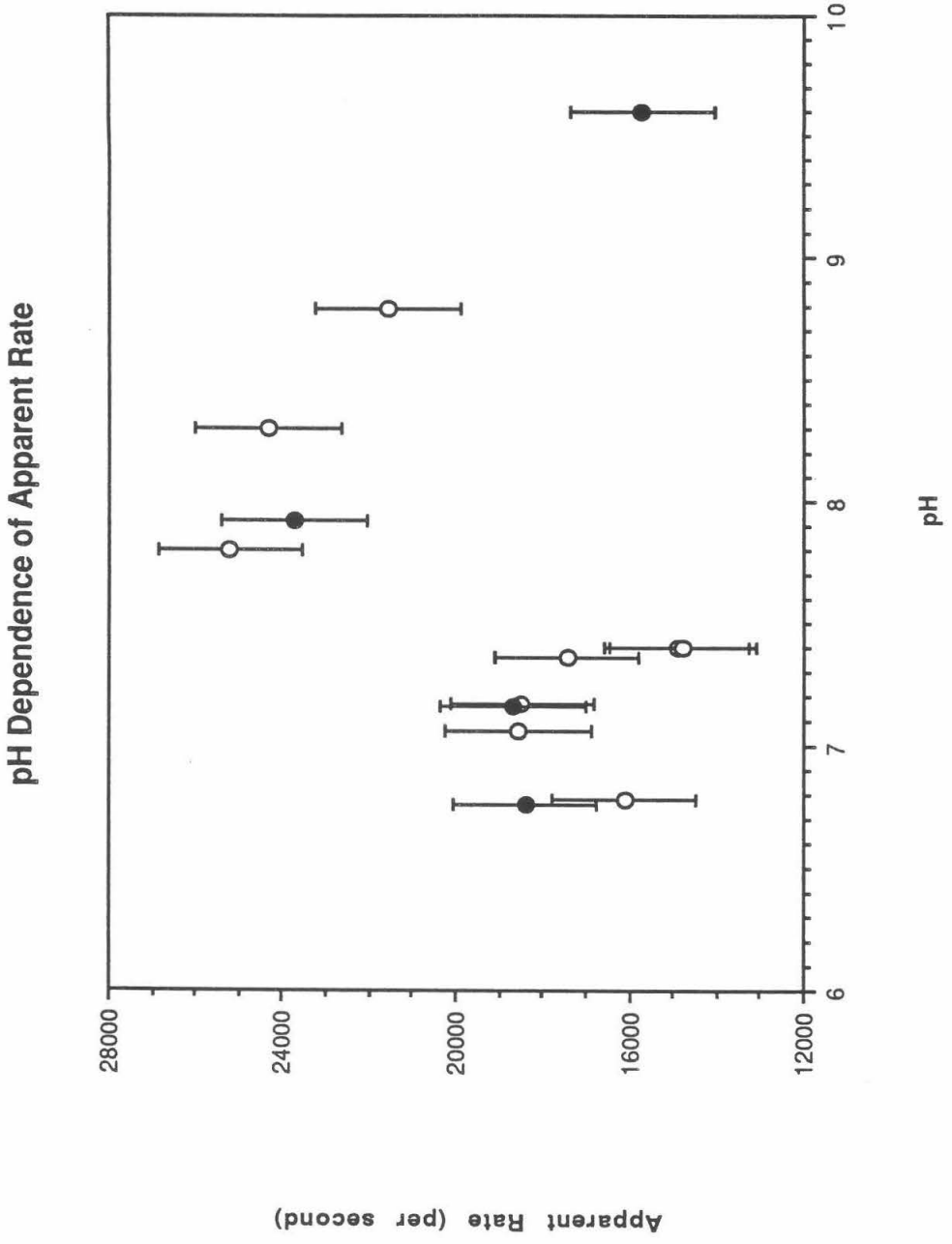
pH Dependence of Apparent Rate
Apparent Rate (per second)
28000
24000
20000
16000
12000
6
7
8
9
10
pH

Figure II.8

Temperature Dependence of Fast Absorbance Change at 598 nm. Buffer: 150 mM NaMOPS, 0.5% Tween-20, pH: 7.36. Data and error bars (1σ) are from 3 parameter fit. Solid dots indicate points where 3-, 4- and 5-parameter fits are in good agreement (see data analysis in materials and methods).

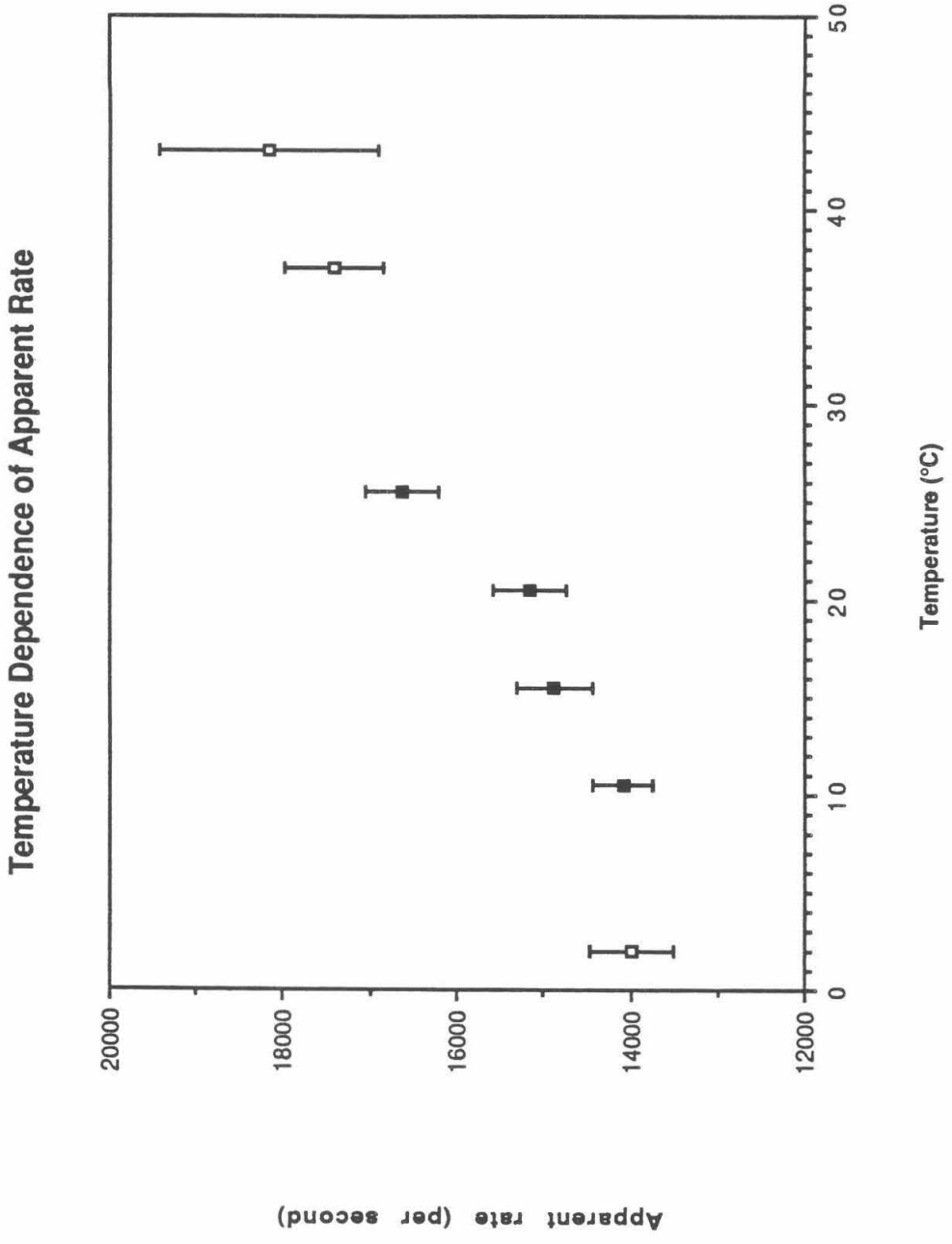
Temperature Dependence of Apparent Rate
Apparent rate (per second)
20000
18000
16000
14000
12000
0
10
20
30
40
50
Temperature (°C)

dependence could be considered insignificant. However, all these data come from the same sample on the same day, and a similar trend was observed at several pH values. The consistency in these data may be partly fortuitous, but the data do illustrate the fact that the process is temperature dependent. The error bars for this figure reflect the uncertainties in the fitted rates (see figure caption).

The assignment of the kinetic phases described above seems clear. Our data support the previous assignment of the 590 nm processes to the photodissociation and recombination of $Fe_{a_3}{}^{2+}$-CO. The processes observed at 598 nm and 830 nm in the COMV+1 samples, are consistent with their assignment as an electron reëquilibration between Fe_a and Cu_A. However, not everything associated with the photolysis of these samples is so straight forward. Figure II.9 shows the absorbance changes in the COMV+1 at 590 nm and 445 nm on an even longer time scale at which the complete return to baseline can be seen. (445 nm is the absorbance maximum for $Fe_{a_3}{}^{2+}$ without CO bound and also contains a significant contribution from $Fe_a{}^{2+}$, Vanneste, 1966.) Figure II.10 shows the absorbance changes in the COMV and COMV+1 at 445 nm on this same time scale. Clearly, there are more complicated processes at work here. The data in these figures illustrate that a good deal remains to be learned about the processes which occur following photolysis of $Fe_{a_3}{}^{2+}$-CO.

Visible spectra of the samples were acquired before and after the experiments. Almost invariably, the level of reduction was greater at the end than at the beginning. Although we did not perform a controlled study, it appeared as though the extent of reduction was greater in samples which had been illuminated for a longer time in the laser beam. This suggests that the

Figure II.9

Absorbance changes at 590 nm and 445 nm in COMV+1 sample following photolysis by 0.6 ns laser pulse. All conditions are the same as for figure II.3.

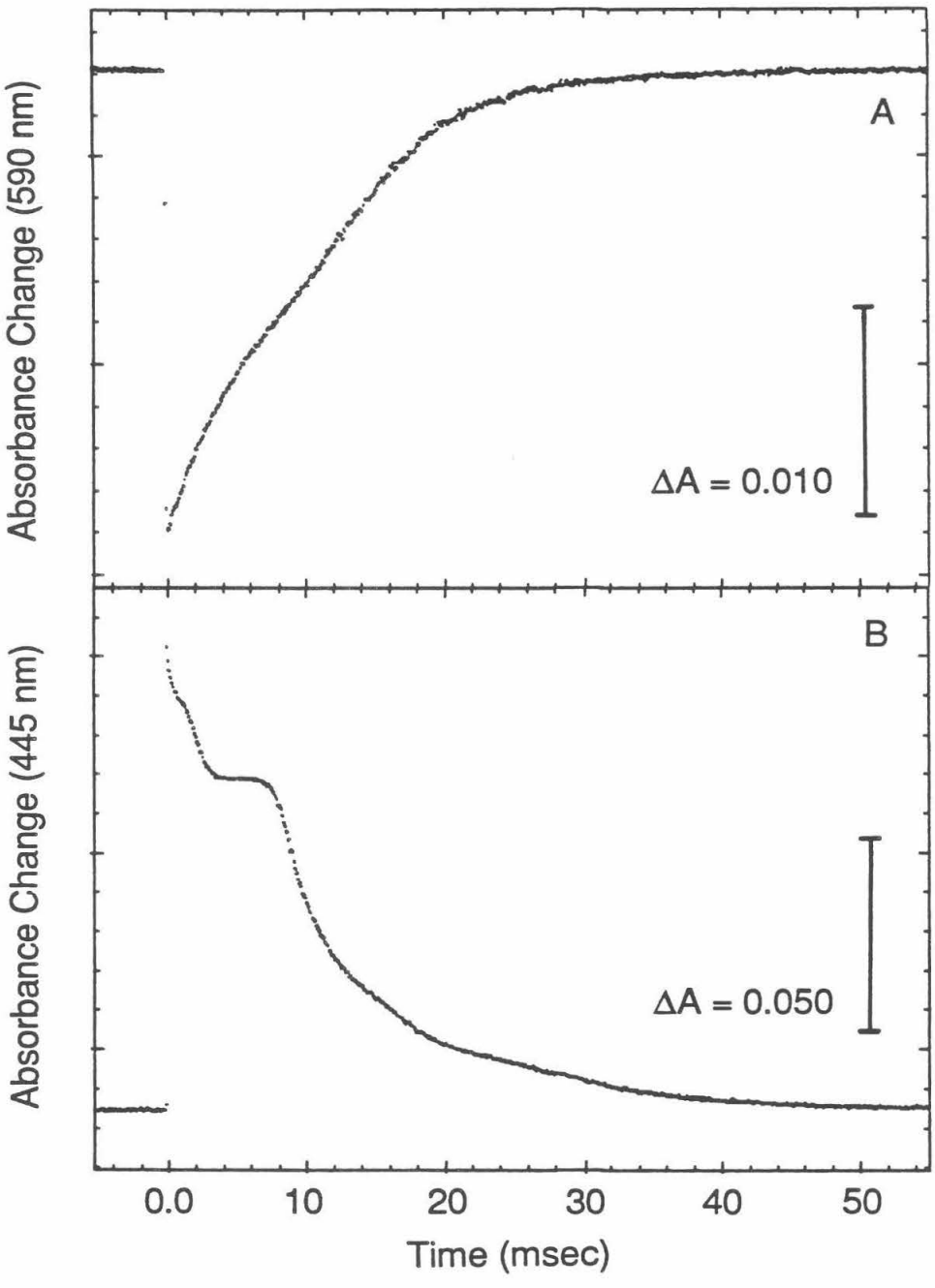
Absorbance Change (590 nm)
A
ΔA = 0.010
Absorbance Change (445 nm)
B
ΔA = 0.050
0.0
10
20
30
40
50
Time (msec)

Figure II.10

Absorbance changes at 445 nm following photolysis by 0.6 ns laser pulse. A: COMV; B: COMV+1. All other conditions are the same as for figure II.3.

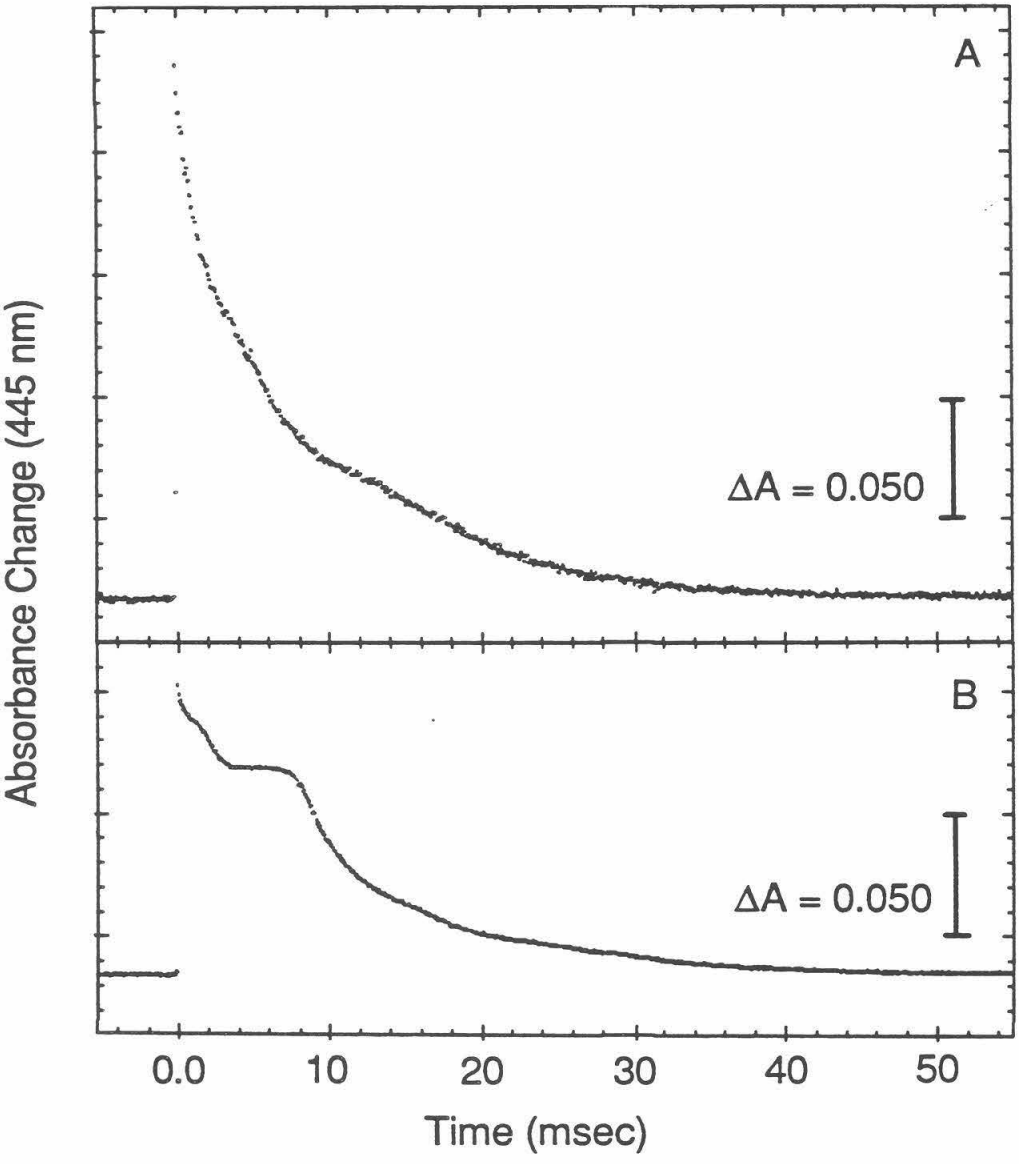
A
ΔA = 0.050
B
ΔA = 0.050
Absorbance Change (445 nm)
0.0
10
20
30
40
50
Time (msec)

samples were being photoreduced. The extent of photoreduction also appeared to be greatest in samples of high pH.

Discussion.

These results show that photolysis of $Fe_{a_3}{}^{2+}$–CO in a three electron reduced COMV+1 sample brings about a redistribution of electrons from Fe_a to Cu_A, with an apparent rate of 17,200 ± 1,700 s^{-1}. In control experiments no electron redistribution was observed in the COMV or COFR compounds.

Boelens et al., (1982), and Brzezinski and Malmström (1987) have studied the changes in absorption which follow photolysis of the COMV compound. In contrast to the above results, Boelens et al. reported that photolysis was followed by electron transfer from the oxygen binding site to Cu_A with an apparent rate of about 7,000 s^{-1}. About 5% of Cu_A became reduced. Brzezinski and Malmström observed the same process but report an apparent rate of about 14,000 s^{-1}. They also found that the reduction of Cu_A was followed by reduction of Fe_a at an apparent rate of about 600 s^{-1}.

These results are not necessarily contradictory. In their experiments, Boelens et al. and Brzezinski and Malmström employed flash sources with temporal pulse widths of 200 ns and 500 ns respectively, and Brzezinski and Malmström reported that their flash energy was 1.0 J per pulse. The present results were obtained using 0.6 ns, 1.0 mJ pulses. We obtained some results similar to theirs using a flash lamp apparatus which had a pulse width greater that one microsecond. It appears, therefore, that the outcome of the photolysis event may be dependent on the duration or total energy of the excitation

pulse. This possibility is discussed below. It is important to note, that these differences in the outcome of the photolysis experiment occurred in the COMV, and not the COMV+1 samples. In the case of the COMV+1 samples, we obtained consistent results regardless of which apparatus was used. Thus, the validity of our results does not depend entirely on the resolution of this issue.

In the COMV+1 samples, photolysis of $Fe_{a_3}{}^{2+}$–CO is followed by a redistribution of electrons from Fe_a to Cu_A at an apparent rate of 17,200 ± 1,700 s^{-1}. The distance between the two metal centers is between 8 and 26 Å (Goodman and Leigh, 1987; Brudvig et al., 1984). In this section, the meaning of this apparent rate will be discussed.

The process is initiated by the photolysis $Fe_{a_3}{}^{2+}$-CO at the oxygen binding site. This apparently brings about a shift in the redox equilibrium between Fe_a and Cu_A, which are about 20 Å away from the oxygen binding site (Goodman and Leigh, 1987; Brudvig et al., 1984). Although the mechanism of this communication is unknown, it is most likely mediated by an enzyme conformational change. One possibility which cannot be ruled out is that the rate of the electron reëquilibration which we observe is limited by this putative conformational change. In that case, the present results would still place a lower limit on the "true" electron equilibration rate, and given that caveat, much of the following discussion would still apply.

On the other hand, the rate limiting step may be the electron transfer itself. As discussed in the introduction, if the process being observed is simply an intramolecular electron reëquilibration between two metal centers, then the relaxation rate is the sum of the forward and reverse electron transfer rates ($k_f + k_r$). The individual rates can be found if the equilibrium constant

($K = k_r/k_f$) is known. The fast kinetic phase observed at 598 nm (at pH 7.0 and 25.5 °C) has a rate of 17,200 ± 1,700 s^{-1}. The redox potentials of Fe_a and Cu_A in the CO inhibited enzyme have been determined electrochemically (Ellis et al., 1986, Wang et al., 1986). At 25 °C the equilibrium constant is 1.46, in favor of the reduction of Cu_A. These values can be used to calculate k_f = 10,200 s^{-1} and k_r = 7,000 s^{-1}.

Two significant assumptions are implicit in this analysis: 1) that the equilibrium constant in the photolyzed enzyme is not significantly different from that measured for the unphotolyzed enzyme; and 2) that the equilibrium constant for the photolyzed enzyme actually governs the observed relaxation. The validity of these assumptions is discussed below.

The first assumption is that the redox potentials of Fe_a and Cu_A in the photolyzed enzyme -- where the observed kinetics take place -- can be reasonably approximated by the corresponding potentials in the unphotolyzed, CO inhibited enzyme. The correct way to solve for k_f and k_r would be to use the redox potentials of Fe_a and Cu_A in the photolyzed enzyme. However, these potentials are not known. They must be different from the corresponding potentials in the unphotolyzed enzyme; the experimental design relies on this change in potential to perturb the electron equilibrium. It appears that this change is small; in the kinetics experiment, the total electron population change upon photolysis of the COMV+1 is less than 2%. The redox potentials of Fe_a and Cu_A have been measured in both the native enzyme and the CO inhibited enzyme (Blair et al., 1986; Ellis et al., 1986; Wang et al., 1986, personal communication from the same authors). There is nothing that would predict that a large shift in the redox equilibrium, towards Cu_A,

should occur upon photolysis; if anything, a small change in the other direction is predicted, but this is probably within the uncertainty of the measurements. However, we cannot be sure that the redox potentials in the freshly photolyzed enzyme are the same as in the native enzyme. (We tried to measure the equilibrium extent of the electron redistribution in a continuous illumination experiment without success, apparently because under these conditions there is electron transfer from the oxygen binding site metal centers, just as there is in the COMV compound, see Boelens and Wever, 1980; Boelens et al., 1982.) Nevertheless, it appears that the first assumption is a reasonable one.

The second assumption is that the redox potentials of Fe_a and Cu_A (in the photolyzed enzyme) are actually the ones which govern the observed reëquilibration. This would be the case if the relaxation is a monophasic exponential decay. However, if the overall relaxation involves more than one step, the energy level(s) of the intermediate(s) would enter into the picture (Hiromi, 1979). The measured relaxation appears to be a single exponential decay, but there is no way to be sure that it is not just the first phase of a more complicated process. There are no equilibrium data with which to compare the extent of the absorbance change, and because of the recombination of $Fe_{a_3}{}^{2+}$–CO, the relaxation cannot be observed for more than a few milliseconds.

The relaxation process might be multiphasic if either the reduction of Cu_A, or the oxidation of Fe_a was followed by a conformational relaxation. This kind of behavior is predicted by many models of the proton pump (Gelles et al., 1986; Blair et al., 1986; Wikström et al., 1981). As discussed in the introduction, the reduction and oxidation kinetics of Fe_a and Cu_A are biphasic at both sites.

(Antalis and Plamer, 1982; Hill et al., 1986). In fact, Wikström and colleagues (1981) and Brzezinski and colleagues (1986) have proposed that biphasicity in the enzyme's kinetics is related to its role as a proton pump. Thus, some multiphasic behavior in the electron redistribution between these two sites would not be unexpected.

Thus, the electron reëquilibration appears to be a simple first order process, but in this experiment there is no way to be sure. If the rebinding of CO could be slowed down, the relaxation could be followed for a longer time. This might be accomplished by lowering the concentration of CO in the solution, since the rate of rebinding has been reported to depend on CO concentration (Sharrock and Yonetani, 1977; Boelens et al., 1982). However, it is not certain that this concentration dependence occurs under the conditions of our experiment (see below).

The next chapter describes a temperature-jump experiment which can potentially overcome these problems. Unfortunately the experiment has not yet been completed.

As discussed above, the events which take place after photolysis of the half reduced COMV enzyme appear to depend on the temporal pulse width, or the total energy of the excitation flash. When a microsecond flash lamp, with about a joule of power was used, electron transfer out of the oxygen binding site was observed. In contrast, when a nitrogen laser with a 0.6 ns pulse length and a pulse energy of about 1.0 mJ was used, no electron redistribution was observed.

The excited states involved in CO photolysis are very short lived compared to the pulse width of either light source, and so it is unlikely that the

difference between the two outcomes has to do with an excited state process (M. Ondrias, personal communication).

The explanation could lie in the fate of the CO molecule after photolysis. Fiamingo et al. (1982) have studied the photolysis and recombination of $Fe_{a_3}{}^{2+}$–CO in fully reduced, CO inhibited cytochrome *c* oxidase at low temperatures, by means of infrared spectroscopy. At low temperature, IR absorption bands corresponding to $Fe_{a_3}{}^{2+}$–CO were observed. When the sample was photolyzed, a copper carbonyl absorption band appeared, indicating that the CO molecule released by Fe_{a_3} had become bound to Cu_B. When the photolyzing lamp was turned off, the $Cu_B{}^{+}$-CO band slowly diminished in intensity and the $Fe_{a_3}{}^{2+}$–CO absorption grew in synchronously. The authors concluded that at low temperature, there was only one molecule of CO in the oxygen binding site. When the sample was illuminated, this CO was photolyzed from Fe_{a_3} and became bound to Cu_B. After the light was turned off, CO recombined with Fe_{a_3}, but at a rate governed by its released from Cu_B. Since the recombination rate did not depend on the concentration of CO in the bulk sample, it was also concluded that the site was closed to exchange of CO with the outside below 210 K.

One possible explanation of our results is that the shorter pulses cause CO to be released from Fe_{a_3} but only the longer, more energetic pulses remove the CO molecule from the oxygen binding pocket, that is, from both Fe_{a_3} and Cu_B. If the complete removal of CO from the pocket was neccessary before either Fe_{a_3} or Cu_B could become oxidized, electron redistribution would only be seen with the longer pulses.

There are at least two ways in which the longer light pulses might bring about this effect. 1) The longer light flashes have a great deal of energy. It could be that the absorption of a large number of photons by Fe_{a_3}, after the dissociation of CO, could increase the local kinetic energy in the pocket, and increase the probability of CO escaping. If the CO molecule did not go straight to Cu_B, but collided with the protein a few times, local motions in the protein might make escape more likely (J. Alben, personal communication). 2) It is possible that under the conditions of our experiment, Cu_B^+-CO is photolabile. With longer pulse widths, CO might be unable to bind to either Cu_B or Fe_{a_3} and might leave the pocket. Cu_B^{2+}-NO has been shown to be photolabile (Boelens, Rademaker et al., 1982), and Denis and Neau (1985) have found evidence that the rebinding of CO to fully reduced cytochrome *c* oxidase at low temperatures is photoactivated. Since this rebinding is thought to be controlled by the release of CO from Cu_B, this result would be consistent with a photolabile Cu_B^+-CO.

Both of these explanations predict that in the short pulse experiments, the photolyzed molecule of CO would remain in the site, and that the rate of recombination of $Fe_{a_3}^{2+}$–CO would be controlled by the release of CO from Cu_B^+. Fiamingo et al. (1982) only studied the release of CO from Cu_B^+ directly below about 180 K. I extrapolated their temperature dependence to room temperature and found that the predicted rate was about 300 s^{-1}, which, given the long extrapolation, is not inconsistent with the rates of about 130 s^{-1} which we observe for the recombination of CO.

Above about 210 K, the rebinding of CO has been found to be dependent on the CO concentration in the sample (Sharrock and Yonetani, 1977; Boelens

et al., 1982). Both of the explanation given above would lead to the prediction that in the short flash experiments, CO would rebind at a rate independent of concentration. We did not measure a CO concentration dependence of the rate of recombination. However, in our experiments the rate of recombination was approximately the same whether a long or short flash was used, which suggests that the rebinding processes in the two experiments are similar.

Thus, neither of the explanations offered above can completely account for the results. However, they may serve to guide further study of the problem. One experimental approach which could be fruitful would be to measure the rate of CO rebinding to the fully reduced enzyme as a function of CO concentration, and flash pulse width.

References.

Antalis, T.M. and Palmer, G. (1982) *J. Biol. Chem.* **257**, 6194-6206.

Bickar, D., Bonaventura, C. and Bonaventura, J. (1984) *J. Biol. Chem.* **259**, 10777-10783.

Blair, D.F., Ellis, W.R. Jr., Wang, H., Gray, H.B. and Chan, S.I. (1986) *J. Biol. Chem.* **261**, 11524-11537.

Boelens, R., Rademaker, H., Pel, R. and Wever, R. (1982) *Biochim. Biophys. Acta*, **672**, 84-94.

Boelens, R. and Wever, R. (1979) *Biochim. Biophys. Acta*, **547**, 296-310.

Boelens, R. and Wever, R. (1980) *FEBS Lett.* **116**, 223-226.

Boelens, R., Wever, R. and Van Gelder, B.F. (1982) *Biochim. Biophys. Acta*, **682**, 264-272.

Brautigan, D.L., Ferguson-Miller, S. and Margoliash, E. (1978) *Meth. Enz.* **53**, 128.

Brudvig, G.W., Blair, D.F. and Chan, S.I. (1984) *J. Biol. Chem.* **17**, 11001-11009.

Brzezinski, P. and Malmström, B.G. (1987) *Biochim. Biophys. Acta*, **894**, 29-38.

Copeland, R.A., Smith, P.A., Chan, S.I. (1987) *Biochemistry*, **26**, 7311-7316.

Denis, M. and Neu, E. (1985) *J. Inorg. Biochem.* **23**, 259-262.

Ellis, W.R. Jr., Wang, H.W., Blair, D.F., Gray, H.B. and Chan, S.I. (1986) *Biochemistry*, **25**,161-167.

Fiamingo, F.G., Altschuld, R.A., Moh, P.P. and Alben, J.O. (1982) *J. Biol. Chem.* **257**, 1639-1650.

Findsen, E.W., Centeno, J., Babcock, G.T. and Ondrias, M.R. (1987) *J. Am. Chem. Soc.* **105**, 5367-5372.

Gelles, J., Blair, D.F. and Chan, S.I. (1986) *Biochim. Biophys. Acta*, **853**, 205-236.

Goodman, G. and Leigh, J.S. Jr. (1987) *Biochim. Biophys. Acta*, **890**, 360-367.

Greenwood, C., Wilson, M.T. and Brunori, M. (1974) *Biochem. J.* **137**, 205-215.

Hartzell, C.R. and Beinert, H. (1974) *Biochim. Biophys. Acta*, **368**, 318-338.

Hill, B.C. and Nicholls, P. (1980) *Biochem. J.* **187**, 809-818.

Hill, B.C., Greenwood, C. and Nicholls, P. (1986) *Biochim. Biophys. Acta*, **853**, 91-113.

Hiromi, K. (1979) *Kinetics of Fast Enzyme Reactions*, N.Y., Halsted Press.

Kuboyama, M., Takemori, S. and King, T.E. (1962) *Biochim. Biophys. Res. Comm.* **9**, 534-539.

Milder, S.J., Goldbeck, R.A., Kliger, D.S. and Gray, H.B. (1980) *J. Am. Chem. Soc.* **102**, 6761-6764.

Morgan, J.E., Blair, D.F. and Chan, S.I. (1985) *J. Inorg. Biochem.* **23**, 295-302.

Nicholls, P. and Chanady, G.A. (1981) *Biochim. Biophys. Acta*, **634**, 256-265.

Petersen, L.C. and Andréasson, L.E. (1976) *FEBS Lett.* **66**, 52-57.

Sharrock, M. and Yonetani, T. (1977) *Biochim. Biophys. Acta*, **462**, 718-730.

Smith, L. (1955) in *Methods in Biochemical Analysis*, Vol. 2 (D. Glick, Ed.) Wiley, N.Y., pp. 427-434.

Vanneste, W.H. (1966) *Biochemistry*, **5**, 838-848.

Veerman, E.C.I., Wilms, J., Casteleijn, G. and Van Gelder, B.F. (1980) *Biochim. Biophys. Acta*, **590**, 117-127.

Wang, H., Blair, D.F., Ellis, W.R. Jr., Gray, H.B. and Chan, S.I. (1986)*Biochemistry*, **25**, 167-171.

Wikström, M. (1981) in *Interaction Between Iron and Proteins in Oxygen and Electron Transport*, (C. Ho and W.C. Eaton, eds), Elsevier, New York.

Chapter III

Temperature Jump Studies of Electron Equilibration in CO Inhibited Cytochrome *c* Oxidase

Introduction.

The last chapter described a flash photolysis experiment to study the Fe_a -- Cu_A electron equilibration rate. In that experiment, the redox equilibrium between Fe_a and Cu_A was perturbed by photolyzing $Fe_{a_3}{}^{2+}$–CO at the oxygen binding site, some distance away. After the photolysis, an electron redistribution from Fe_a to Cu_A with an apparent rate of about 17,200 s^{-1} was observed. However, the meaning of this apparent rate is still open to question. One reason for this is that it is not possible to tell from the data whether the observed kinetics are a true single exponential decay, or whether they are the first part of a longer multiphasic process. This question could be answered if the process could be followed for a sufficiently long time, or if the true equilibrium extent of the reëquilibration were known. Unfortunately, for reasons described in the previous chapter, these solutions may not be possible for the flash photolysis experiment.

Another possible way to perturb this Fe_a -- Cu_A equilibrium is by means of a rapid temperature-jump. This would be possible if the redox equilibrium between these two sites is sufficiently temperature sensitive. The temperature dependences of the redox potentials of Fe_a and Cu_A in the CO inhibited enzyme have been measured by Ellis et al. (1986) and Wang et al. (1986), but their results are not sufficiently precise to decide whether this experiment would be possible. However, results presented here demonstrate that upon warming, the redox equilibrium shifts enough for the change to be measured using conventional T-jump techniques.

If the reëquilibration could be measured using this technique, some of the limitations in interpreting the rate might be overcome. First, the extent of the reëquilibration can be determined, because equilibrium measurements can be made at different temperatures. Second, using the T-jump method, it is possible to observe the reaction for a longer time. In principle, a T-jump measurement can be followed until the thermostat begins to cool the cell back down, a time of over a second. (In our apparatus, an electronic artifact has thus far limited this time to about 0.1 s.)

Compared to the laser flash experiment, the T-jump technique also has it's drawbacks. The biggest of these is that the dead time of the instrument (the length of the heating pulse) is typically ten to thirty microseconds. The half time of the reëquilibration measured in the flash experiment is about 35 μs. This means that, in a T-jump experiment, the reaction could be largely complete during the heating pulse time, and if any of the kinetic progress could be observed, the finite length of the heating pulse would be convoluted into it (for a discussion of this see Stewart). Thus, the T-jump technique might only provide a lower limit to the apparent rate.

This would not actually be so bad. A lower limit on this rate, and the forward and backward rates would still be very useful in understanding the function of the enzyme. Furthermore, this information could be complementary to the data from the flash experiment. The T-jump results might help with the interpretation of the flash photolysis data. If, in the T-jump experiment, the entire relaxation was complete on a time scale consistent with the rate seen in the flash experiment, this would suggest that the fast process in the latter experiment was also the complete relaxation. This, in

turn, could lend some credence to the separation of forward and reverse rates, suggested in the previous chapter.

One complication to this kind of experiment is that raising the temperature of the sample may cause other changes besides shifting the redox equilibrium in question. This is especially true in the case of a system as large and complicated as an enzyme. It is known that when cytochrome *c* oxidase is heated above about 43 °C, the enzyme undergoes irreversible structural changes at both the Cu_A site and at the oxygen binding site (Sone and Nicholls, 1984; Sone et al., 1986; Li et al., 1988). However, no perturbations of functional significance would be expected for an increase of 5 °C in the 5 to 25 °C range, where these T-jump experiments are carried out. The main concern is temperature dependent changes in the visible spectrum of the enzyme which would interfere with the measurement itself. Orii and Miki (1979) reported temperature dependent band shifts in the visible spectrum of both the oxidized and the reduced forms of the native enzyme. They report that the changes which resulted from warming the oxidized enzyme were completely reversible, but that the changes observed in the reduced enzyme had a reversible and an irreversible component. They attributed these changes to conformational changes in the enzyme. In this context, temperature dependent spectral changes are of interest only because they must not be mistaken for redox related changes in the spectrum. However, this experiment would provide the opportunity to measure the rate of these non-redox related changes as well.

The results in this chapter demonstrate that the T-jump experiment is feasible. Equilibrium measurements are presented which show that the

temperature dependence of the Fe_a -- Cu_A redox equilibrium is large enough that a reëquilibration should be visible using standard T-jump techniques. Then preliminary kinetic data are presented. Unfortunately, the present data are not unambiguous, but they do indicate that the measurement is possible. In addition, temperature dependent band shifts have been observed in the CO inhibited enzyme which are similar to the reversible component reported by Orii and Miki (1979); no changes were found to correspond to their irreversible component. T-jump measurements show that, at least in the COFR enzyme, the band shift is very fast ($k_{app} > 20{,}000\ s^{-1}$).

As noted in the introduction, a T-jump kinetic measurement has been reported on a similar system. Greenwood et al. (1976) poised a sample containing cytochrome *c* and CO inhibited cytochrome *c* oxidase at a level of reduction at which Fe_a , Cu_A and cytochrome *c* were all partially reduced, and then perturbed this system by T-jump. They monitored the levels of reduction of Fe_a and cytochrome *c* and observed a two phase relaxation. They assigned the fast phase to the cytochrome *c* to Fe_a equilibration, and the slow phase (apparent rate 40-100 s^{-1}) to the Fe_a to Cu_A equilibration. As discussed earlier, there may be an alternative explanation for their slow phase. The present experiment has the advantage that this reëquilibration could be observed directly.

Materials and Methods.

The preparation of cytochrome *c* oxidase, and the preparation and handling of the CO inhibited enzyme has been described in an earlier chapter. (A few variations in sample preparation and handling are described below.)

Temperature-Jump Apparatus. Temperature-jump measurements were made using a Dionex-Durrum D-150 temperature-jump apparatus installed in a Dionex-Durrum D-100 stopped-flow apparatus. Because the samples were air sensitive, the apparatus was enclosed in a glove box (Vacuum Atmospheres Corporation). The lamp and monochromator were located outside of the box, and the probing light was brought into the box by means of a fiber optic bundle (Polymicro Technologies.) Due to space constraints, the mirror box -- a periscope arrangement which focuses the light from the monochromator onto the cell -- was removed. Instead, the output of the monochromator was focused onto the fiber optic bundle with a lens (50 mm focal length, 1.5 inches diameter, S1-UV quartz, Oriel Corporation.) A heat exchange system was used to control the temperature of the instrument without compromising the anaerobicity of the glove box. The water from the instrument's cooling circuit was pumped out of the box, through a coil of steel tubing immersed in a temperature control water bath (Haake FK2) and then back into the glove box. The entire loop outside of the glove box was sealed and made of steel tubing except for the pump and pump connections which were plastic. The pump was a sealed unit driven by magnetic coupling.

In order to cover the desired time window, two different arrangements were used for amplification of the photomultiplier (PMT) output. 1) The logarithmic amplifier in the stopped-flow apparatus was used to give an output in absorbance units. The shortest time constant available with this amplifier is 0.5 ms. There is also an electronic baseline artifact which has the form of a rising exponential decay with a characteristic time of about 0.4 s. Thus, there are upper and lower limits to the time window observable with this amplifier. 2) The output from the PMT was applied across a 100 KΩ resistor, and the voltage across this resistor was fed into an AC amplifier (Hewlett-Packard model 465A operated at the 20 dB gain setting.) The input capacitance of this amplifier is less that 20 pF giving a detection time constant of about 2 μs. The AC coupling time constant of this amplifier is about 0.1 s. This system produced a signal proportional to change in transmittance. In both cases, the output was read out on a storage oscilloscope and recorded photographically.

The amplitude of the temperature jump was calibrated using a dye solution with a temperature sensitive absorbance, as described by Hiromi (1979). The dye solution consisted of phenolphthalien in a buffer containing 100 mM glycine and 500 mM NaCl at pH 9.5. The pK_a of glycine is temperature sensitive, and so the pH of the solution varies with temperature. The pH of 9.5 is chosen to be near the color transition pK_a of phenolphthalien. The end result is that the absorbance of the phenolphthalien varies as a function of temperature. In the course of these calibrations it was found that when the temperature increase was extrapolated to zero, the corresponding pulse width was about negative 8 μs. Apparently, the actual pulse width produced by this instrument is 8 μs larger than the setting on the dial. This technique was also

used to calibrate the AC amplifier. The T-Jump cell was found to have a shorter light path than the specified 20 mm. However, because the temperature change was calibrated this way, the data should be self-consistent, and no correction was applied.

The enzyme samples used in kinetic experiments were initially prepared in concentrated form (as described in the previous chapter) and then diluted anaerobically to the desired concentration. The concentrated samples were typically in a buffer of 50 mM NaMOPS, 0.5% Tween-20. They were diluted about 30 fold into a buffer of 100 mM NaMOPS, 500 mM NaCl, 0.5% Tween-20. The conductivity of the diluting buffer (at room temperature) was within 5% of that of the calibrating buffer. In calculating the results, no correction was made for differences between the conductivities of the standard solution and the samples.

Optical Spectroscopy. Optical spectra in the visible and near infrared region (350-900 nm) were collected on a Beckman Acta (Model C-III) dual beam spectrophotometer, the digital output of which was recorded on a Spex Scamp computer. Baseline spectra were digitally subtracted. Temperature control was maintained by means of a water cooled metal cell holder attached to a refrigerated water bath. The system was calibrated by measuring the temperature in a cell, and at the cell holder at various bath temperatures. Temperatures at the cell holder were measured at the cell holder by the "Beckman TM Programmer" temperature controller, or with a digital thermometer (Fluke, model 51K/J).

Anaerobic Techniques. The samples for the pilot equilibrium temperature difference measurements were made as described in the previous

chapter except for the following differences: 1) The samples were made at the concentration at which they were to be used; i.e., they were not diluted after reduction. 2) The NADH was added anaerobically. The samples used in the kinetics experiments were made as described in the previous chapter except that the fully reduced samples were made by adding solid sodium dithionite to partially reduced samples inside the glove box.

Before samples were injected into the T-jump apparatus they were partially de-gassed (inside the glove box) by placing them in a large plastic syringe, covering the tip of the syringe with parafilm, and drawing back the plunger. After each kinetic experiment, some of the remaining sample was taken from the loading syringe and placed in a sealed optical cuvette. These samples were taken out of the glove box and used for equilibrium temperature difference measurements.

Water and buffers were made anaerobic before they were introduced into the glove box. This was achieved by placing the solution in a sealed container, and then stirring with a magnetic stirrer while flowing anaerobic nitrogen or argon through the container's headspace. Teflon covered stir bars used for this purpose were first pumped to down on the vacuum line to remove absorbed oxygen. Nitrogen was made oxygen free by bubbling it through solutions of containing vanadium (II).

Samples and supplies were brought into the glove box through the air lock. Typically, the air lock with the supplies inside was evacuated for twenty minutes before being opened to the interior of the box. However, when oxygen absorbing plastic items such as parafilm or syringes were brought in, the air lock was usually evacuated overnight. Samples, water, and buffers

enclosed in vacuum line glassware posed a special problem since they contained an atmosphere of gas. If the containers were not sealed tightly enough, they could explode or blow out their stopcocks against the force of the retaining springs. However, if extra springs were used and the stopcock was blown open, the container could be shattered when the springs recoiled. The best solution found was to hold the stopcocks on weakly with springs and also tie them down with copper wire. Under this arrangement, the stopcock could move out far enough to vent the atmosphere, but would not travel far enough to do damage when the springs recoiled.

Results and Discussion.

The kinetic studies presented in the previous chapter made use of three different classes of CO inhibited samples: the CO mixed valence enzyme, the fully reduced CO inhibited enzyme, and samples poised at an intermediate three electron level of reduction. These were designated as COMV, COFR and COMV+1 respectively. (Example spectra are shown in fugure II.2) Since the COMV+1 is partially reduced, it contains a subpopulation in which Fe_a and Cu_A are in a dynamic redox equilibrium. In the previous experiment, a flash photolysis technique was used to perturb this equilibrium. The COMV and COFR were used as controls for changes which were not related to the movement of electrons. The objective of the experiments in this chapter is to use a temperature-jump method to study these same kinetics.

The first step was to investigate whether an electron reëquilibration occurred upon warming the COMV+1 sample. Figure III.1 shows the changes

Figure III.1.

Temperature difference spectra of CO inhibited cytochrome oxidase at various reduction levels. A) COMV; B) COMV+1; C) COFR. Dots, 14°C minus 6.5°C; dashes, 21.5°C minus 6.5°C; solid line, 28.5°C minus 6.5°C. Enzyme concentration: 48 μM; buffer 5 mM NaMOPS, 100 mM NaCl, 0.5% Tween-20; path length, 10 mm.

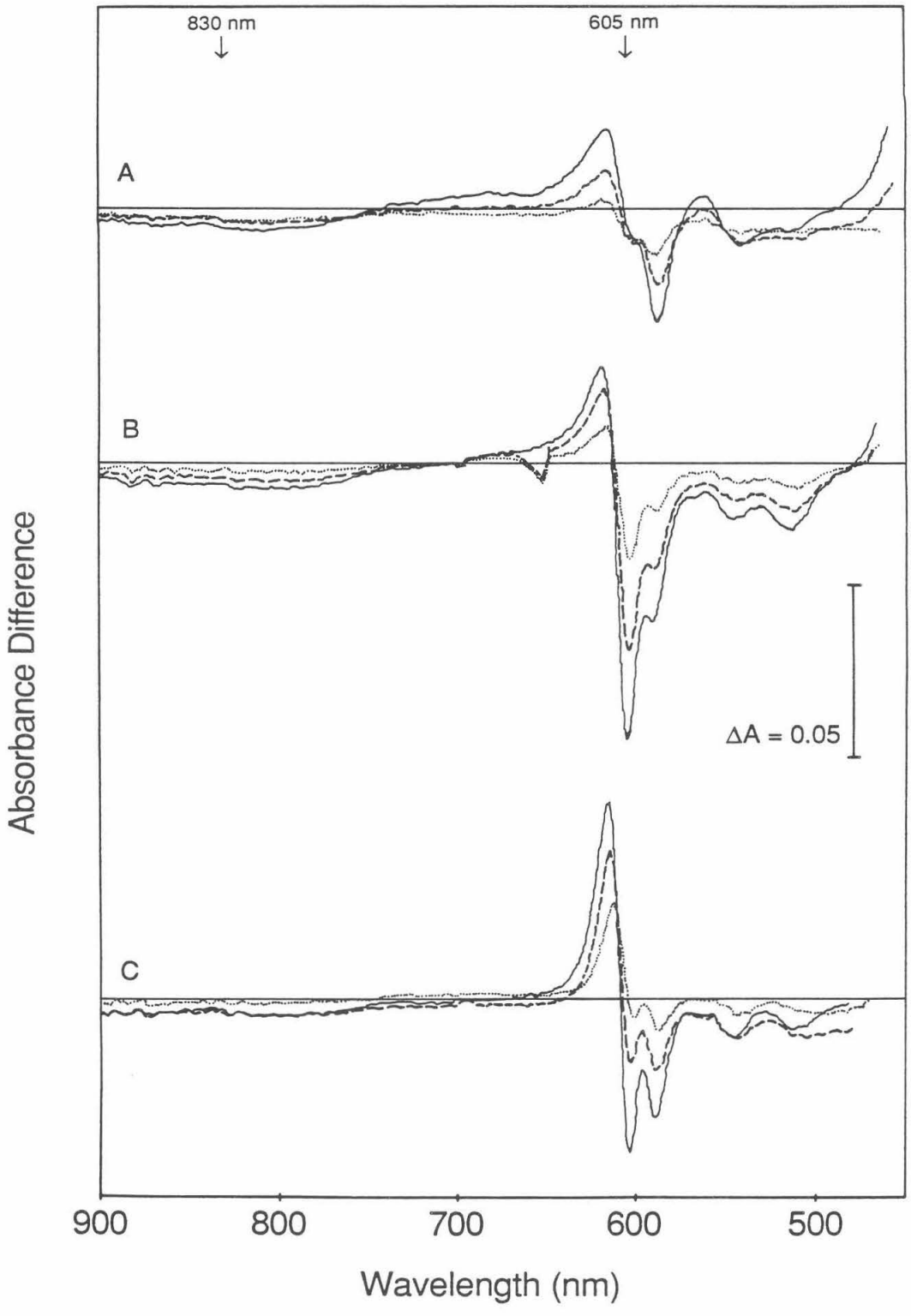
830 nm
605 nm
A
B
C
ΔA = 0.05
Absorbance Difference
900
800
700
600
500
Wavelength (nm)

in absorbance at which occurred in COMV, COMV+1 and COFR samples as the temperature was raised in a series of steps. In each case the sample was allowed tens of minutes to equilibrate at the new temperature. The temperature difference spectra for the COMV+1 sample are shown in figure III.1b. As the temperature of this sample was raised, there were parallel decreases in absorbance at 605 nm and in the near infrared, corresponding to the alpha band of Fe_a^{2+} and the 830 nm band arising from Cu_A^{2+} respectively. A decrease in absorbance at both of these wavelengths is consistent with an electron redistribution from Fe_a to Cu_A. However, the magnitude of the absorbance changes is what would be expected if slightly more that half as much Cu_A was reduced as Fe_a was oxidized. Figure III.1a shows that when the COMV compound was warmed, there was very little change in absorbance at 605 nm. Small changes were observed in the near infrared but they did not appear to come from a systematic change in the 830 nm band intensity. In the case of the COFR compound (Figure III.1c), a large decrease in absorbance at 605 nm was observed. Again, there were small changes in absorbance in the near IR, but there did not appear to be a systematic change in the 830 nm band. There was significant variation in the temperature difference spectra for the COFR compound. In a different run through the same temperature steps, the decrease in absorbance at 605 nm was as large as that observed in the COMV+1 sample, and almost no changes at all were observed in the near infrared.

Thus, the absorbance change at 605 nm in the COMV+1 is twice as large as it would be if the only contribution was an electron redistribution from Fe_a to Cu_A. However, the temperature difference spectrum of the COFR shows a

large decrease in absorbance at 605 nm. Since no electron distribution is possible in the COFR, this must be due to a temperature dependent shift in the Fe_a^{2+} absorption band. These data suggest that upon warming, an electron redistribution does occur in the COMV+1 samples, but that about half of the absorbance change observed at 605 nm arises from a temperature dependent shift in the Fe_a^{2+} spectrum.

In order to check this conclusion, the contribution of non-redox related absorbance changes to the COMV+1 temperature difference spectrum was estimated. If no electron reëquilibration took place, the temperature difference spectrum of the COMV+1 should be a linear combination of the difference spectra for the COFR and COMV samples with contributions proportional to the fraction of reduced and oxidized Fe_a in the sample. Based on this assumption, a COMV+1 temperature difference spectrum without any electron reëquilibration component was simulated. The change in absorbance at 605 nm in this simulated difference spectrum accounted for slightly less that half of the absorbance difference in the real COMV+1 sample, indicating that at least half of the absorbance change in the real difference spectrum was unique to the COMV+1 compound, and presumably represented the oxidation of Fe_a^{2+}. Since this analysis was based on the largest absorbance changes observed at 605 nm in the COFR enzyme, the contribution of that component should be taken as an upper limit.

This agrees with the estimate based on the size of the 830 nm absorbance changes. (The estimate from the 830 nm data involves an implicit assumption that any near infrared absorbance changes in the COFR and COMV are not present in the COMV+1.) Thus, an electron redistribution does take place upon

warming the COMV+1 sample, and it makes a significant contribution to the temperature difference spectrum.

The next step was to try to measure the rate of these absorbance changes using the temperature-jump apparatus. Figure III.2, 3 and 4 showstemperature-jump kinetic data for COMV+1, COFR and COMV samples subjected to aproximately a 6 °C jump in temperature (but see Materials and Methods.) These data are presented as progress towards the goal stated in the introduction. This is not a finished experiment, and the data must not be overinterpreted. For this reason, more technical details are presented that might be usual.

As noted in the Materials and Methods section, two different amplifiers were used, a fast AC amplifier, and a slower logarithmic amplifier. The logarithmic amplifier gave an output which could be read directly in absorbance units, and the data are marked accordingly. The output of the AC amplifier was in voltage, proportional to transmittance, and the scale for those traces is given in voltage units. (The calibration factor used for these data was: ΔTransmittance = -0.09 ΔV.)

Figure III.2 shows the T-jump data for the COMV+1 sample. Fast absorbance changes were observed at 605 nm and 615 nm. In both cases, the changes appeared to occur during the heating pulse, and no slower phases were observed. The slow processes in Figure III.2b.and d are electronic artifacts. Figure III.3 shows parallel data for the COFR compound. Once again, a fast absorbance changes was observed at 615 nm. At 605 nm, there was a decrease in absorbance which was resolved with the slower amplifier. Although a small apparent change was observed using the faster amplifier,

Figure III.2.

Temperature-jump kinetics data (oscilloscope photographs) of COMV+1 sample at 605 nm and 615 nm*. Pulse width setting: 20 μs, except for b. where 30 μs was used (in most cases where the 30 μs pulse width was used the termination spark gap switch failed to fire and the heating pulse was not terminated); pulse voltage 5 KV; thermostat temperature: 6 °C; approx temperature increase 5.8 C; slit width 1 mm, except for c. and d where 0.2 mm slit width was used. Oscilloscope settings are indicated. The upper two traces were recorded using the fast AC amplifier. The lower two traces were recorded using the logarithmic amplifier. Enzyme concentration: 9.4 μM; buffer: 100 mM NaMOPS, 500 mM NaCl, 0.5% Tween-20; optical path length: 20 mm (see materials and methods). *In the case of d. the instrument had been calibrated at 605 nm and the monochromator set to 615 nm without recalibration.

Carbon Monoxide Inhibited Cytochrome *c* Oxidase -- Partially Reduced (COMV+1)

Temperature-Jump Kinetic Traces

605 nm.

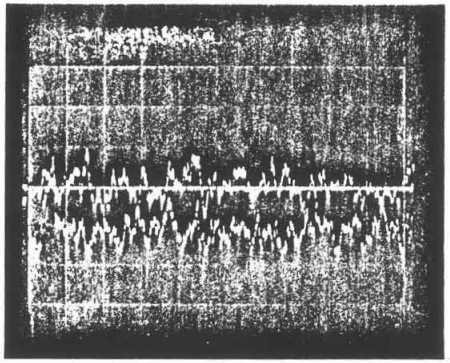

← baseline

50 μs per division.
50 mV per division.

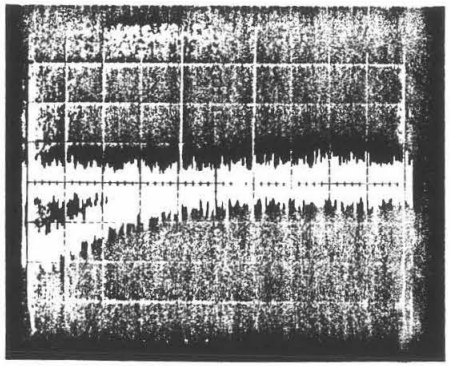

← baseline

100 ms per division.
ΔA 0.005 per division.
0.2 mm slit width.

615 nm*.

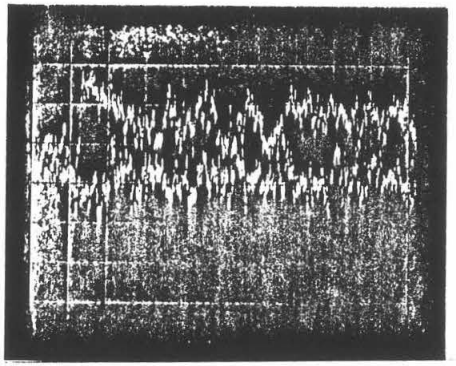

← baseline

100 μs per division.
50 mV per division.
30 μs heating pulse width.

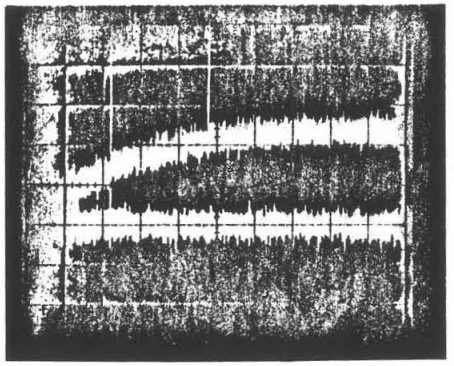

← baseline

100 ms per division.
ΔA 0.005 per division.
0.2 mm slit width.
*See figure caption.

Figure III.3.

Temperature-jump kinetics data (oscilloscope photographs) of COFR sample at 605 nm and 615* nm. Pulse width setting: 20 μs,; pulse voltage 5 KV; thermostat temperature: 6 °C; approx temperature increase 5.8 C; slit width 1 mm. Oscilloscope settings are indicated. The upper two traces were recorded using the fast AC amplifier. The lower two traces were recorded using the logarithmic amplifier. Enzyme concentration: 9.4 μM; buffer: 100 mM NaMOPS, 500 mM NaCl, 0.5% Tween-20; optical path length: 20 mm (see materials and methods). *In the case of b. the instrument had been calibrated at 605 nm and the monochromator set to 615 nm without recalibration.

Carbon Monoxide Inhibited Cytochrome *c* Oxidase -- Fully Reduced

Temperature-Jump Kinetic Traces

605 nm.

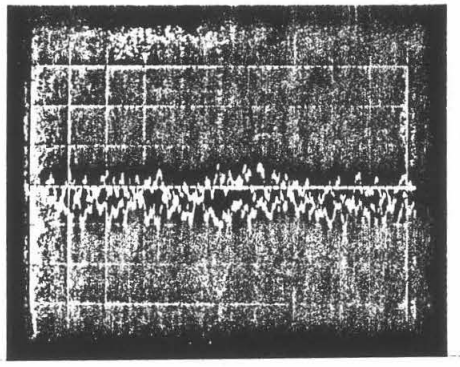

← baseline

50 μs per division.
50 mV per division.

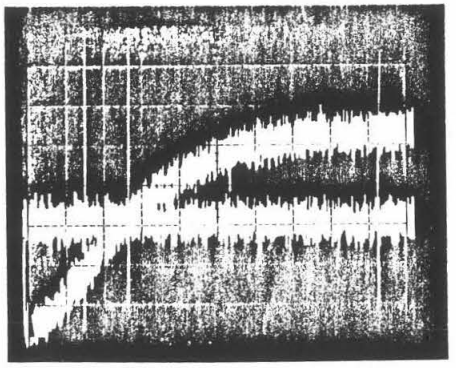

100 ms per division
ΔA 0.002 per division

← baseline

615 nm*.

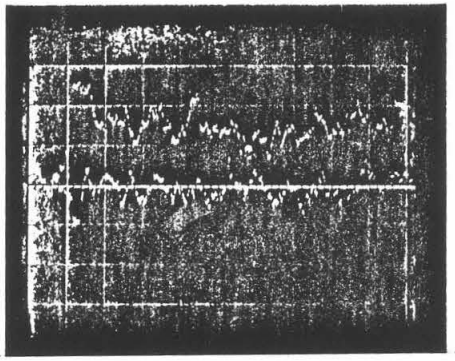

← baseline

20 μs per division.
50 mV per division.
*See figure caption.

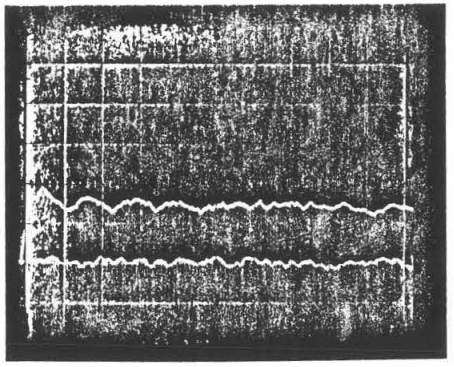

2 ms per division.
ΔA 0.005 per division

← baseline

Figure III.4.

Temperature-jump kinetics data (oscilloscope photographs) of COMV sample at 605 nm. Pulse width setting: 20 μs,; pulse voltage 5 KV; thermostat temperature: 6 °C; approx temperature increase 5.8 C; slit width 0.2 mm. Oscilloscope settings are indicated. The upper two traces were recorded using the fast AC amplifier. The lower trace was recorded using the logarithmic amplifier. Enzyme concentration: 11.8 μM; buffer: 100 mM NaMOPS, 500 mM NaCl, 0.5% Tween-20; optical path length: 20 mm (see materials and methods).

Carbon Monoxide Mixed Valence Cytochrome *c* Oxidase

Temperature-Jump Kinetic Traces

605 nm.

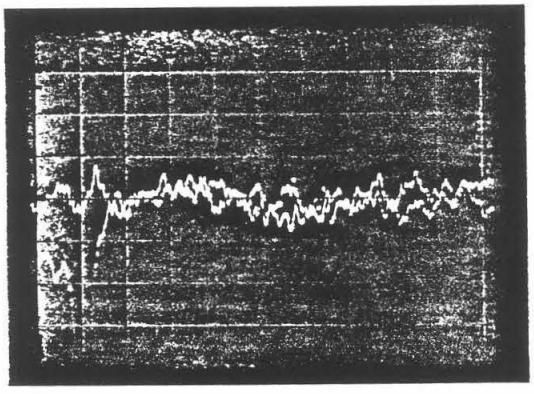

← baseline

20 μs per division.
100 mV per division.
0.2 mm slit width.

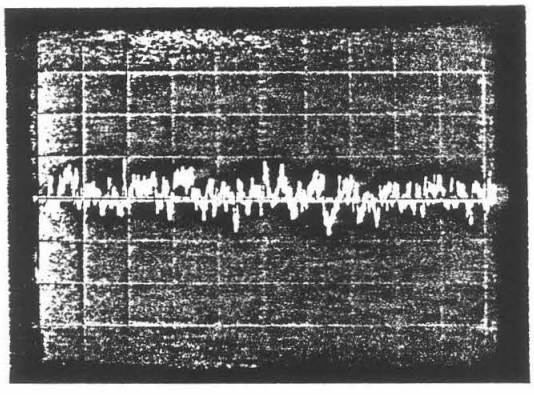

← baseline

100 μs per division.
100 mV per division.
0.2 mm slit width.

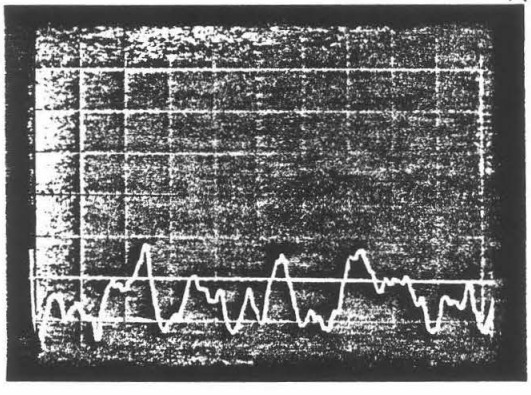

1.0 ms per division.
ΔA 0.002 per division.
0.2 mm silt width.

← baseline

the noise level was too large to be sure. In the case of the COMV sample (figure III.4), no absorbance changes were resolvable using either amplifier.

As indicated in the figure legend, some of these data were recorded using a 0.2 mm slit width and some using a 1.0 mm slit width. The smaller slit was originally chosen in order to minimize photolysis of $Fe_{a_3}{}^{2+}$–CO in the sample by the probe light. If CO is photolyzed from the oxygen binding site, redox activity at Fe_{a_3} and Cu_B would be possible, and the kinetic processes could not be assigned unambiguously. However, with the 0.2 mm slit width, it was never possible to resolve any absorbance changes at the fast time scale. In order to investigate the possibility of photolysis when the larger slit width was used, the absorbance of a COMV sample at 590 nm, a wavelength characteristic of $Fe_{a_3}{}^{2+}$–CO (Vanneste, 1966), was measured at both slit widths. The absorbance measured with the 1.0 mm slit width was slightly smaller than that measured with the 0.2 mm silt width. This could have been a direct result of measuring with a larger slit width, or a result of photolysis of $Fe_{a_3}{}^{2+}$–CO in the brighter probe beam. The latter possibility should be investigated further (see below).

Figure III.5 shows temperature difference spectra for the same samples which were used for the T-jump measurements above. Two important differences between these samples and the ones used in the earlier equilibrium study should be noted. First, the concentration of the kinetics samples was significantly lower. The concentration in these samples was chosen so that the absorbance of the COMV+1 sample at 605 nm would be 0.8 or less in the T-jump cell, which has an optical path length of 20 mm. (The actual path length is slightly smaller; see Materials and Methods. Also, the actual

Figure III.5

Temperature difference spectra (20 °C minus 4 °C) of CO inhibited cytochrome *c* oxidase at various levels of reduction: a, COMV; b, COMV+1, c, COFR. The vertical I-bar beside each trace represents the extent of the absorbance change at 605 nm or 615 nm observed in the T-jump experiment (see text). The T-jump conditions are described in figures III.2,3 and 4 but the extents have been scaled to reflect the differences in optical path length and temperature change. Optical path length for spectra: 10 mm. All data have been scaled to represent an enzyme concentration of 9.4 μM.

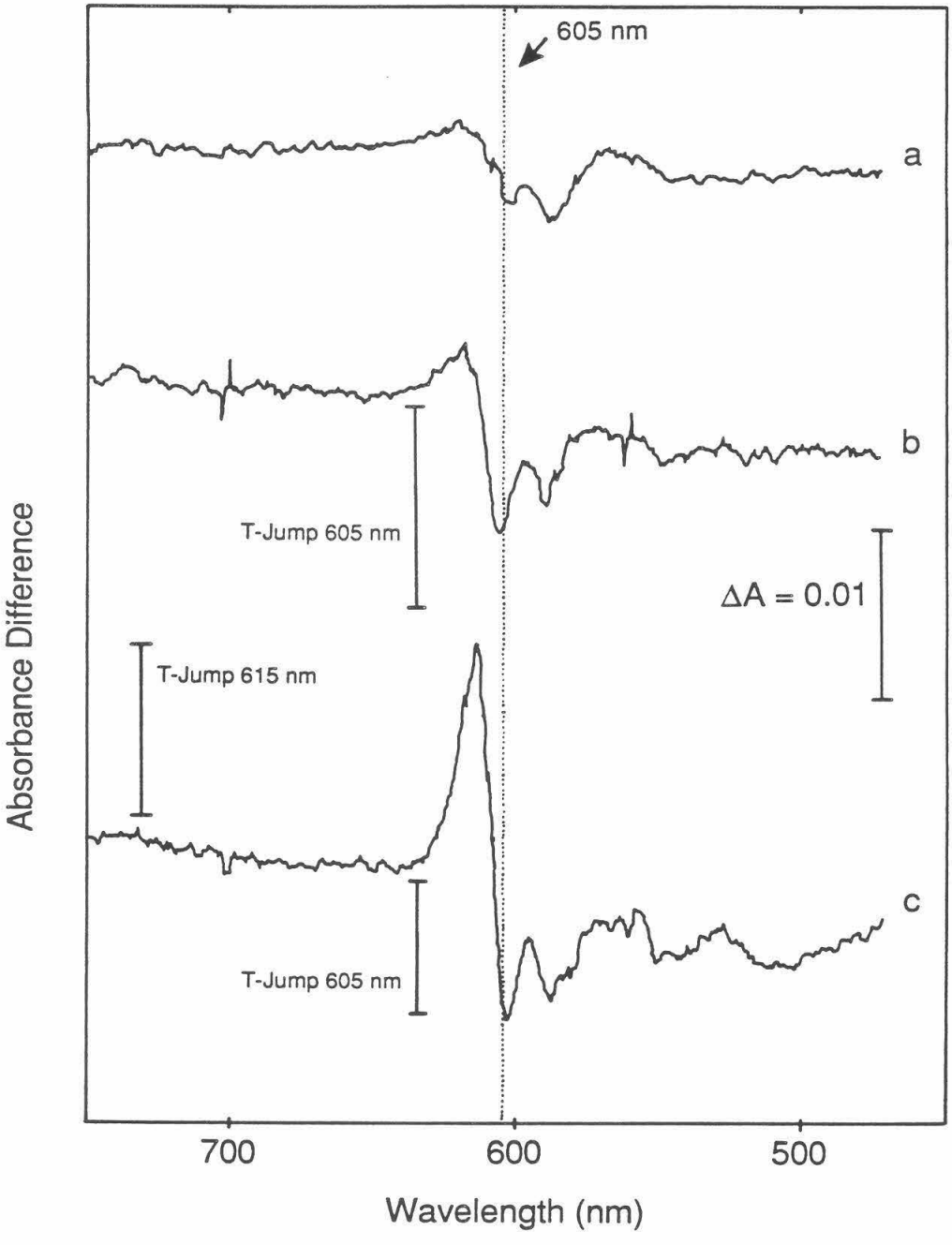
605 nm
a
b
T-Jump 605 nm
ΔA = 0.01
T-Jump 615 nm
c
T-Jump 605 nm
Absorbance Difference
700
600
500
Wavelength (nm)

absorbance of the samples at 605 nm was closer to 0.54.) At this lower concentration, the noise in the visible region difference spectra was significant, and observation of temperature dependent changes in the 830 nm band was out of the question. Second, the ionic strength of the buffer was increased from about 100 mM to above 500 mM. This was done in order to increase the conductivity of the solution so that the heating pulse width could be decreased. It should also be noted that once this ionic strength had been selected, the starting temperature of the T-jump experiment could not be increased, because increasing the temperature would increase the conductivity of the solution to a point where the the rapid heating might shatter the cell.

These temperature difference spectra are generally similar to the earlier ones. However, based on these spectra, the evidence for an electron redistribution in the COMV+1 sample is not unambiguous. The same simulation of non-redox related changes was repeated here. There is a component in the COMV+1 temperature difference spectrum which cannot be accounted for in terms of temperature dependent band shifts, but the amplitude of this component is largest at about 608 nm, and it is small at 605 nm (where Fe_a^{2+} absorbs maximally). The interpretation is also complicated by some relatively large changes in the baseline.

The results of the T-jump kinetics are also summarized in figure III.5. The vertical I-bars represent the amplitude of the absorbance changes observed in the T-jump experiment, corrected for the size of the temperature change and the optical path length. The data from the absorbance amplifier were used to calculate these amplitides. The results calculated from the AC

amplifier data were consistently about 20% smaller. However, since no slow changes in transmittance were observed, and since this difference was seen fairly consistently, it probably reflects an inaccuracy in the calibration of this amplifier (see Materials and Methods).

The data clearly show that the fast absorbance changes observed in the T-jump experiment are large enough to account completely for the increase at 615 nm and the decrease at 605 nm in the COFR temperature difference spectrum. The fast absorbance decrease at 605 nm appears to be a little bit larger that the measured equilibrium change.

The temperature-jump results show that if an electron redistribution as large as the one in the COMV+1 pilot experiment (figure III.1) occurred, it could be observed by the T-jump experiment. Thus, the experiment we set out to do is feasible. The fast absorbance change observed at 605 nm in the COMV+1 sample accounts for all of the change observed at equilibrium, but unfortunately, this change cannot be unambiguously assigned to a redox process. As described above, the temperature difference spectrum for the COMV+1 sample (figure III.3) contains a component which cannot be accounted for in terms of temperature dependent band shifts. However, this component was largest at 608 nm, and was small at 605 nm. It is possible that at very high ionic strength, the Fe_a^{2+} absorbance band is shifted to 608 nm in which case, the T-jump measurement could be made at that wavelength. However, a T-jump measurement made at 607 nm on the same sample was not significantly different. Alternatively, the apparent shift could be an artifact of light scattering baseline changes. With the dilute samples, baseline shifts were sometimes as large as the difference peaks. In the case of the T-jump

kinetic data, baseline shifts do not appear to have been a problem, demonstrated by the fact that both increasing and decreasing absorbances could be measured in the same sample at different wavelengths.

Several minor changes should be made in the experiment. First, the ionic strength should be lowered to 150 mM. The existence of the electron reëquilibration under those conditions has been confirmed. Second, in view of the 20 to 30 μs heating pulse width, the PMT grounding resistor used with the fast amplifier could be increased to give a time constant of 10 to 15 μs without an increase in the effective dead time. Third, the kinetic data should be acquired in digital form, so that several transients can be averaged. This would be time consuming, but it is apparent that a small improvement in the signal quality could make a significant difference. Fourth, the possibility that a significant amount of $Fe_{a_3}{}^{2+}$–CO is photolyzed by the probe beam should be investigated using neutral density filters. Beyond this, it would be instructive to repeat the T-jump experiment of Greenwood et al. (1976) which included cytochrome *c* in the samples, under conditions where the results could be compared directly to the results with the COMV+1 system.

Temperature dependent band shifts are observed in all of the difference spectra, but the nature of these changes is not known. The largest component of the COMV temperature difference spectrum has a maximum at around 615 nm and a minimum at around 590 nm where the absorbance maximum of $Fe_{a_3}{}^{2+}$–CO is found. The temperature difference spectrum of the COFR appears to be made up of two components, one which is like the COMV difference described above, and a larger one which has a minimum at about 605 nm and a maximum at about 615 nm. The first of these components appears to arise from

$Fe_{a_3}{}^{2+}$–CO. It is present in the difference spectra of both the half- and the fully-reduced CO inhibited compounds and has a minimum corresponding to the absorbance maximum of $Fe_{a_3}{}^{2+}$–CO. The second component appears to arise from reduced Fe_a. It is not present in the COMV where Fe_a is in the ferric form, and it has its minimum at 605 where the absorbance maximum for $Fe_a{}^{2+}$ is found. Apparently, upon warming, some heme A species which has an absorbance maximum at about 615 nm is being reversibly populated. These temperature dependent band shifts are similar to changes observed by Orii and Miki (1979) in the native oxidized and fully reduced enzyme. In the native oxidized enzyme, the difference maximum and minimum they observe are at different wavelengths from those observed in the COMV. In the case of the reduced enzyme, they observe a reversible and an irreversible component. Their reversible component appears to be very similar to the component of the COFR difference spectrum which was assigned to Fe_a above. In the present work, there is no evidence of their irreversible component. One explanation would be that their irreversible component arises from reduced (native) Fe_{a_3}. The binding of CO might restructure the oxygen binding site in such a way that this temperature dependent band shift would be reversible.

The T-jump results on the fully reduced CO inhibited enzyme demonstrate that these temperature dependent band shifts in the COFR compound occur very quickly. Since these changes are apparently complete within the pulse width of the T-jump apparatus (28 μs) they presumably have apparent rate of greater than 20,000 s^{-1}.

References.

Ellis, W.R. Jr., Wang, H.W., Blair, D.F., Gray, H.B. and Chan, S.I. (1986) *Biochemistry*, **25**, 161-167.

Greenwood, C., Brittain, T., Wilson, M. and Brunori, M. (1976) *Biochem. J.* **157**, 591-598.

Hiromi, K. (1979) *Kinetics of Fast Enzyme Reactions*, N.Y., Halsted Press.

Li, P.M., Morgan, J.E., Nilsson, T., Ma, M., and Chan, S.I. (1988) *Biochemistry*, in press.

Orii, Y. and Miki, T. (1979) in *Cytochrome Oxidase*, (T.E. King et al., eds.) Elsevier/North-Holland Biomedical Press, pp. 251-256.

Sone, N. and Nicholls, P. (1984) *Biochemistry*, **23**, 6550-6554.

Sone, N., Ogura, T., and Kitigawa, T. (1986) *Biochim. Biophys. Acta*, **850**, 139-145.

Stewart, J.E. *Optimization of Instrument Conditions in Stopped-Flow and Temperature-Jump Experiments*, Application Notes, number 8, Dionex instrument corporation, Sunneyvale, CA.

Vanneste, W.H. (1966) *Biochemistry*, **5**, 838-848.

Wang, H., Blair, D.F., Ellis, W.R. Jr., Gray, H.B. and Chan, S.I. (1986) *Biochemistry*, **25**, 167-171.

Chapter IV

Temperature Jump Studies of Electron Equilibration in Cyanide Inhibited Cytochrome *c* Oxidase

Introduction.

In the previous chapter, results were presented which showed that in CO inhibited cytochrome *c* oxidase, the redox equilibrium between Fe_a and Cu_A shifts towards Cu_A as the temperature is raised. Progress towards measuring the rate of this redistribution using the temperature-jump technique was described, but the data were still inconclusive. In this chapter, a similar experiment involving the cyanide inhibited form of the enzyme is presented. Cyanide binds to ferric Fe_{a_3} and lowers its reduction potential, effectively preventing its reduction (Erecinska and Wilson, 1980). Fe_a and Cu_A are still redox active, as is Cu_B (Nicholls and Chanady, 1982).

Samples analogous to the two-, three- and four-electron reduced, CO inhibited samples described in the previous chapters can be made in the cyanide inhibited enzyme. They are: 1) the fully oxidized, cyanide inhibited enzyme (CNOx); 2) the "mixed valence cyanide compound" (CNMV), made by adding sodium dithionite to the oxidized cyanide inhibited enzyme; and 3) a sample made by adding between one and two electron equivalents of NADH to the cyanide inhibited enzyme. This third class of samples (which will be called CN+1), is roughly analogous to the COMV+1 samples in that there is a redox equilibrium between the partially reduced metal centers.

There are, however, at least three major differences between COMV+1 samples and CN+1 samples: First, in the CN+1 samples, Fe_{a_3} is in the oxidized, and not the reduced state. Second, in the CO inhibited enzyme, Cu_B is always in the reduced form, while in the cyanide inhibited enzyme, it may change redox state. The third difference is that although Fe_a and Cu_A are almost

equipotential in the CO inhibited enzyme, the redox potential of Fe_a in the cyanide inhibited enzyme, is about 48 mV higher than that of Cu_A (Goodman, 1984). This is a consequence of the redox anticoöperativity between Fe_a and the metals of the oxygen binding site. Oxidation of Fe_{a_3} causes the redox potential of Fe_a to be raised by about 35 mV (Blair et al., 1986). One result of this is that when the cyanide inhibited enzyme is partially reduced, the electron distribution between Fe_a and Cu_A will substantially favor the reduction of Fe_a.

The experimental design was the same as that used with the CO inhibited enzyme in the last chapter. These cyanide inhibited samples were subjected to small changes in temperature with the primary objective of studying the intramolecular movement of electrons in the partially reduced (CN+1) sample. To this end, equilibrium measurements were first made by recording the spectra of the samples at different temperatures and then subtracting to arrive at temperature difference spectra. As before, the temperature difference spectra for the various samples were compared in order to identify absorbance changes corresponding to temperature dependent electron redistributions. Then the temperature-jump method was used to investigate the kinetics of the temperature dependent absorbance changes. However, unlike the work with the CO inhibited enzyme, this experiment met with success, although from an unexpected quarter.

Materials and Methods.

The apparatus and techniques for the temperature-jump measurement

are described in the previous chapter. Thus, this section is devoted to the preparation of cyanide inhibited samples.

Cyanide inhibited cytochrome c *oxidase.* Cyanide inhibited cytochrome *c* oxidase was prepared by adding potassium cyanide from a concentrated solution to the enzyme to a final concentration of 1-6 mM and incubating the sample in the refrigerator for about 24 hours. Formation of the cyanide bound form of the enzyme was judged by the shift of the Søret band to 427 nm (Blair et al., 1982).

The CN+1 samples were prepared from the cyanide bound species by first making the sample anaerobic, adding one to two electron equivalents of NADH (not anaerobic), and then de-aerating the sample once again. The sample was then allowed to incubate in the refrigerator until reduced, as judged by its visible spectrum. As in the case of the COMV+1 samples, this compound was prepared at high concentration and then when necessary, diluted anaerobically to produce the desired concentration and pH.

Results.

The upper panel of figure IV.1 shows the visible spectra of fully oxidized cyanide inhibited cytochrome *c* oxidase (CNOx), the mixed valence cyanide enzyme (CNMV); i.e, cyanide inhibited enzyme subsequently reduced with excess sodium dithionite, and a sample poised at an intermediate level of reduction (CN+1). The lower panel of figure IV.1 shows the absorbance changes, which occur when each of these samples is warmed from 4 to 20 °C.

Figure IV.1

Upper frame: Visible absorption spectra of cyanide inhibited cytochrome *c* oxidase with increasing amounts of added reductant: CNOx (solid line); CN+1 (dashes); CNMV (dots). Lower frame: Temperature difference spectra of the same samples: a, CNOX; b, CN+1; c, CNMV. The spectra in the lower frame are the results of subtracting 4 °C spectra from 20 °C spectra. The spectra in the upper frame were measured at 20 °C. Enzyme concentration: 13 μM. (The CNOx and CNMV samples were actually at 15.6 μM and so the spectra have been scaled accordingly.) Buffer composition: 100 mM NaMOPS, 500 mM NaCl, 0.5% Tween-20, pH 7.4. This composition is approximate since samples were prepared in concentrated form in a buffer of lower ionic strength, typically 50 mM NaMOPS, and then into the higher ionic strength buffer. Approx. cyanide concentration before dilution, a and c: 2 mM; b: 5 mM; after dilution, a and c: 0.3 mM; b: 0.2 mM.

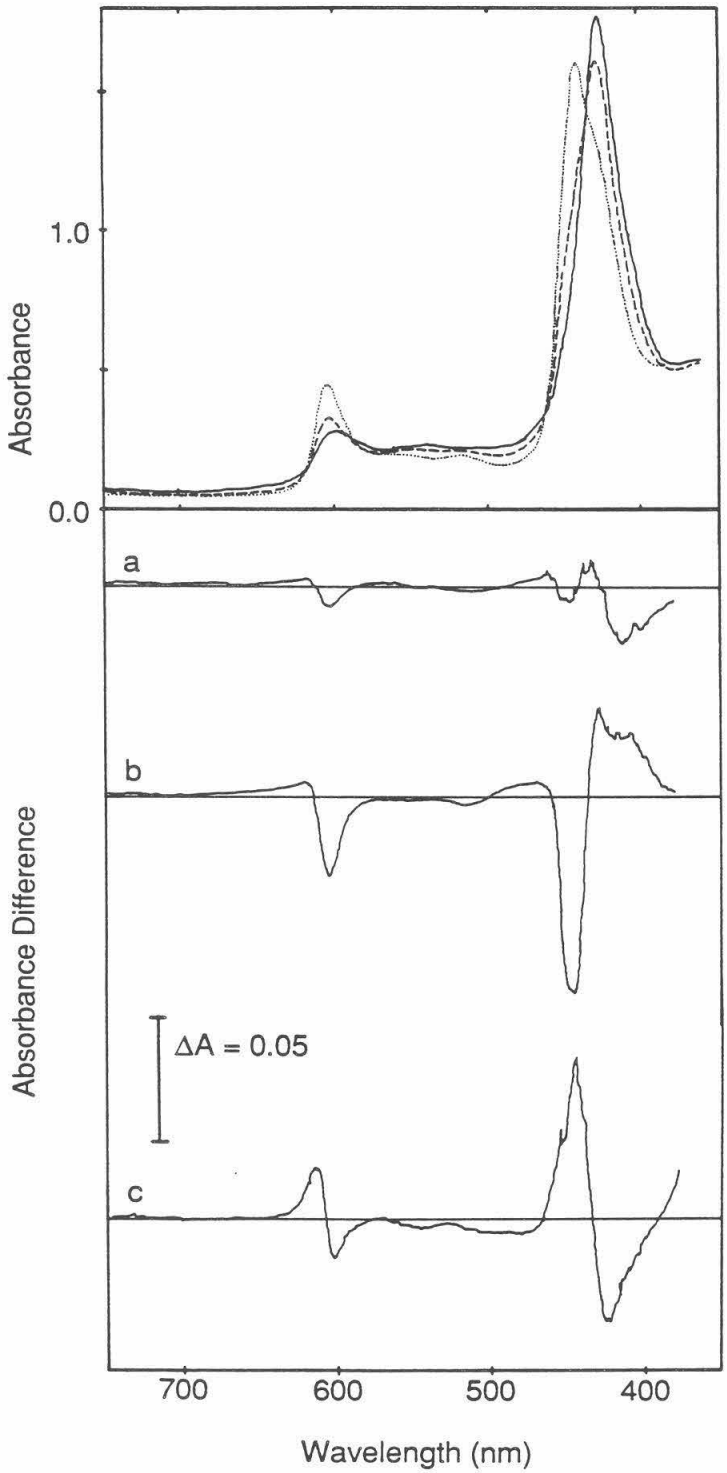
Absorbance
1.0
0.0
a
b
c
Absorbance Difference
ΔA = 0.05
700
600
500
400
Wavelength (nm)

All three temperature difference spectra show absorbance band shifts, but the CN+1 difference spectrum clearly contains a component which is not present in the other two samples. Changes are evident in both the alpha and Søret band regions which suggest that Fe_a is becoming more oxidized as the temperature is increased.

This is similar to what was seen when the partially reduced CO inhibited (COMV+1) samples were warmed. In that case, the oxidation of Fe_a was accompanied by the reduction of Cu_A, evidenced by a decrease in the intensity of the 830 nm absorption. In order to see whether the same electron redistribution was occurring in this experiment, the CN+1 temperature difference spectrum was measured again at a higher enzyme concentration at which the 830 nm band could be measured. Figure IV.2 shows the results of this measurement. In contrast to the results obtained with the COMV+1 samples (see figure III.1), there was no apparent reduction of Cu_A in this sample.

If these changes in the visible spectrum actually indicate the oxidation of Fe_a, then the electron acceptor must be Cu_B. There are only four redox active metal centers in the enzyme, and all the others can be discounted; Fe_a is the apparent donor, Fe_{a_3} is inhibited by cyanide, and will not accept an electron, and no redox changes are observed at Cu_A.

The kinetics of the absorbance changes at 605 nm were then investigated using the temperature-jump apparatus. Figures IV.3, 4 and 5 show the actual T-jump data for CN+1, CNOx and CNMV samples observed at 605 nm over a range of time scales. In each figure, the top two traces were measured using a fast AC amplifier, while the lower two traces were recorded

Figure IV.2

Upper frame: Absolute spectra of partially reduced, cyanide inhibited cytochrome *c* oxidase (CN+1) at 20 °C (dashes and trace A) and 4 °C (solid line and trace B). Inset: 830 nm region expanded vertically 14X. These traces have been offset vertically from one another for clarity. **Lower frame: Temperature difference spectrum (A-B above).** Enzyme concentration: 245 μM, path length 2 mm. Buffer composition: 100 mM NaMOPS, 500 mM NaCl, 2mM KCN, 0.5% Tween-20. In this case, the sample was dialyzed into this buffer.

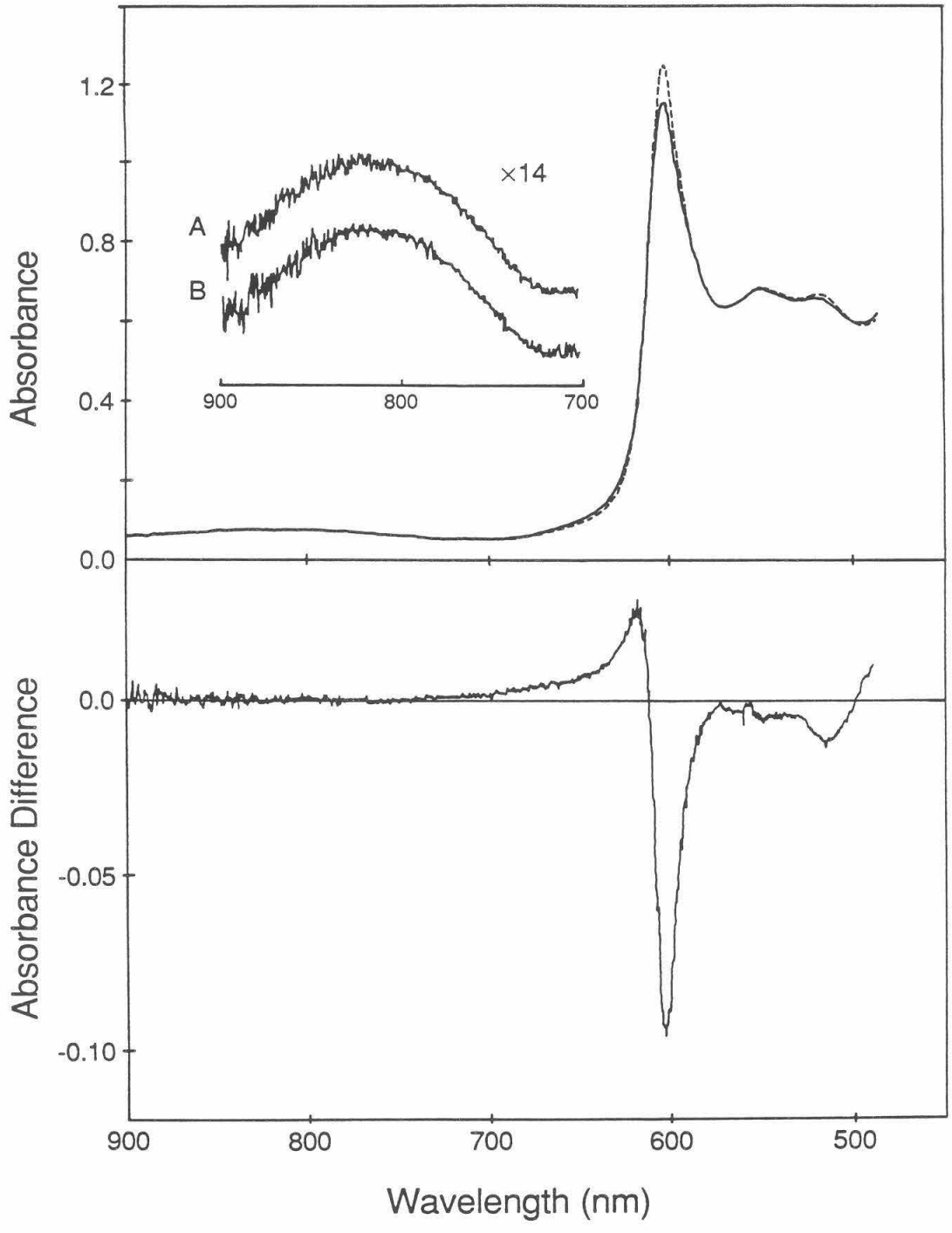
1.2
0.8
0.4
0.0
Absorbance
×14
A
B
900
800
700
0.0
-0.05
-0.10
Absorbance Difference
900
800
700
600
500
Wavelength (nm)

Figure IV.3

Temperature-jump kinetics data (oscilloscope photographs) of CN+1 sample at 605 nm. Pulse width setting: 20 μs; pulse voltage 5 KV; thermostat temperature: 6 °C; aprox temperature increase 5.8 C; slit width 1 mm. Oscilloscope settings are indicated. The upper two traces were recorded using the fast AC amplifier. The lower two traces were recorded using the logarithmic amplifier. Enzyme concentration: 13 μM; approx. cyanide concentration before dilution: 5 mM; after dilution: 0.2 mM; optical path length: 20 mm.

Cyanide Inhibited Cytochrome *c* Oxidase -- "CN+1"

Temperature-Jump Kinetic Traces

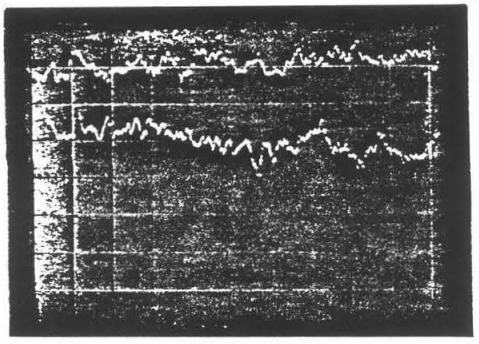

← baseline

605 nm

20 μs per division
50 mV per division

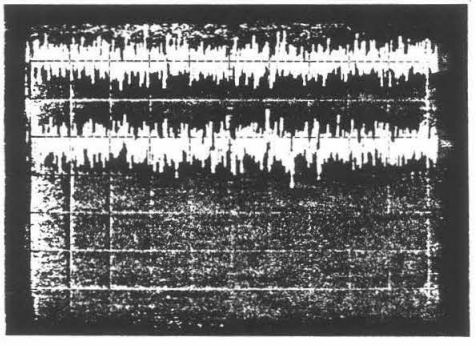

← baseline

100 μs per division
50 mV per division

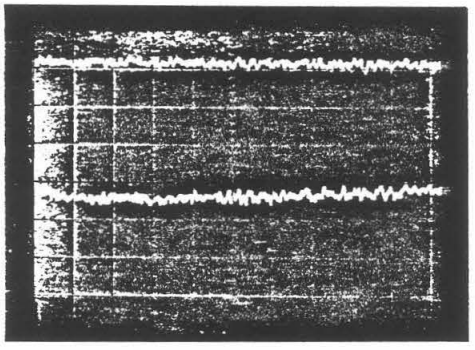

← baseline

10 ms per division
ΔA 0.005 per division

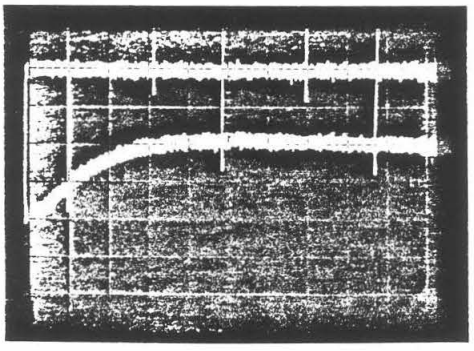

← baseline

200 ms per division
ΔA 0.005 per division

Figure IV.4

Temperature-jump kinetics data (oscilloscope photographs) of CNMV sample at 605 nm. Enzyme concentration: 15.6 μM; approx. cyanide concentration before dilution: 2 mM; after dilution: 0.3 mM. All other conditions as indicated for figure IV.3.

Cyanide Inhibited Cytochrome *c* Oxidase Mixed Valence

Temperature-Jump Kinetic Traces

605 nm

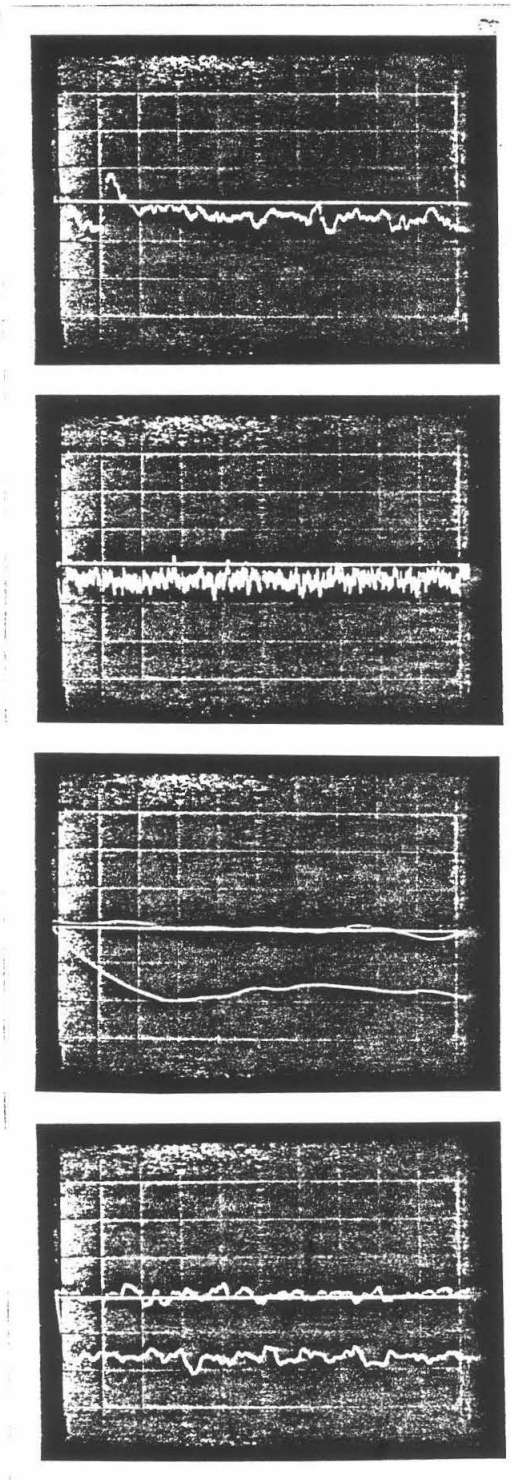

← baseline

20 μs per division
50 mV per division

← baseline

200 μs per division
50 mV per division

← baseline

200 μs per division
ΔA = 0.005 per division

← baseline

2 ms per division
ΔA = 0.005 per division

Figure IV.5 Temperature-jump kinetics data (oscilloscope photographs) of CNOx sample at 605 nm. Enzyme concentration 15.6 μM; approx. cyanide concentration before dilution: 2 mM; after dilution: 0.3 mM. All other conditions as indicated for figure IV.3.with a slower logarithmic amplifier which has a longer time constant (0.1 ms) but is consequently more sensitive.

Cyanide Inhibited Cytochrome *c* Oxidase -- Fully Oxidized

Temperature-Jump Kinetic Traces

605 nm

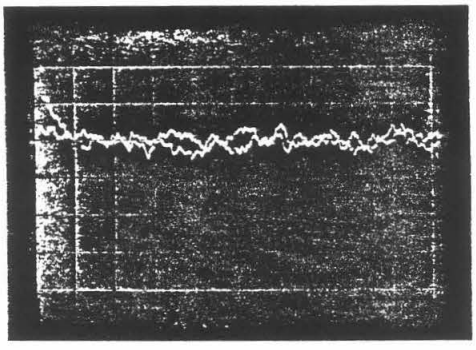

← baseline

20 μs per division
100 mV per division

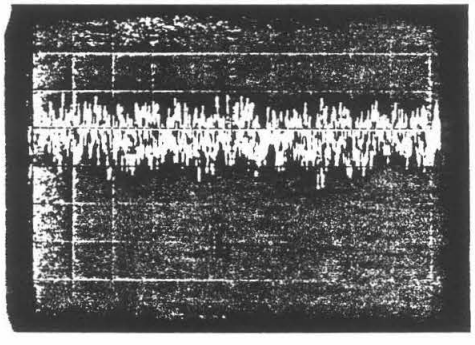

← baseline

200 μs per division
50 mV per division

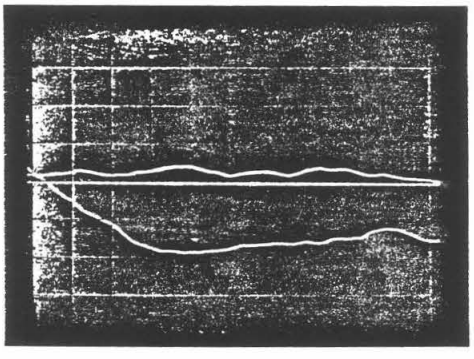

← baseline

200 μs per division
ΔA 0.002 per division

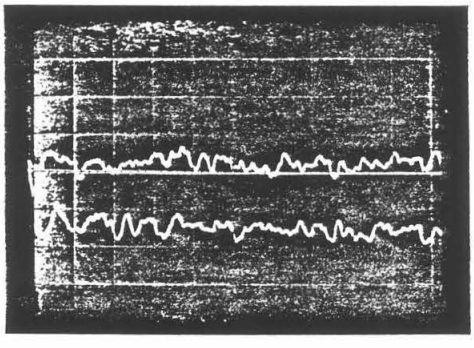

← baseline

2 ms per division
ΔA 0.002 per division

In the CN+1 sample (figure IV.3), rapid heating produces a fast decrease in absorbance at 605 nm. Most of this change occurs within the dead time of the measurement (i.e. during the 28 μs heating pulse width), and all of the observed change is over within 100 μs. (The upward trend in figure IV.4d is an artifact from the detection electronics.) The absorbance change is clearly visible even though the rate cannot be resolved. In the case of the CNOx and CNMV samples (figures IV.4 and 5), small decreases in absorbance at 605 nm were observed using the absorbance amplifier, but the changes were too small to measure reliably with the fast AC amplifier. While there is no reason to think that these changes are slow, the data only demonstrate that the absorbance changes are over within about 0.6 ms (the slow changes in figures IV.5.c and IV.6c are amplifier response curves).

These kinetic data are summarized and compared to the equilibrium temperature difference spectra in figure IV.6. The vertical I bar beside each spectrum indicates the amplitude of the absorbance change in the T-jump experiment, for that sample at 605 nm. These amplitudes were calculated from the (slower) absorbance amplifier data. The T-jump data were obtained for a 5.7 °C increase in temperature beginning at 6 °C, while the equilibrium data represent 20 °C-minus-4 °C difference spectra. The T-jump data have been rescaled to match the equilibrium data (see Materials and Methods, Chapter III).

In every case, the amplitudes of the absorbance change in the T-jump measurement are in reasonable agreement with the extents in the equilibrium data. These data suggest that the entire absorbance change at 605 nm in the CN+1 sample occurs with an apparent rate of at least 10,000 s^{-1} ($t_{1/2} < 60$ μs).

Figure IV.6 Temperature difference spectra (20 °C minus 4 °C) of cyanide inhibited cytochrome *c* oxidase with increasing amounts of added reductant: A, CNOx; B, CN+1; C, CNMV. The vertical I-bar beside each trace represents the extent of the absorbance change at 605 nm observed in the T-jump experiment (see text). The difference spectra are the same ones shown in figure IV.1. The T-jump conditions are described in figure IV.3, 4 and 5, but the extents have been scaled to reflect the differences in optical path length and temperature change. All data have been scaled to represent an enzyme concentration of 13 μM.

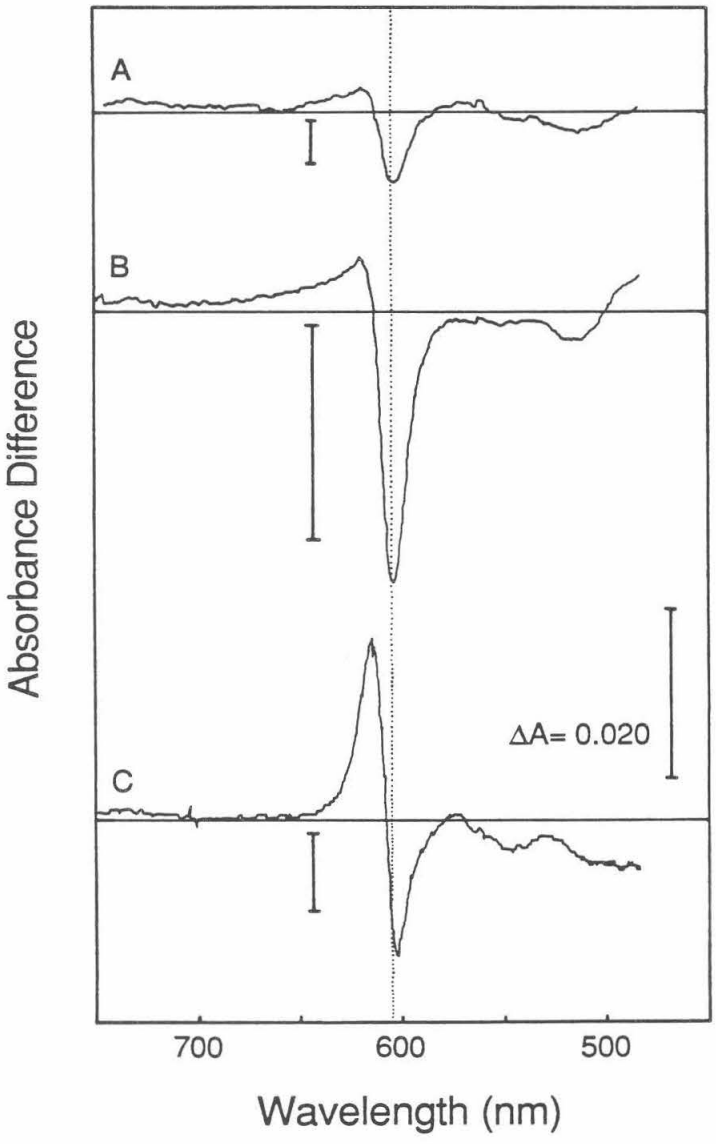
A
B
C
ΔA= 0.020
Absorbance Difference
700
600
500
Wavelength (nm)

The change in absorbance in the CN+1 sample calculated using the data from the fast amplifier is 83% of that calculated from the absorbance amplifier, but since there is no indication of any further change in absorbance level between 100 μs and 0.1 s, this is probably best ascribed to the fact that the calibration in the fast measurement is less precise.

It is possible that the progress of this reëquilibration could actually be observed, and its rate measured. It would be necessary to signal average over a number of temperature jump events, and it might also be necessary to reduce the heating pulse width slightly.

The absorbance changes in the CNOx and CNMV samples, are presumably temperature dependent band shifts of the type seen in the CO inhibited enzyme and reported in the native enzyme by Orii and Miki (1979). Absorbance changes at 605 nm in these samples could not be measured on the fast time scale. However, when the CNMV sample was observed at 620 nm, there was a clear absorbance increase during the heating pulse. Figure IV.7 shows the kinetic data for this sample at 620 nm together with the (equilibrium) temperature difference spectrum. The unlabelled I bar in the spectrum plot represents the amplitude of the absorbance change at 620 nm during the T-jump (scaled as before). In this case, the amplitude was calculated from the AC amplifier data. The extent of the absorbance change observed during the heating pulse, accounts for almost all of the change expected at equilibrium. No further absorbance changes were observed during the next 0.2 seconds. This suggests that, as in the case of the CO inhibited samples, the process which is responsible for the band shift has an apparent rate greater than 20,000 s^{-1}.

Figure IV.7

Temperature-jump kinetic data at 620 nm and equilibrium temperature difference spectrum for CNMV sample. The T-jump traces were recorded using the fast AC amplifier. Other conditions in the T-jump experiment are the same as shown in figure IV.4. The temperature difference spectrum is the same as figure IV.6C. The unlabelled vertical I-bar represents the extent of the absorbance change in the T-jump data shown above, scaled to reflect differences in optical path length and temperature change. The data have been scaled to represent an enzyme concentration of 13 μM.

Cyanide Inhibited Cytochrome *c* Oxidase -- Mixed Valence

Temperature-Jump Kinetic Traces 620 nm

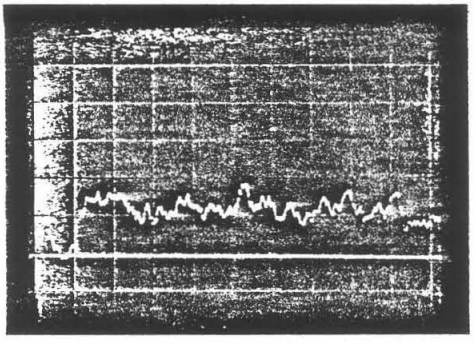

20 μs per division
100 mV per division

← baseline

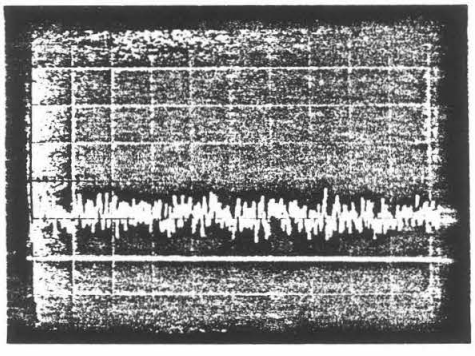

200 μs per division
100 mV per division.

← baseline

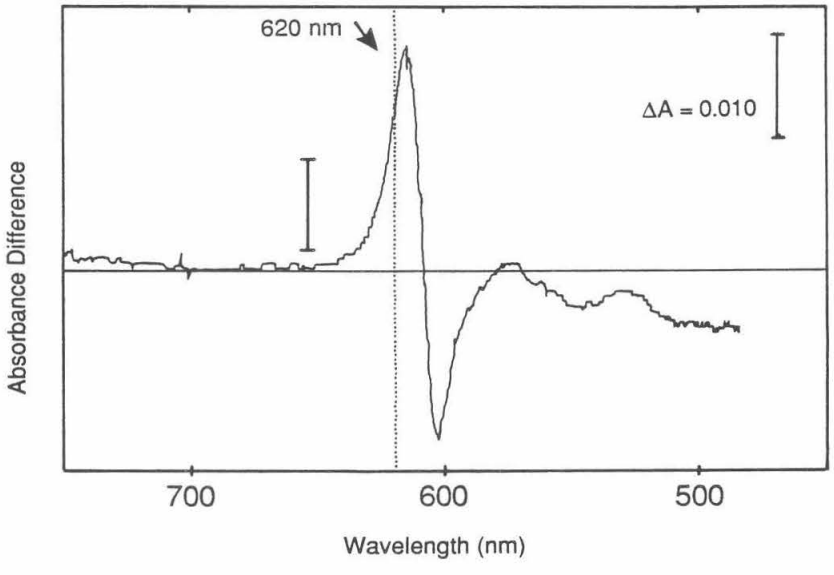

Discussion.

The temperature difference spectra of the oxidized cyanide inhibited (CNOx) and cyanide mixed valence (CNMV) compounds of cytochrome *c* oxidase show absorbance band shifts in their alpha and Søret regions. The T-jump data shown above demonstrate that the alpha band shift observed in the CNMV compound occurs very quickly. The absorbance change is complete within the 28 μs heating pulse width, which means that the apparent rate must be larger than 20,000 per second.

Another cyanide inhibited sample was prepared at an intermediate level of reduction. The temperature difference spectrum of this CN+1 sample was different from that of either the oxidized or the mixed valence sample and is consistent with Fe_a becoming increasingly oxidized as the temperature is raised. There is a large negative peak at 605 nm which cannot be accounted for by considering the CN+1 sample to be a mixture of the oxidized and mixed valence compounds. While it appears that Fe_a is becoming more oxidized, the 830 nm band region of the temperature difference spectrum shows clearly that Cu_A is not being reduced. Since Fe_{a_3} in these samples is bound by cyanide which prevents its reduction, it can be inferred by elimination that the electron acceptor is Cu_B.

The absorbance changes at 605 nm in the CN+1 sample were studied in the T-jump apparatus. Rapid heating of the sample produced a fast absorbance decrease after which the absorbance remained unchanged out to about 0.1 seconds. Most of the change occurred during the heating pulse, and the

change was almost certainly complete within 100 μs. This suggests that the putative electron reëquilibration has an apparent rate of at least 10,000 s^{-1}.

The redox potential of Cu_B in the cyanide inhibited enzyme is not well characterized. However, a redox potential interaction between Fe_a and Cu_B has been observed (Goodman, 1984) which indicates that the redox potentials of these sites are within about 60 mV (See Blair et al., 1986). In a system of this kind, a potential difference of 60 mV would correspond to an equilibrium constant of about 0.1. Thus, neither the forward or the reverse electron transfer rate would be exected to be less that 1000 s^{-1}.

This result was unexpected. We undertook this experiment to try to measure a Fe_a to Cu_A equilibration rate in a sample in which the oxygen binding site metal centers were in their oxidized forms. This was to be a complement to the data on the CO inhibited enzyme. Instead, we have apparently observed an electron reëquilibration between Fe_a and Cu_B. The data indicate that in the cyanide inhibited enzyme, electron transfer from Fe_a to the oxygen binding site can occur on a faster time scale than enzyme turnover.

It is impossible to tell from these data whether this is a direct electron transfer between Fe_a and Cu_B, or whether the electrons go via Cu_A. It is interesting to note that the lower limit we have place on the apparent rate (10,000 s^{-1}) is not very different from the apparent rate for Fe_{a_3} to Cu_A electron transfer in the experiments of Boelens et al. (1982) and Brzezinski et al. (1987); 7,000, and 14,200 s^{-1} respectively. Since these are both measurements of the electron transfer between the the "low potential" metal

centers and the oxygen binding site, they may have a common rate limiting step.

The possible involvement of Cu_A could be investigated by repeating the experiment in either *p*HMB modified (Gelles and Chan, 1985) or "heat treated" (Sone and Nicholls, 1986; Li et al., 1988) cytochrome *c* oxidase. In these forms of the enzyme, Cu_A is effectively no longer redox active, and electron transfer through Cu_A would not be feasible. Thus, we would predict that an electron reëquilibration which proceeded via Cu_A would be much slower in these Cu_A-modified forms of the enzyme.

The experiment would not be definitive, since these modifications are likely to affect more than just Cu_A (Li et al., 1988), but the results would be interesting nevertheless. The results could suggest an answer to the question of whether electrons are transferred to the oxygen binding site from Fe_a or Cu_A under enzyme turnover conditions.

References.

Blair, D.F., Bocian, D.F., Babcock, G.T. and Chan, S.I. (1982) *Biochemistry*, **21**, 6928-6935.

Blair, D.F., Ellis, W.R. Jr., Wang, H., Gray, H.B. and Chan, S.I. (1986) *J. Biol. Chem.* **261**, 11524-11537.

Boelens, R., Wever, R. and Van Gelder, B.F. (1982) *Biochim. Biophys. Acta*, **682**, 264-272.

Brzezinski, P. and Malmström, B.G. (1987) *Biochim. Biophys. Acta*, **894**, 29-38.

Erecinska, M. and Wilson, D.F. (1980) *Pharmacol. Ther.* **8**, 1-20.

Gelles, J. and Chan, S.I. (1985) *Biochemistry*, **24**, 3693-3972.

Goodman, G. (1984) *J. Biol. Chem.* **259**, 15094-15099.

Li, P.M., Morgan, J.E., Nilsson, T., Ma, M. and Chan, S.I. (1988) *Biochemistry*, in press.

Nicholls, P. and Chanady, G.A. (1982) *Biochem. J.* **203**, 541-549.

Orii, Y. and Miki, T. (1979) in *Cytochrome Oxidase*, (T.E. King et al., eds.) Elsevier/North-Holland Biomedical Press, pp. 251-256.

Sone, N. and Nicholls, P. (1984) *Biochemistry*, **23**, 6550-6554.

Chapter V

Discussion

We have prepared samples of CO inhibited cytochrome *c* oxidase in which Fe_a and Cu_A are both partially reduced and in dynamic redox equilibrium. Photolysis of $Fe_{a_3}^{2+}$–CO in these samples resulted in an electron redistribution from Fe_a to Cu_A, with an apparent rate of 17,000 ± 1,700 s^{-1}. The interpretation of this apparent rate was discussed at the end of the experimental chapter. It appears that this number reflects the sum of the forward and reverse electron transfer rates between these two metal centers, but this could not be shown conclusively. It is possible the rate of the process we observe is limited by a conformational change. Alternatively, since the experimental conditions do not allow the relaxation process to be followed for more than a few milliseconds, the fast relaxation which we observe could be the first phase of a multiphasic process. However, the results do suggest that the Fe_a to Cu_A electron transfer can be very fast.

In the introduction, I reviewed a number of previous results which have been interpreted to mean that the Fe_a -- Cu_A electron equilibration rate is considerably slower than this. For some of these experiments, there were alternative interpretations of the data which would be consistent with a faster Fe_a --Cu_A equilibration rate. However, three of these experiments should be discussed further:

1) In 1975 Wilson et al. reported a stopped flow experiment in which cytochrome *c* oxidase was reduced by ferrocytochrome *c*. As the concentration of cytochrome *c* was increased, Fe_a became reduced more quickly, and a lag was observed between the reduction of Fe_a and Cu_A. At the higher cytochrome *c* concentrations, the rate of reduction of Cu_A was

reported to be independent of cytochrome *c* concentration, with a half time of about 8 ms. The fact that the lag in the reduction of Cu_A was observed only at higher concentrations, and at faster rates, indicates that it is a kinetic phenomenon and does not arise from a difference between the redox potentials of Fe_a and Cu_A. This result does not appear to be consistent with fast electron equilibration between these two sites.

Other workers have reported similar experiments in which no such lag was observed (Antalis and Palmer, 1982; Andréasson et al., 1972). The experiments of Wilson et al. (1975) were all carried out in the presence of some oxygen; in some cases the cyanide inhibited form of the enzyme was used. In contrast, the other experiments referred to above were all carried out anaerobically. Andréasson et al. (1972) reported that, when they allowed air into their reactions, the absorbance changes at 550 nm (oxidation of cytochrome *c*) no longer tracked linearly with absorbance changes at 830 nm. This could occur because, in the native enzyme, some electron transfer to the oxygen binding site can take place on this time scale (see also Beinert et al., 1976). However, these authors did not report whether the reduction of Fe_a and Cu_A (i.e. absorbance changes at 605 nm and 830 nm) still tracked together under aerobic conditions.

2) Halaka et al. (1984) observed a similar lag between the reduction of Fe_a and Cu_A when the enzyme was reduced using PMS. In this case, a rate of about 20 s^{-1} was resolved for Fe_a to Cu_A electron transfer. Although the reduction of Fe_a was a second order process, the rate of reduction of Cu_A did not change significantly when the concentrations of the reactants were varied (Barnes, 1986), suggesting that here also, the lag is a kinetic and not a

thermodynamic phenomenon. The authors noted the fast Fe_a to Cu_A electron transfer invoked by Antalis and Palmer (1982) and suggested that this rate could be different under different experimental conditions.

3) Brzezinski and Malmström (1987) studied electron transfer in cytochrome *c* oxidase following photolysis of the CO mixed valence compound of the enzyme. They reported that photolysis of $Fe_{a_3}{}^{2+}$–CO was followed by partial reduction of Cu_A at an apparent rate of about 14,000 s^{-1}, and partial reduction of Fe_a at an apparent rate of about 600 s^{-1}. They interpreted these results in terms of fast electron transfer from the oxygen binding site to Cu_A, followed by slower electron transfer from Cu_A to Fe_a.

The rate which they measured for the Fe_a -- Cu_A electron equilibration (k_{app} = 600 s^{-1}), is at least ten times slower than the one we have observed. The authors pointed out that their data are consistent with a model in which Cu_A and Fe_a both accept electrons directly from the oxygen binding site but with different rates. However, this explanation is still inconsistent with the faster Fe_a -- Cu_A electron equilibration rate, because if there was fast equilibration, Fe_a and Cu_A should reduce synchronously.

In the experiment of Brzezinski et al. (1987), either Fe_{a_3} or Cu_B must become reoxidized in order for Cu_A or Fe_a to be reduced, whereas, in our experiment, it appears that both Fe_{a_3} or Cu_B remain reduced throughout. This could be the key to understanding the difference between the two results. It is possible that the reoxidation of one of the oxygen binding site metal centers causes the Fe_a -- Cu_A electron equilibration rate to become much slower. Alternatively, the reduction of Fe_a which Brzezinski et al. observe at 600 s^{-1} could be driven by a conformational change which alters the redox potential

of Fe_a or Cu_A. The apparent rate of electron redistribution would then reflect the rate of this conformational change and not the electron transfer rate. If this putative conformational change could occur only when Fe_{a_3} or Cu_B becomes oxidized, it would not be observed during in our experiment.

Thus we cannot be sure either that a) the fast rate which we have measured actually corresponds to the complete Fe_a -- Cu_A electron reëquilibration, or b) if so, that this rate applies under all circumstances. The experiments discussed above provide some compelling evidence that this rate can be slower, at least in some states of the enzyme. The rate could vary with experimental conditions (Halaka et al., 1984), or even be controlled or "gated" as part of the enzyme's proton pumping mechanism (see Blair et al., 1985). However, for the sake of discussion, it is useful to explore the ramifications of a consistently fast Fe_a -- Cu_A electron equilibration rate.

We have measured an apparent rate of about 17,000 s^{-1} for electron equilibration between Fe_a and Cu_A and calculated forward and reverse rates of about 10,000 s^{-1} and 7,000 s^{-1} respectively. If the rate of electron exchange between these two sites were this fast under enzyme turnover conditions, then it would not matter whether electrons entered the enzyme through Fe_a or Cu_A. The maximum turnover rate of the enzyme under typical experimental conditions is 50 to 100 (electrons) s^{-1}, and is never more than a few hundred (Sinjorgo et al., 1986). Given these rates, electrons from cytochrome *c* could enter the enzyme at Fe_a, and be transferred to oxygen out of Cu_A (or vice versa), without ever disturbing the redox equilibrium between Fe_a and Cu_A. This would not resolve the question of whether electrons could enter the enzyme from more than one cytochrome *c* binding site, but the question of

which metal center(s) recieved electrons directly from cytochrome *c* would be moot.

If the Fe_a -- Cu_A redox equilibration is fast under turnover conditions, it is unlikely that electrons are transferred to the oxygen binding site from more than one of the two centers at a significant rate. As discussed in the introduction, the pumping of protons is probably driven by electron transfer from Fe_a or Cu_A but not both. Electron transfer out of the non-pumping site would not drive the proton pump; i.e., it would not be "coupled" (see Blair et al., 1985). The proton pump site is generally assumed to be a 1.0 H^+/e^- device (see Chan et al., 1987). If this is indeed the case, then in order to achieve a real stoichiometry of 0.9 H^+/e^- (Sarti et al., 1985), almost all of the electrons moving through the enzyme would have to pass through a coupled pathway. Thus, the system must be able to run with a minimum uncoupled electron flow. However, if the non-pumping site could transfer electrons to oxygen at an appreciable rate, and if that site was in fast redox equilibrium with the pumping site, a significant fraction of the electron flow would not be coupled.

The fast rate we have measured also suggests an alternative explanation of the flow flash, reoxidation data (Hill and Greenwood, 1984a,b; Hill et al., 1986). Three phases have been resolved in the reoxidation of cytochrome *c* oxidase by oxygen. In the first phase, which is very fast (30,000 s^{-1}), Fe_{a_3} is oxidized along with about 40% of Fe_a. In the second phase, about 60% of Cu_A is oxidized at a rate of about 7,000 s^{-1}. In the final phase, the balance of both Fe_a and Cu_A are oxidized at a rate of about 700 s^{-1}. The reoxidation of Cu_B cannot be followed in these experiments. These data have been interpreted in terms of a branched mechanism in which two subpopulations of the enzyme follow

different paths to reoxidation (Hill and Greenwood, 1984a,b). In one (40%) subpopulation of the enzyme, Fe_a would be reoxidized quickly (30,000 s^{-1}), and Cu_A would be reoxidized slowly (700 s^{-1}). In the other (60%) subpopulation, Cu_A would be reoxidized quickly (7,000 s^{-1}), and Fe_a would be reoxidized slowly (700 s^{-1}).

The experiment was repeated in the five electron reduced, cytochrome *c*, cytochrome *c* oxidase, 1:1 high affinity complex. Under these conditions, about 40% of the bound cytochrome *c* was reoxidized at a rate of 6,000 s^{-1}, and the remainder at about 500 s^{-1}. The fraction of Fe_a, which in the absence of cytochrome *c* was reoxidized at 700 s^{-1}, was reoxidized much more slowly in the presence of cytochrome *c* (Hill and Greenwood, 1984b). This was explained as follows (see figure V.1A): In 40% of the enzyme, Fe_a is reoxidized at 30,000 s^{-1}. If cytochrome *c* could donate electrons to Fe_a at 6,000 s^{-1}, then in this subpopulation, cytochrome *c* would immediately begin to reoxidize at that rate. Presumably these electrons would be passed on immediately to the oxygen binding site. In the other 60% of the enzyme, the reoxidation of Fe_a occurs at 700 s^{-1}. However, if cytochrome *c* could donate electrons to Fe_a at a much higher rate (6000 s^{-1}), the electrons leaving Fe_a would be immediately replaced by electrons from cytochrome *c*, and instead of the reoxidation of Fe_a, the reoxidation of cytochrome *c* would be observed at 700 s^{-1}.

This model requires electron transfer to the oxygen binding site from both Fe_a and Cu_A. Furthermore it requires that each of these two processes take place at two different rates in different subpopulations of the enzyme. As discussed earlier, fast electron transfer to the oxygen binding site from both

Figure V.1.

Possible electron transfer pathways for the reoxidation of the five electron reduced cytochrome *c* -- cytochrome *c* oxidase complex.

A. A scheme based on the model of Hill and Greenwood (1984a,b) and Hill et al., (1986); B. A scheme base on very fast Cu_A to Fe_a electron transfer.

A.

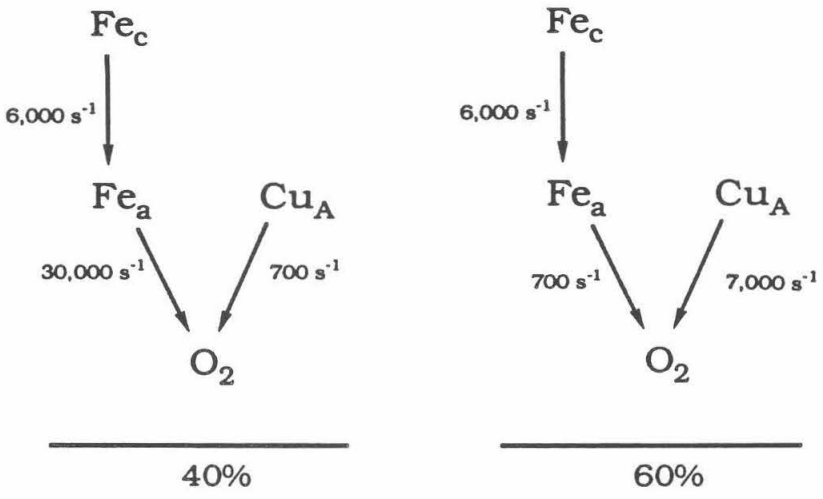
Fe$_c$
6,000 s^{-1}
Fe$_a$
Cu$_A$
30,000 s^{-1}
700 s^{-1}
O$_2$
40%
Fe$_c$
6,000 s^{-1}
Fe$_a$
Cu$_A$
700 s^{-1}
7,000 s^{-1}
O$_2$
60%

B.

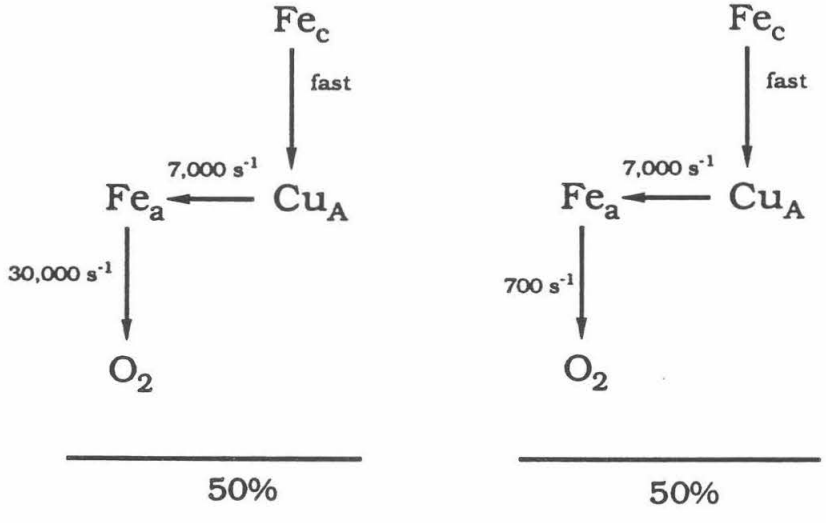
Fe$_c$
fast
7,000 s^{-1}
Fe$_a$
Cu$_A$
30,000 s^{-1}
O$_2$
50%
Fe$_c$
fast
7,000 s^{-1}
Fe$_a$
Cu$_A$
700 s^{-1}
O$_2$
50%

Fe_a and Cu_A is not easy to reconcile with a model in which the proton pump mechanism has an ideal 1.0 H^+/e^- stoichiometry.

The present kinetic results suggest a simpler explanation. This was suggested by the fact that, in the flow flash experiment, a fraction of Cu_A reoxidized at a rate of 7,000 s^{-1}, and a fraction of the bound cytochrome *c* reoxidized at a rate of 6,000 s^{-1}. These rates are close to the Cu_A to Fe_a electron transfer rate of about 7,000 s^{-1} (tentatively) derived from our flash photolysis experiment, a fact which suggests that Cu_A to Fe_a electron transfer might be the rate limiting step in reoxidation of both Cu_A and cytochrome *c* . This might be the case if: 1) electron transfer from Fe_a to the oxygen binding site was inherently biphasic, with a rate of about 30,000 s^{-1} in about half of the enzyme, and about 700 s^{-1} in the other half; 2) cytochrome *c* donated electrons directly to Cu_A at a very fast rate; 3) there was no electron transfer at any significant rate from Cu_A to the oxygen binding site.

According to this scheme, the reaction would proceed as follows (see figure V.1B): First, in about half of the enzyme, Fe_a would be reoxidized at 30,000 s^{-1}. In that subpopulation, Cu_A and cytochrome *c* would then begin to reoxidize via Fe_a. The bottleneck for this process would be the Cu_A to Fe_a electron transfer (7,000 s^{-1}). In the remaining half of the enzyme, Fe_a would donate electrons to the oxygen binding site at 700 s^{-1}. However, Fe_a would be continuously rereduced by Cu_A and cytochrome *c* as fast as it was oxidized. Thus the oxidation of Cu_A and cytochrome *c* would be observed instead of the oxidation of Fe_a. The proposed pathway is not new (see Holm et al., 1987), but our results do suggest that the Cu_A to Fe_a electron transfer is fast enough to explain the flow flash data this way.

In this scheme, only Fe_a would transfer electrons to the oxygen binding site. This step would still have to be biphasic; that is, it would have to have strikingly different rates in different subpopulations of the enzyme. One difficulty with this explanation is that compared to the model of Hill and Greenwood (1984a,b), the assignments of subpopulations in the slower phase would be reversed. The 60% subpopulation in the fast phase would have to correspond to the 40% subpopulation in the second phase and vice versa. This would be most easily done by assuming that the enzyme is divided into two equal subpopulations. Whether this is consistent with the flow flash kinetic data is not completely clear.

Our flash photolysis results suggest that, at least under some conditions, the Fe_a -- Cu_A electron transfer rate can be far faster than enzyme turnover rates. Even this conclusion cannot be stated unequivocally, but the temperature-jump experiment of chapter III indicates that a firm answer is within reach.

The temperature-jump study in chapter IV shows that, in cyanide bound cytochrome *c* oxidase, there is fast electron exchange between Fe_a and Cu_B (kapp > 10,000 s^{-1}). The electron transfer could go directly from Fe_a to Cu_B, or could go via Cu_A. As discussed above, this question could be explored with the aid of Cu_A-modified forms of the enzyme. Since this electron transfer occurs along a pathway which could be involved in proton pumping, it would also be of interest to investigate the pH dependence of this process, as well as the effects of ^2H_2O as the solvent.

Finally, the flash photolysis experiments have suggested that some unusual photochemistry occurs when $Fe_{a_3}{}^{2+}$–CO, in the oxygen binding site of

cytochrome *c* oxidase, is photolyzed. It appears that photolysis can have a different outcome dependent on either the temporal pulse width or the total energy of the light pulse. At the end of chapter II, some experiments were suggested which might clarify this matter. The electron transfer events which follow photolysis will not be completely understood until the photochemistry at the oxygen binding site is explained.

References.

Andréasson, L.E., Malmström, B.G., Strömberg, B.G. and Vänngård, T. (1972) *FEBS Lett.* **28**, 297-301.

Antalis, T.M. and Palmer, G. (1982) *J. Biol. Chem.* **257**, 6194-6206.

Barnes, Z.K. (1986) Ph.D. Thesis, Michigan State University.

Beinert, H., Hansen, R. and Hartzell, C.R. (1976) *Biochim. Biophys. Acta*, **423**, 339-355.

Blair, D.F., Witt, S.F. and Chan, S.I. (1985) *J. Am. Chem. Soc.* **107**, 7389-7399.

Brudvig, G.W., Blair, D.F. and Chan, S.I. (1984) *J. Biol. Chem.* **17**, 11001-11009.

Brzezinski, P. and Malmström, B.G. (1987) *Biochim. Biophys. Acta*, **894**, 29-38.

Chan, S.I., Li, P.M., Nilsson, T., Gelles, J., Blair, D.F. and Martin, C.T. (1987) in *Proc. of the Fourth Int. Conf. on Oxidases.*

Halaka, F.G., Barnes, Z.K., Babcock, G.T. and Dye, J.L. (1984) *Biochemistry*, **23**, 2005-2011.

Hill, B.C. and Greenwood, C. (1984a) *Biochem. J.* **218**, 913-921.

Hill, B.C. and Greenwood, C. (1984b) *FEBS Lett.* **166**, 362-366.

Hill, B.C., Greenwood, C. and Nicholls, P. (1986) *Biochim. Biophys. Acta*, **853**, 91-113.

Holm, L., Saraste, M. and Wikström, M. (1987) *EMBO J.* **6**, 2819-2823.

Sarti, P., Jones, M.G., Antonini, G., Matatesta, F., Colosimo, A., Wilson, M.T. and Brunori, M. (1985) *Proc. Natl. Acad. Sci. U.S.A.* **82**, 4876-4880.

Sinjorgo, K.M.C., Steinebach, O.M., Dekker, H.L. and Muijsers, A.O. (1986) *Biochim. Biophys. Acta*, **850**, 108-115.

Wilson, M.T., Greenwood, C., Brunori, M. and Antonini, E. (1975) *Biochem. J.* **147**, 145-153.

Appendix.

```
C       SASHIMI
C
C       CONVERTS TRANSMITTANCE (BIOMATION) DATA TO RELATIVE ABSORBANCE
C
C       WRITTEN BY: PETER MARK LI
C       ALGORITHM: JOEL MORGAN AND PETER MARK LI
C       DOCUMENTATION: JOEL MORGAN
C
C       RELATIVE ABSORBANCE MEANS THAT THE CHANGES IN ABSORBANCE
C       DURING A KINETIC TRACE REFLECT CORRECTLY SCALED ABSORBANCE
C       DIFFERENCES, BUT THAT THE ENTIRE KINETIC TRACE WILL HAVE AN
C       UNKNOWN OFFSET.
C
C       THE PROGRAM IS DESIGNED TO TAKE DATA FILES FROM THE
C       BIOMATION/APPLESACII SYSTEM IN DR. MOUSTAFA EL-SAYED'S LAB
C       AT UCLA AND PREPARE THEM FOR CURVE FITTING BY THE MAGURO
C       PROGRAM.
C
C       THE BASELINE FILE (FILEB) IS A NO-LIGHT BIOMATION BACKGROUND
C       SCAN.
C
C       THE NAMES OF THE DATA FILES ARE READ FROM A LIST FILE, THE
C       THREE LINES OF WHICH ARE IGNORED.  THIS IS SO THAT LIST FILES
C       PREPARED BY DIRECTORY CREATION PROGRAMS CAN BE USED.
C
C       ALGORITHM:
C
C       THE BASELINE FILE IS USED FOR TWO PURPOSES:
C       1)POINTS 900 TO 1000 ARE AVERAGED AND USED TO CALCULATE
C         A BASELINE OFFSET (IMAX)
C       2)IMAX IS SUBTRACTED FROM EACH POINT IN THE FILE TO GIVE A
C         BASELINE CORRECTION FILE (ITBP) WHICH CAN BE SUBTRACTED FROM
C         THE DATA FILE TO CORRECT FOR IRREGULARITIES IN THE BASELINE
C         WITHOUT INTRODUCING AN OFFSET IN THE DATA.  THE CORRECTED
C         DATA FILE IS STORED AS ITP
C
C       THE BIOMATION OUTPUT IS LARGEST FOR MINIMUM LIGHT AND SMALLEST
C       FOR MAXIMUM LIGHT.  FOR THIS REASON, THE VALUES IN THE
C       INPUT FILE (IT) ARE ACTUALLY A REPRESENTATION OF THE DIFFERENCE
C       BETWEEN THE ACTUAL LIGHT FLUX AND THE LIGHT FLUX WHICH WOULD
C       UNDERFLOW THE BIOMATION VOLTAGE WINDOW (NOT NECCESSARILY
C       100%T.)  VALUES PROPORTIONAL TO THE ACTUAL TRANSMITTANCE
C       ARE OBTAINED BY SUBTRACTING THE DATA (IT) FROM IMAX.  (IMAX IS
C       REPRESENTS THE DIFFERENCE BETWEEN ZERO LIGHT FLUX AND THE
C       LIGHT FLUX WHICH WOULD UNDERFLOW THE BIOMATION VOLTAGE
C       WINDOW.)
C
C       FINALLY, IMAX IS USED IN LIEU OF A 100%T VALUE WHICH IS NOT
C       AVAILABLE.  THIS INTRODUCES A CONSTANT ADDITIVE UNKNOWN
C       INTO THE ABSORBANCE VALUES.
C
C       INPUT/OUTPUT UNIT DESIGNATIONS:
C       1: INPUT--BASELINE FILE
C       2: INPUT--KINETIC DATA FROM BIOMTION.  EXPECTED EXTENSION:.DAT
C       3: OUTPUT--ABSORBANCE DATA (ALSO CONTAINS RAW DATA AND
C                  BASELINE-SUBTRACTED RAW DATA.)  USES SAME FILE NAME
C                  AS INPUT FILE BUT CHANGES EXTENSION TO .ABS.
C       4: INPUT--LIST FILE
C
        DIMENSION IT(1024), ITB(1024), A(1024), ITP(1024), ITBP(1024)
        CHARACTER FILE*20, FILEB*20, LIST*20
        INTEGER*4 IMAX
C
C       ***** READ NAME OF DIRECTORY FILE, BASELINE FILE AND CHANNEL
C             TIME FROM KEYBOARD
```

```
C
 5      TYPE 10
 10     FORMAT(1X,'DIRECTORY FILE > ',$)
        READ(5,'(A)')LIST
 30     TYPE 35
 35     FORMAT(1X,'BASEFILE > ',$)
        READ(5,'(A)')FILEB
        TYPE 50
 50     FORMAT(1X,'CHTIME > ',$)
        ACCEPT *,CHX
C
C       ***** READ LIST FILE AND BASELINE FILE.
C
        OPEN(UNIT=4,NAME=LIST,DEFAULTFILE='.LIS',TYPE='OLD',READONLY)
        OPEN(UNIT=1,NAME=FILEB,DEFAULTFILE='.DAT',TYPE='OLD',READONLY)
        READ(4,'(A)')FILE
        READ(4,'(A)')FILE
        READ(4,'(A)')FILE
        DO 55 I=1,1024
        READ(1,*)ITB(I)
 55     CONTINUE
C
C       ***** LOOP TO READ DATA FILES, PROCESS AND WRITE ABSORBANCE
C             FILES
C
           DO 100 L=1,100
           READ(4,'(A)')FILE
           OPEN(UNIT=2,NAME=FILE,DEFAULTFILE='.DAT',TYPE='OLD',READONLY)
           J=INDEX(FILE(1:),'.DAT')
           FILE(J:J+3)='.ABS'
           OPEN(UNIT=3,NAME=FILE,DEFAULTFILE='.ABS',TYPE='NEW')
              DO 60 I=1,1024
              READ(2,*,END=70) IT(I)
 60           CONTINUE
           NCH=1024
           GO TO 75
 70        NCH=I-1
 75        CLOSE(UNIT=2)
C
C          ***** FIND IMAX AND USE IT TO CALCULATE BASELINE WITHOUT
C                OFFSET.  WRITE TO ITP
C
           IMAX=0
              DO 80 J=900,1000
              IMAX=ITB(J)/101+IMAX
 80           CONTINUE
           DO 82 I=1,NCH
           ITBP(I)=ITB(I)-IMAX
           ITP(I)=IT(I)-ITBP(I)
82         CONTINUE
C
C              ***** CALUCLATE ABSORBANCE AND WRITE OUTPUT FILE
C
85             DO 90 J=1,NCH
               IF(ITP(J).EQ.0)ITP(J)=1
               RI=FLOAT(IMAX)/FLOAT(IMAX-ITP(J))
               XJJ=FLOAT(J)*CHX
               A(J)=ALOG10(RI)
89             WRITE (3,*) XJJ,A(J),ITP(J),IT(J)
90             CONTINUE
            CLOSE(UNIT=3)
100         CONTINUE
        STOP
        END
```

```
C     MAGURO.FOR: A PROGRAM TO ANALYZE KINETIC DATA
C
C     READS FILE NAME (DEFAULT: .ABS) AND CHANNEL TIME (SECONDS) FROM
C     FROM TERMINAL
C     READS XD,YD (TIME,OBSERVATION) FROM FILE
C     DISPLAYS ENTIRE DATA SET ON SCREEN
C     ALLOWS SELECTION BY USE OF CURSOR MOVEMENT OF:
C          REGION TO PLOT (X)
C          REGION FROM WHICH TO SCALE Y
C          EXPANDED Y SCALING
C          ZERO TIME POINT FOR FIT
C          REGION OF DATA TO USE IN FIT
C          Y EXPANSION IN PLOT
C     FITS A SINGLE EXPONENTIAL CURVE (THREE PARAMETERS) TO THE DATA
C     USING AN IMSL LIBRARY ROUTINE CALLED ZXSSQ.
C     PLOTS DATA, THEORETICAL CURVE AND PRINTS PARAMETERS TO SCREEN.
C     ALLOWS RESULTS TO BE PRINTED ON TRILOG LINE PRINTER.
C
C     CAUTION!  THE PROGRAM IS NOT BUG FREE.
C     SOME OPTIONS IN THIS PROGRAM WORK WELL BUT OTHERS WILL CAUSE IT
C     TO CRASH OR WRITE INCORRECT FILE NAMES -- CHECK IT OUT
C     CAREFULLY.
C
C     LIBRARY ROUTINES: PGPLOT, ZXSSQ (IMSL)
C     LINK TO: [BJW.GRAPHICS]GRPCKG2/L, PUB:IMSL/L, PUB:QMSPLOT/L
C
      EXTERNAL SINGLE
      COMMON XF,YF
      DIMENSION XD(1024), YD(1024), XP(1024), YFIT(1024), XF(1024)
      DIMENSION YF(1024), F(1024), X(3), PARM(4), XJAC(1024,6)
      DIMENSION XJTJ(21), WORK(3000)
      CHARACTER DEVICE*128, CHAR*1, FILE*20, DEV2*20, TOP(1)
      CHARACTER*20 NOUT(20), TOUT(20)*35
      DATA TOP/'T'/
      DATA TOUT(1)/'FILENAME:       '/
      DATA TOUT(2)/'PARAMETER 1:    '/
      DATA TOUT(3)/'PARAMETER 2:    '/
      DATA TOUT(4)/'PARAMETER 3:    '/
      DATA TOUT(5)/'SUM OF SQUARES:'/
      DATA TOUT(6)/'IER:            '/
      DATA TOUT(7)/'INFER:          '/
      DATA TOUT(8)/'WORK(1):        '/
      DATA TOUT(9)/'WORK(2):        '/
      DATA TOUT(10)/'WORK(3):        '/
      DATA TOUT(11)/'WORK(4):        '/
      DATA TOUT(12)/'WORK(5):        '/
      DATA TOUT(13)/'POINTS IN FIT: '/
      DATA TOUT(14)/'SET ZERO (s):  '/
      DATA TOUT(15)/'START FIT (s): '/
      DATA TOUT(16)/'END FIT (m):   '/
      DATA TOUT(17)/'CH TIME (m):   '/
C
C     ----- READ FILENAME AND TIME PER CHANNEL.
C
      JFLAG=0
    5 CONTINUE
      WRITE(6,10)
   10 FORMAT(1X,'FILENAME > ',$)
      READ(5,'(A)') FILE
      WRITE(6,15)
   15 FORMAT(1X,'CHANNEL TIME (SECONDS)> ',$)
      READ(5,20)CHT
   20 FORMAT(F15.8)
C
C     ----- READ FILE -- UP TO 1024 POINTS.
```

```
C           NCH IS SET TO NUMBER OF POINTS.
C
      OPEN(UNIT=1,NAME=FILE, DEFAULTFILE='.ABS',
     +TYPE='OLD',READ ONLY)
         DO 50 I=1,1024
         READ (1,*,END=60) XD(I),YD(I)
   50    CONTINUE
      NCH=1024
      GO TO 70
   60 NCH=I-1
   70 CONTINUE
      CLOSE(UNIT=1)
C
C     ----- FIND THE LIMITS OF THE COMPLETE DATA SET
C
    75 YFMIN=YD(1)
      YFMAX=YD(1)
      XFMIN=XD(1)
      XFMAX=XD(1)
         DO 80 I=1,NCH
         IF (YD(I).LT.YFMIN) THEN
         YFMIN=YD(I)
         MINCH=I
         END IF
         IF (YD(I).GT.YFMAX) THEN
         YFMAX=YD(I)
         MAXCH=I
         END IF
         IF (XD(I).LT.XFMIN) XFMIN=XD(I)
         IF (XD(I).GT.XFMAX) XFMAX=XD(I)
   80    CONTINUE
C
C           NOTE: DEVICE CODE IS /VT FOR VT125.  ADDING A FILE
C                 DESCRIPTION BEFORE THE "/" WOULD WRITE TO THE
C                 FILE (ALSO?)
C
      CALL PGBEGIN(0,'/VT',1,1)
C
C     ----- MAKE SOME ROOM AT TOP AND BOTTOM OF PLOT
C
      YRANGE=YFMAX-YFMIN
      YFMAX=YFMAX+0.125*YRANGE
      YFMIN=YFMIN-0.125*YRANGE
C
C
C
      IF(JFLAG.EQ.0)THEN
      JFLAG=1
      GO TO 88
      END IF
   83 WRITE(6,85)
   85 FORMAT(1X,'SET NEW SCALING LIMITS? (Y/N): ',$)
      READ(5,'(A)')CHAR
      IF(CHAR.EQ.'N')THEN
      GO TO 200
      ELSE IF(CHAR.EQ.'Y')THEN
      GO TO 88
      ELSE
      GO TO 83
      END IF
C
C     ----- SET ALL OTHER PLOTTING AND FITTING LIMITS TO
C           THE FULL ENVELOPE TO BEGIN WITH.
C
   88 XZERO=XFMIN
```

```
      XSMIN=XFMIN
      XSMAX=XFMAX
      YPMIN=YFMIN
      YPMAX=YFMAX
      YSMIN=YFMIN
      YWMIN=YFMIN
      YSMAX=YFMAX
      YWMAX=YFMAX
      XSCALEA=XFMIN
      XSCALEB=XFMAX
      XSTART=XFMIN
      XSTOP=XFMAX
C
C     ----- PLOT FULL DATA SET -----
C
C
      CALL PGENV(XFMIN,XFMAX,YFMIN,YFMAX,0,0)
      CALL PGPOINT(NCH,XD,YD,1)
C
C     ----- ASSIGN STARTING POSITION FOR CURSOR.
C
      XCURSOR=XSMIN
      YCURSOR=YSMAX
C
C     ----- CALL CURSOR SUBROUTINE PGCURSE(XCURSOR,YCURSOR,CHAR)
C
C           PGCURSE POSITIONS THE CURSOR AT XCURSOR, YCURSOR IN THE
C           PLOT COORDINATES.  THE CURSOR CAN THEN BE MOVED LOCALLY
C           BY THE VT125.  WHEN THE CURSOR IS AT THE DESIRED PLACE,
C           TYPING A CHARACTER WILL RETURN THE NEW CURSOR POSITION
C           AS XCURSOR, YCURSOR.  THE CHARACTER TYPED IS USED TO
C           DIRECT THE NEXT STEP.
C
   90 WRITE(6,100)
  100 FORMAT(1X,'CURSOR: [SLN-OMT] [Z] [Y] [P] [F]')
      CALL PGCURSE(XCURSOR,YCURSOR,CHAR)
C
C     ------------------------------------------------------------
C
C     ------------ <D> RETURN TO DEFAULT PARAMETERS, I.E. FULL ENVELOPE
C
      IF(CHAR.EQ.'D')THEN
      GO TO 75
C
C     ------------ <N> MIN X FOR FIT
C
      ELSE IF(CHAR.EQ.'N')THEN
      XSTART=XCURSOR
      CALL GRSETLS(4)
      CALL PGMOVE(XSTART,YPMAX)
      CALL PGDRAW(XSTART,YPMIN)
      CALL GRSETLS(1)
C
C     ------------ <O> MAX X FOR FIT
C
      ELSE IF(CHAR.EQ.'O')THEN
      XSTOP=XCURSOR
      CALL GRSETLS(4)
      CALL PGMOVE(XSTOP,YPMAX)
      CALL PGDRAW(XSTOP,YPMIN)
      CALL GRSETLS(1)
C
C     ------------ <L> MIN X OF SCALING REGION
C
```

```
      ELSE IF(CHAR.EQ.'L')THEN
      XSCALEA=XCURSOR
      CALL GRSETLS(5)
      CALL PGMOVE(XSCALEA,YPMAX)
      CALL PGDRAW(XSCALEA,YPMIN)
      CALL GRSETLS(1)
C
C     ------------ <M> MAX X OF SCALING REGION
C
      ELSE IF(CHAR.EQ.'M')THEN
      XSCALEB=XCURSOR
      CALL GRSETLS(5)
      CALL PGMOVE(XSCALEB,YPMAX)
      CALL PGDRAW(XSCALEB,YPMIN)
      CALL GRSETLS(1)
C
C     ------------ <S> MIN X OF PLOT
C
      ELSE IF(CHAR.EQ.'S')THEN
      XSMIN=XCURSOR
      CALL PGMOVE(XSMIN,YPMAX)
      CALL PGDRAW(XSMIN,YPMIN)
C
C     ------------ <T> MAX X OF PLOT
C
      ELSE IF(CHAR.EQ.'T')THEN
      XSMAX=XCURSOR
      CALL PGMOVE(XSMAX,YPMAX)
      CALL PGDRAW(XSMAX,YPMIN)
C
C     ------------ <U> MIN Y OF PLOT
C
      ELSE IF(CHAR.EQ.'U')THEN
      YMMIN=YCURSOR
      CALL PGMOVE(XSMIN,YMMIN)
      CALL PGDRAW(XSMAX,YMMIN)
C
C     ------------ <V> MAX Y OF PLOT
C
      ELSE IF(CHAR.EQ.'V')THEN
      YMMAX=YCURSOR
      CALL PGMOVE(XSMIN,YMMAX)
      CALL PGDRAW(XSMAX,YMMAX)
C
C     ------------ <Y> RESTORE AUTOMATIC Y SCALING
C
      ELSE IF(CHAR.EQ.'Y')THEN
      YMMIN=YSMIN
      YMMAX=YSMAX
C
C     ------------ <Z> SET ZERO FOR FIT
C
      ELSE IF(CHAR.EQ.'Z') THEN
      XZERO=XCURSOR
      CALL PGMOVE(XZERO,YPMAX)
      CALL PGDRAW(XZERO,YPMIN)
C
C     ------------ <P> PLOT -- EXECUTES RESCALING
C
      ELSE IF(CHAR.EQ.'P')THEN
C
C           ------ ARE PLOT X-LIMITS SWITCHED?
C
         IF(XSMIN.GT.XSMAX)THEN
         SQUID=XSMIN
```

```
          XSMIN=XSMAX
          XSMAX=SQUID
          END IF
C
C             ------ ARE PLOT AND SCALE LIMITS INSIDE DATA ENVELOPE?
C
      IF(XSMIN.LT.XFMIN)XSMIN=XFMIN
      IF(XSMAX.GT.XFMAX)XSMAX=XFMAX
      IF(XSCALEA.LT.XSMIN)XSCALEA=XSMIN
      IF(XSCALEB.GT.XSMAX)XSCALEB=XSMAX
      IF(XZERO.LT.XSMIN)XZERO=XSMIN
      IF(XZERO.GT.XFMAX)XZERO=XFMAX
      IF(XSTART.LT.XZERO)XSTART=XZERO
C
C             ------ FIND CHANNEL NUMBERS CORRESPONDING TO SCALING
C                    LIMITS AND RESCALE Y-LIMITS ACCORDINGLY
C
      NA=XSCALEA/CHT
      NB=XSCALEB/CHT
      IF(NB.GT.NCH)NB=NCH
      YSMIN=YD(NA)
      YSMAX=YD(NA)
          DO 125 I=NA,NB
          IF(YD(I).LT.YSMIN)YSMIN=YD(I)
          IF(YD(I).GT.YSMAX)YSMAX=YD(I)
 125      CONTINUE
C
C             ------ ARE MANUAL Y-LIMITS SWITCHED?
C
          IF(YMMIN.GT.YMMAX)THEN
          SQUID=YMMIN
          YMMIN=YMMAX
          YMMAX=SQUID
          END IF
C
C             ------ MAKE SOME ROOM AT THE TOP AND BOTTOM
C                    NOTE NEW VARIABLES; SCALED VALUES ARE RETAINED
C
      YRANGE=YSMAX-YSMIN
      YPMIN=YSMIN-0.125*YRANGE
      YPMAX=YSMAX+0.125*YRANGE
C
C             ------ INSERT MANUAL Y-LIMITS IF APPROPRIATE
C
      IF(YMMIN.GT.YPMIN)YPMIN=YMMIN
      IF(YMMAX.LT.YPMAX)YPMAX=YMMAX
C
C             ------ PLOT DATA, ASSIGNED ZERO, AND FIT LIMITS
C
      CALL PGENV(XSMIN,XSMAX,YPMIN,YPMAX,0,0)
      CALL PGPOINT(NCH,XD,YD,1)
      CALL PGMOVE(XZERO,YPMAX)
      CALL PGDRAW(XZERO,YPMIN)
      CALL GRSETLS(4)
      CALL PGMOVE(XSTART,YPMAX)
      CALL PGDRAW(XSTART,YPMIN)
      CALL PGMOVE(XSTOP,YPMAX)
      CALL PGDRAW(XSTOP,YPMIN)
      CALL GRSETLS(1)
C
C     ------------ <F> MOVE ON TO FIT
C
      ELSE IF(CHAR.EQ.'F')THEN
      GO TO 200
C
```

```
C
C
C     ------------ <ANY OTHER> TYPE MESSAGE AND RETURN TO PCURSE
C
      ELSE
      WRITE(6,190)
  190 FORMAT(2X,'TRY AGAIN')
      GO TO 90
      END IF
      GO TO 90
  200 CONTINUE
C
C
C
C
C
C
C           ------ ARE PLOT X-LIMITS SWITCHED?
C
         IF(XSMIN.GT.XSMAX)THEN
         SQUID=XSMIN
         XSMIN=XSMAX
         XSMAX=SQUID
         END IF
C
C           ------ ARE PLOT AND SCALE LIMITS INSIDE DATA ENVELOPE?
C
      IF(XSMIN.LT.XFMIN)XSMIN=XFMIN
      IF(XSMAX.GT.XFMAX)XSMAX=XFMAX
      IF(XSCALEA.LT.XSMIN)XSCALEA=XSMIN
      IF(XSCALEB.GT.XSMAX)XSCALEB=XSMAX
      IF(XZERO.LT.XSMIN)XZERO=XSMIN
      IF(XZERO.GT.XFMAX)XZERO=XFMAX
      IF(XSTART.LT.XZERO)XSTART=XZERO
C
C           ------ FIND CHANNEL NUMBERS CORRESPONDING TO SCALING
C                  LIMITS AND RESCALE Y-LIMITS ACCORDINGLY
C
      NA=XSCALEA/CHT
      NB=XSCALEB/CHT
      IF(NB.GT.NCH)NB=NCH
      YSMIN=YD(NA)
      YSMAX=YD(NA)
         DO 205 I=NA,NB
         IF(YD(I).LT.YSMIN)YSMIN=YD(I)
         IF(YD(I).GT.YSMAX)YSMAX=YD(I)
  205    CONTINUE
C
C           ------ ARE MANUAL Y-LIMITS SWITCHED?
C
         IF(YMMIN.GT.YMMAX)THEN
         SQUID=YMMIN
         YMMIN=YMMAX
         YMMAX=SQUID
         END IF
C
C           ------ MAKE SOME ROOM AT THE TOP AND BOTTOM
C                  NOTE NEW VARIABLES; SCALED VALUES ARE RETAINED
C
      YRANGE=YSMAX-YSMIN
      YPMIN=YSMIN-0.125*YRANGE
      YPMAX=YSMAX+0.125*YRANGE
C
C           ------ INSERT MANUAL Y-LIMITS IF APPROPRIATE
C
```

```
      IF(YMMIN.GT.YPMIN)YPMIN=YMMIN
      IF(YMMAX.LT.YPMAX)YPMAX=YMMAX
C
C
C     ----- CHOOSES DATA FOR FIT INTO TWO NEW ARRAYS
C
      NZERO=XZERO/CHT+0.001
      NSTART=XSTART/CHT+0.001
      NSTOP=XSTOP/CHT+0.001
      NFIT=NSTOP-NSTART+1
         DO 210 I=1,NFIT
         XF(I)=XD(I+NSTART-1)-XD(NZERO)+XFMIN
         YF(I)=YD(I+NSTART-1)
 210     CONTINUE
C
C
         DO 220 I=1,NCH
         XP(I)=XD(I)-XD(NZERO)
 220     CONTINUE
C
C
      XSFMIN=XSMIN-XZERO+XFMIN
      XSFMAX=XSMAX-XZERO+XFMIN
C
C     ----- CHOOSE INITIAL GUESSES FOR FIT PARAMETERS -----
C
      CALL PGADVANCE
 225  WRITE(6,230)
 230  FORMAT(1X,'INITIAL ESTIMATES FOR FIT:')
      WRITE(6,231)
 231  FORMAT(1X,'INTERNAL ESTIMATES: E, RESUTS OF PREVIOUS FIT: F',
     +' INPUT NEW VALUES: N')
 232  FORMAT(1X,'>>>> ',$)
      READ(5,'(A)')CHAR
C
C     ----- USING PREVIOUS RESULTS AS NEW GUESSES -----
C
      IF(CHAR.EQ.'F')THEN
      GO TO 510
C
C     ----- CALCULATED GUESSES -----
C
      ELSE IF(CHAR.EQ.'E')THEN
      X(1)=YF(NFIT)
      X(2)=YF(1)-YF(NFIT)
      X(3)=1.0/(XF(1)-XF(NFIT))
      GO TO 510
C
C     ----- GRAPHICAL ENTRY OF GUESSES -----
C
      ELSE IF(CHAR.EQ.'N')THEN
      GO TO 240
      ELSE
      GO TO 225
      END IF
C
C
C
 240  AXX=XF(NFIT)
      AYY=YF(NFIT)
      BXX=XF(1)
      BYY=YF(1)
      CXX=AXX
      CYY=AYY
      XCURSOR=0.0
```

```
      YCURSOR=YPMAX
C
C
 370  CONTINUE
      CALL PGENV(XSFMIN,XSFMAX,YPMIN,YPMAX,0,0)
      CALL PGPOINT(NFIT,XF,YF,1)
 373  CALL PGPOINT(1,AXX,AYY,26)
      CALL PGPOINT(1,BXX,BYY,24)
      CALL PGDRAW(CXX,CYY)
      CALL PGPOINT(1,CXX,CYY,24)
C
      WRITE(6,375)
 375  FORMAT(1X,'CURSOR INPUTS: A,B,C, KEYBOARD: K, TRY ESTIMATE: T',
     + ' FIT: F')
      CALL PGCURSE(XCURSOR,YCURSOR,CHAR)
C
C
C
      IF(CHAR.EQ.'A')THEN
      AXX=XCURSOR
      AYY=YCURSOR
      GO TO 373
C
      ELSE IF(CHAR.EQ.'B')THEN
      BXX=XCURSOR
      BYY=YCURSOR
      GO TO 373
C
      ELSE IF(CHAR.EQ.'C')THEN
      CXX=XCURSOR
      CYY=YCURSOR
      GO TO 373
C
C     ----- DRAW CURVE BASED ON INITIAL PARAMETERS -----
C
      ELSE IF(CHAR.EQ.'T')THEN
      X(1)=AYY
      X(2)=BYY-AYY
      X(3)=1.0/(BXX-CXX)
      YSS=X(1)+X(2)*EXP(X(3)*XF(1))
      WRITE(6,389)(X(I),I=1,3),YSS,XF(1)
 389  FORMAT(1X,5E15.6////)

C
      DO 390 I=1,NFIT
      YFIT(I)=X(1)+X(2)*EXP(X(3)*XF(I))
 390  CONTINUE
C
      CALL PGLINE(NFIT,XF,YFIT)
C
C     ----- READ GUESSES FROM KEYBOARD -----
C
      ELSE IF(CHAR.EQ.'K')THEN
      WRITE(6,400)
 400  FORMAT(1X,'PARAMETER 1 > ',$)
      READ(5,410)X(1)
 410  FORMAT(F10.4)
      WRITE(6,420)
 420  FORMAT(1X,'PARAMETER 2 > ',$)
      READ(5,410)X(2)
      WRITE(6,430)
 430  FORMAT(1X,'PARAMETER 3 > ',$)
      READ(5,410)X(3)
      GO TO 500
C
```

```
      ELSE IF(CHAR.EQ.'F')THEN
      GO TO 500
      ELSE
      GO TO 370
      END IF
      GO TO 370
C
 500  CONTINUE
C
C     ----- SET INITIAL GUESSES FOR FITTING PROGRAM ----
C
      X(1)=AYY
      X(2)=BYY-AYY
      X(3)=1.0/(BXX-CXX)
C
C     ----- SET OTHER PARAMETERS FOR FITTING PROGRAM -----
C
 510  NSIG=6
      EPS=0.0
      DELTA=0.0
      MAXFN=1000
      IOPT=1
      IXJAC=1024
C
C     ----- CALL FITTING SUBPROGRAM -----
C
       CALL ZXSSQ (SINGLE,NFIT,3,NSIG,EPS,DELTA,MAXFN,IOPT,PARM,X,
     + SSQ,F,XJAC,IXJAC,XJTJ,WORK,INFER,JIER)
C
C     ----- CALCULATE THEORETICAL CURVE AND SET PLOT LIMITS -----
C
       YFMIN=X(1)+X(2)*EXP(X(3)*XF(1))
       YFMAX=YFMIN
       DO 700 I=1,NFIT
       YFIT(I)=X(1)+X(2)*EXP(X(3)*XF(I))
       IF(YFIT(I).LT.YFMIN)YFMIN=YFIT(I)
       IF(YFIT(I).GT.YFMAX)YFMAX=YFIT(I)
 700   CONTINUE
C
C
C
       IF(YFMIN.LT.YPMIN)YPMIN=YFMIN
       IF(YFMAX.LT.YPMIN)YPMAX=YFMAX
       IF(YSMIN.LT.YPMIN)YPMIN=YSMIN
       IF(YSMAX.GT.YPMAX)YPMAX=YSMAX
C
C
C     ----- ENCODE PARAMETERS TO PRINT -----
C
 750  FORMAT(E15.6)
 760  FORMAT(I15)
      ENCODE(20,750,NOUT(2))X(1)
      ENCODE(20,750,NOUT(3))X(2)
      ENCODE(20,750,NOUT(4))X(3)
      ENCODE(20,750,NOUT(5))SSQ
      ENCODE(20,760,NOUT(6))JIER
      ENCODE(20,760,NOUT(7))INFER
      ENCODE(20,750,NOUT(8))WORK(1)
      ENCODE(20,750,NOUT(9))WORK(2)
      ENCODE(20,750,NOUT(10))WORK(3)
      ENCODE(20,750,NOUT(11))WORK(4)
      ENCODE(20,750,NOUT(12))WORK(5)
      ENCODE(20,760,NOUT(13))NFIT
      ENCODE(20,750,NOUT(14))XZERO
      ENCODE(20,750,NOUT(15))XSTART
```

```
      ENCODE(20,750,NOUT(16))XSTOP
      ENCODE(20,750,NOUT(17))CHT
C
C
      TOUT(1)(16:35)=FILE(1:20)
      DO 770 I=2,17
      TOUT(I)(16:35)=NOUT(I)(1:20)
 770  CONTINUE
C
C     ----- PRINT RESULTS TO SCREEN -----
C
      CALL PGENV(XSFMIN,XSFMAX,YPMIN,YPMAX,0,0)
      CALL PGPOINT(NCH,XP,YD,1)
      CALL PGLINE(NFIT,XF,YFIT)
      SPACE=-1.0
      DO 775 I=1,7
      CALL PGMTEXT(TOP,SPACE,0.5,0.0,TOUT(I))
      SPACE=SPACE-2.0
 775  CONTINUE
 776  CONTINUE
C
C     ----- ADJUSTMENT OF Y PLOT LIMITS -----
C
 1000 WRITE(6,1001)YPMIN,YPMAX
 1001 FORMAT(1X,'Y PLOT LIMITS: ',2F12.4,' REPLACE? (Y/N): ',$)
      READ(5,'(A)')CHAR
      IF(CHAR.EQ.'Y')THEN
      WRITE(6,1100)
 1100 FORMAT(1X,'NEW MIN-Y PLOT LIMIT: ',$)
      READ(5,1200)DOWN
 1200 FORMAT(F12.8)
      WRITE(6,1300)
 1300 FORMAT(1X,'NEW MAX-Y PLOT LIMIT: ',$)
      READ(5,1200)UP
      YPMIN=DOWN
      YPMAX=UP
      GO TO 770
      ELSE IF(CHAR.EQ.'N')THEN
      GO TO 1400
      ELSE
      GO TO 1000
      END IF
 1400 CALL PGADVANCE
      CALL PGEND
C
C     ----- WRITE FILE FOR TRILOG PRINTER OUTPUT -----
C
 777  WRITE(6,778)INFER
 778  FORMAT(1X,'INFER=',I4,' WRITE FILE FOR TRILOG PRINTER? (Y/N):
     + ',$)
      READ(5,'(A)')CHAR
      IF(CHAR.EQ.'Y')THEN
      GO TO 779
      ELSE IF(CHAR.EQ.'N')THEN
      GO TO 905
      ELSE
      GO TO 777
      END IF
C
 779  CONTINUE
      J=INDEX(FILE(1:),' ')
      DEV2(1:J-1)=FILE(1:J-1)
      DEV2(J:J+3)='.TRI'
      DEV2(14:20)='/TRILOG'
C
```

```
C
      CALL PGBEGIN(0,DEV2,2,2)
      CALL PGENV(XSFMIN,XSFMAX,YPMIN,YPMAX,0,0)
      CALL PGPOINT(NCH,XP,YD,1)
      CALL PGLINE(NFIT,XF,YFIT)
C
C
C
      CALL PGADVANCE
      SPACE=-1.0
      DO 780 I=1,17
      CALL PGMTEXT(TOP,SPACE,0.1,0.0,TOUT(I))
      SPACE=SPACE-2.0
 780  CONTINUE
C
C
C
      XFSTART=XSTART-XZERO
      XFSTOP=XSTOP-XZERO
      YPMIN=F(1)
      YPMAX=F(1)
      DO 800 I=1,NFIT
      IF(YPMIN.GT.F(I))YPMIN=F(I)
      IF(YPMAX.LT.F(I))YPMAX=F(I)
 800  CONTINUE
C
C
C
      RANGE=YPMAX-YPMIN
      YPMAX=YPMAX+0.5*RANGE
      YPMIN=YPMIN-0.5*RANGE
C
C
C
      CALL PGADVANCE
      CALL PGENV(XSFMIN,XSFMAX,YPMIN,YPMAX,0,0)
      CALL PGPOINT(NFIT,XF,F,1)
      CALL PGMTEXT(TOP,-4.0,0.1,0.0,'RESIDUALS')
      CALL GRSETLS(4)
      CALL PGMOVE(XFSTART,YPMAX)
      CALL PGDRAW(XFSTART,YPMIN)
      CALL PGMOVE(XFSTOP,YPMAX)
      CALL PGDRAW(XFSTOP,YPMIN)
      CALL GRSETLS(1)
      CALL PGEND
C
C     ----- OPTION TO LOOP TO BEGINNING -----
C
 905  WRITE(6,910)
 910  FORMAT(1X,'DO YOU WANT IT AGAIN? ',$)
      READ(5,'(A)')CHAR
      IF(CHAR.EQ.'Y')THEN
      GO TO 944
      ELSE IF(CHAR.EQ.'N')THEN
      GO TO 950
      ELSE
      GO TO 905
      END IF
C
 944  WRITE(6,945)
 945  FORMAT(1X,'SAME DATA SET (S) OR A NEW ONE (N)? ',$)
      READ(5,'(A)')CHAR
      IF(CHAR.EQ.'S')THEN
      GO TO 75
      ELSE IF(CHAR.EQ.'N')THEN
```

```
      GO TO 5
      ELSE
      GO TO 944
      END IF
  950 CONTINUE
      STOP
      END
C
C     ----- FUNCTION SUBROUTINE FOR ZXSSQ FITTING PROGRAM -----
C
      SUBROUTINE SINGLE(X,M,N,F)
      COMMON XF,YF
      DIMENSION XF(1024), YF(1024), F(1024), X(3)
      DO 300 I=1,M
      F(I)=YF(I)-X(1)-X(2)*EXP(X(3)*XF(I))
  300 CONTINUE
      RETURN
      END
```